universität wien

MASTERARBEIT

Titel der Masterarbeit

A zebrafish model of Letm1 and Letm2 deficiency

verfasst von

Stefan Hajny, BSc

angestrebter akademischer Grad

Master of Science (MSc)

Wien, 2015

Studienkennzahl lt. Studienblatt:	A 066 834
Studienrichtung lt. Studienblatt:	Masterstudium Molekulare Biologie (UG2002)
Betreut von:	Priv. Doz. Dr. Karin Novikovsky

Table of contents

Acknowledgements

Within the scope of the conducted Master thesis, I had the opportunity to participate at an interesting collaborative research project between the *Anna Spiegel Center for Translational Research* (ASCTR) and the *Max F. Perutz Laboratories* (MFPL).

I would like to express my gratitude to all members of the laboratories of Karin Nowikovsky (ASCTR), Kristin Tessmar-Raible (MFPL) and Florian Raible (MFPL).

Working with zebrafish was a new process for me during the first period. Therefore I want to particularly thank Marcus Dekens, Bruno Fontinha and Poonam Sharma for their supportive help and advice during the whole study. Furthermore, I also like to acknowledge Stephanie Bannister for beneficial support at the genomic engineering approaches.

Conducting experiments at two different institutes is never an easy endeavour. Hence, special thanks go to Shane Austin who supported me during comprehensive studies and gave supportive advice whenever needed.

Especially I want to thank my supervisors Karin Nowikovsky and Kristin Tessmar-Raible for guidance throughout the study, valuable discussions and the enjoyable collaboration.

Finally, I also want to mention all involved person of my private environment who were important for a healthy work-life-balance.

Abbreviations

5mC	5-methylated cytosine
AMP	Ampicillin
CBD	Calcium binding domain
CDS	coding sequence
CRSIPR/Cas9	Clustered regularly interspaced palindromic repeats/CRISPR associated
DPF	Days post fertilization
DSB	Double strand break
HMR	Homologous recombination
IPTG	Isopropyl β-D-1-thiogalactopyranoside
ISH	*In situ* hybridization
IVT	*In vitro* transcription
KAN	Kanamycin
LETM	Leucine zipper-EF-hand containing transmembrane
mRNA	Messenger RNA
NHEJ	Non homologous end joining
RT	Room temperature
RVD	Repeat variable di-residue
SPEC	Spectinomycin
TALEN	Transcription activator like effectors nuclease
WHS	Wolf Hirschhorn syndrome
WHSCR	WHS critical region
WT	Wildtype
X-Gal	5-bromo-4-chloro-3-indolyl-β-D-galactopyranoside

1. Introduction

1.1. Wolf Hirschhorn Syndrome

In 1961, the geneticists Cooper and Hirschhorn described a patient with gene deletions on chromosome 4 or 5 accompanied with a characteristic phenotype. Decades of scientific research revealed that these findings were the first ones, which describe the severe gene deletion disorder termed *Wolf Hirschhorn syndrome* (WHS).

With an incidence of around 1:50,000 live births the syndrome is categorized as a rare disorder (Shannon, Maltby, Rigby, & Quarrell, 2001). Furthermore, the many linked pathogenic symptoms makes it difficult to diagnose WHS (Paradowska-Stolarz, 2014). To overcome that issue, a core phenotype (minimal diagnostic criteria) including a typical facial appearance, growth retardation, intellectual disability and seizures was defined. Several further studies demonstrated that women are twice more often affected than male patients (Battaglia, Filippi, & Carey, 2008).

Besides the rather complex phenotype, the genotype is characterized by a multigenic deletion within a distinct area of the short end of chromosome 4. While the deletion is restricted to the 4p16.3 region in 20% of the diagnosed patients (approx. 5Mb), the vast majority suffers from larger deletions beyond that area (Bergemann, Cole, & Hirschhorn, 2005). Further studies described that pure *de novo* deletions are the most common underlying mechanisms behind the genomic loss. (Paradowska-Stolarz, 2014).

Early genomic mapping approaches demonstrated that the deletions always affect a very distinct set of genes, termed as the WHS-critical-region 1 (WHSCR 1; Wright et al., 1997). Few years later, Zollino and colleagues described a more distal located region (WHSCR2) overlapping with WHSCR1 and linked to WHS related phenotypes (Marcella Zollino et al., 2003).

It is further supposed that the complexity of the disease phenotype reflects the genotypic variability in WHS patients. Basically, the size of the deleted chromosomal portion determines the phenotypical appearance and pathogenic symptoms (Hammond et al., 2011; M Zollino et al., 2000). In a more recent research paper, Zollino proposed to classify the WHS patients according to their size of chromosomal deletion into a severe (≥22 Mb deletion), classical (5-18 Mb deletion) and mild phenotype (≤3.5 Mb deletion; Zollino et al., 2008).

1.2. LETM1, an important protein for mitochondrial potassium homeostasis

The *Leucine Zipper-EF-hand containing transmembrane* 1 (*LETM1*) gene is located less than 80 kb distal to the WHSCR1 and falls within WHSCR2. WHS patients who suffer of epileptic seizures are found to be letm1 haploinsufficient, respectively carry a deletion within WHSCR2. Hence, it

is suggested that LETM1 is the most prominent key player in this distinct phenotype. (Schlickum et al., 2004). However, one study described a *LETM1* haploinsufficient patient without the typical seizure phenotype which suggests another associated gene (Maas et al., 2008).

LETM1 is an evolutionary conserved and nucleus encoded, mitochondrial protein located in the inner membrane (Dimmer et al., 2008). Based on various sequencing and alignment approaches, LETM1 and respective orthologues were detected in each eukaryotic organism so far (Karin Nowikovsky, Pozzan, Rizzuto, Scorrano, & Bernardi, 2012; Schlickum et al., 2004). Moreover, data collected from mice and human tissue samples fortified the ubiquitous abundance (Sabine Endele, Fuhry, Pak, Zabel, & Winterpacht, 1999). The mature protein displays one or two putative Ca^{2+} binding domains (CBD), one highly conserved transmembrane region (TMR), a leucine zipper motif and has an estimated mass of approximately 83 kDa (Endele, Fuhry, Pak, Zabel, & Winterpacht, 1999;).

First experiments in yeast revealed that Mdm38p, the best studied of the two known orthologues of LETM1, is required for growth on non-fermentable substrate. This implied that Mdm38p is crucial for mitochondrial functionality. It was further demonstrated that the identified yeast protein controls the mitochondrial potassium and consequently the volume homeostasis (Froschauer, Nowikovsky, & Schweyen, 2005; Zotova et al., 2010).

The group of Martin et al. identified a protein with a mass of approximately 83 kDa as a candidate for mitochondrial K^+/H^+ exchange (Martin, Beavis, & Garlid, 1984). These findings support the notion that *LETM1* encodes an essential regulatory factor of the long sought after the mitochondrial K^+/H^+ exchanger (KHE) protein complex. The fact that LETM1 carries only one transmembrane domain further strengthen the idea that the protein may be a crucial regulatory subunit of the KHE (Froschauer et al., 2005). Subsequent investigations revealed that a homozygote *MDM38* deletion, associated with mitochondrial dysfunctions, was lethal in yeast and other eukaryotic organism.

Besides, Mdm38p was reported to be involved in the mitochondrial translation machinery and required for the assembly of the *cytochrome bc1 complex* and the *cytochrome c oxidase* (Lupo et al., 2011). Hence, it can be hypothesized that Mdm38p and maybe also LETM1 may be involved in more processes than initially assumed.

A study in *Drosophila melanogaster* illustrated that a ubiquitous knock-down of the DmLetm1 gene resulted in early lethality during development. Tissue specific knock-downs led to various pathogenic phenotypes, such as growth retardation or decreased locomotion. Assessment of the latter showed that downregulation of neuronal DmLetm1 led to significantly higher immobile

phases when compared to WT. Furthermore, the characteristic phenotype of swollen mitochondria was also observed in DmLetm1 deficient flies (McQuibban et al., 2010).

By means of siRNA, the group of Jiang and colleagues generated a *Letm1* haploinsufficient mouse strain. These animals clearly showed embryonic growth retardation at day 9.5. However, this effect subsided over the following 4 days and the embryos were even sized at day 13.5, pointing to the importance of LETM1 during the first days of development. Furthermore, *Letm1*$^{+/-}$ mice were treated with kainic acid to artificially induce seizures. Mutant animals showed a 25% higher sensitivity to the applied treatment when compared to related WT, fortifying the seizure related role of LETM1 (Jiang et al., 2013).

The group of Xiaogang Zhang investigated the relationship between LETM1 and seizures in rats. Using a lentiviral approach, *Letm1* expression was conditionally knocked-down in the hippocampal formation. However, disruption of *Letm1* expression did not lead to spontaneous seizures unless in combination with the injection of Pilocarpine. Comparisons between mutant and WT animals showed elevated duration and frequency levels of seizures in the *Letm1* knock-down group. The ionophore Nigericin was further injected into the hippocampus to study its effect on seizure intensity. However, treatment with the substance did not show any changes, suggesting a secondary mechanism behind the seizure phenotype (X. Zhang et al., 2013).

Based on the comprehensive findings in different model systems, it can be proposed that LETM1 haploinsufficient neurons are one of the most affected tissue types. For instance, to maintain excitability, synaptical vesicle docking or endocytosis, neurons heavily rely on oxidative phosphorylation (Streck et al., 2014). LETM1 deficient cells display a pathogenic mitochondrial phenotype. Hence it can be concluded that insufficient ATP production and/or outer mitochondrial membrane disruption substantially alters neuronal functionality or induce cell death, respectively.

1.3. The KHE is an indispensable complex to maintain mitochondrial volume and pH homeostasis

Peter Mitchell was rewarded with the Nobel Prize for his Chemiosmotic Hypothesis which he postulated in the early 1960s (Reviewed by Mitchell, 2011). This fundamental theory of the mitochondrial energy conservation relies on the existence of a tightly regulated cation and anion transport and exchange system across the mitochondrial membrane as described in the third and fourth postulation, as cited below:

3. Chemiosmotic energy conservation depends on substrate specific exchange-diffusion carrier systems in the mitochondrial membrane. These transport complexes are capable to catalyse the reversible exchange of anions against OH^- and cations against H^+. Furthermore, these systems also regulate the mitochondrial pH and the osmotic differential, without disrupting the membrane potential.

4. The third (but also first and second) postulates describe systems which are located in a specialized coupling membrane, characterized by a low permeability to protons, cations and anions.

Decades of research revealed that especially the inner mitochondrial membrane has a low permeability to differently charged ions and that this membrane harbours several ion transport systems which are regulated by conductance (reviewed in Nowikovsky, Schweyen, & Bernardi, 2009). Potassium transport and exchange systems regulating the mitochondrial potassium homeostasis are particularly important. The present study focuses on LETM1, a protein proposed to be the primary regulatory subunit of the KHE. Hence, mitochondrial potassium homeostasis will be emphasized in the upcoming section.

Principally, mitochondrial swelling depends on the organelles energetic state (Azzone & Azzi, 1965). Highly energized mitochondria can accumulate K^+ due to unbalanced K^+ fluxes (influx > efflux). Potassium uptake is usually compensated by the KHE via electroneutral extrusion of one K^+ for one H^+. However, in case of leaks, and/or opening of potassium channels, inefficiently counteracted by the efflux system, the limits of the system will be reached which results in the disturbance of the equilibrium, associated with swelling.

Low energized, respectively depolarized mitochondria on the other side are no longer capable to maintain stable ion gradients. Hence, non-diffusible matrix proteins and macromolecular complexes increase the osmotic pressure leading to mitochondrial swelling.

Potassium swelling assays in yeast mitochondria showed that Mdm38p is indispensable for K^+/H^+ exchange, thus a crucial factor of the KHE (Karin Nowikovsky et al., 2004).

Knock-down of *LETM1* in HeLa cells (Dimmer et al., 2008) or depletion of the *MDM38* gene product in yeast (Karin Nowikovsky et al., 2004) caused severe mitochondrial swelling and fragmentation. Further studies in Mdm38p deficient yeast revealed an impaired KHE activity, mitophagy and eventually cell death (Froschauer et al., 2005; K Nowikovsky, Reipert, Devenish, & Schweyen, 2007). Importantly, it was shown that nigericin, an ionophore catalysing K^+/H^+

exchange, was capable to revert the Mdm38p/LETM1 deletion/knock-down phenotypes, respectively (Figure 1). This was another strong evidence linking the function of LETM1 or Mdm38p to the KHE.

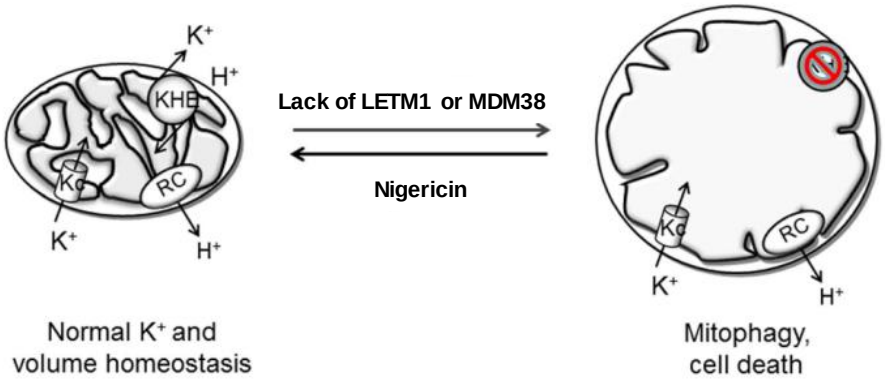

***Figure 1**: Mitochondrial volume homeostasis is tightly controlled by well-regulated potassium fluxes. While related potassium channels (K_c) provide a constant K^+ influx, driven by the inner membrane potential, the electroneutral potassium/proton exchanger (KHE) complex is indispensable for its extrusion. The thereby imported protons are further processed by the respiratory chain (RC). Studies in yeast and HeLa cells demonstrated a swollen mitochondrial phenotype in MDM38, respectively LETM1 deficient mutants. However, treatment with the ionophore nigericin fully reverted the observed pathogenic condition. Hence, the ablated protein plays an essential role in mitochondrial K^+/H^+ exchange. (Picture adapted and modified from* Nowikovsky et al., 2012*).*

1.4. The elusive role of LETM2, a protein closely related to LETM1

Besides LETM1, most eukaryotes also encode a LETM1-like protein, termed *Leucine Zipper-EF-hand containing transmembrane* 2 (Letm2). Sequence alignments showed that these proteins share various domains with LETM1 (Section 3.1). However, the role and function of LETM2 is still elusive. Based on the similar sequence to LETM1 it can be speculated that the protein may have a similar function, structure and localization. However, only three studies investigated different aspects of LETM2 or related proteins so far.

Organ specific northern and immunoblotting studies in rats revealed that LETM2 expression was restricted to almost all developmental stages of sperm (Tamai et al., 2008a).

In yeast, as mentioned before, *MDM38* has a homologous gene, *YPR125W*, also termed *MRS7*. While disruption of *MRS7* does not show any phenotype, double deletion of *MDM38* and *MRS7* shows the same phenotype as the single knock-out of *MDM38*. However, overexpression of MRS7 in *MDM38* deficient yeast cells restored the growth phenotype which points to a functional homology (Karin Nowikovsky et al., 2004).

In *Arabidopsis thaliana*, two orthologues *LETM* genes were found and named AtLetm1 and AtLetm2. Interestingly, *Arabidopsis* is viable without AtLetm1 transcripts. While the AtLetm1

deficiency just caused mild growth retardations, no phenotype was observed in plants of depleted AtLetm2. Establishing a knock-out strain, lacking AtLetm1 and AtLetm2 in a homozygote manner was not possible, due to impaired development. However, plants with a homozygous deletion of any of the two *letm* genes combined with the heterozygous deletion of the other *letm* gene was viable. While AtLetm1$^{+/-}$ / AtLetm2$^{-/-}$ strains showed the same phenotype as AtLetm1$^{-/-}$ specimens, the AtLetm1$^{-/-}$ / AtLetm2$^{+/-}$ strain was characterized by growth retardations during the first few weeks after germination, impaired early root growth and deformations. However, the deficiencies disappeared during maturation (B. Zhang et al., 2012).

1.5. The zebrafish as a model organism

Over past decades the zebrafish (*Danio rerio*) emerged to one of the most important model organism in molecular biology. Besides the fast regeneration times, high progeny, easy handling, *ex vivo* development and well established resources, the fish is a suitable model for the present study (Grunwald & Eisen, 2002). Moreover, a recent review highlighted the advantages of the zebrafish fish in terms of mitochondrial research (Steele, Prykhozhij, & Berman, 2014). The natural environment supports easy, reliable and exact administration of various compounds. The size makes the species furthermore perfect for various high throughput drug screening approaches. For instance, larvae can be raised and subsequently screened in 96-well microtiter plates (Parng, Seng, Semino, & McGrath, 2002). Moreover, the well-established pentylenetetrazole model (PTZ) was used in the present thesis to study behavioral alteration in zebrafish larvae. (Berghmans, Hunt, Roach, & Goldsmith, 2007; Ellis, Seibert, & Soanes, 2012).

The zebrafish model system was initially established for forward genetic screening approaches. However, due to their transparent and “simple to image” character, *Danio rerio* became increasingly important for reverse genetic procedures (Goldsmith & Jobin, 2012).

Several techniques for genomic engineering were adapted from other model systems or newly established over the last years. The TALEN and CRISPR/Cas9 system are currently the state of the art methods to establish a stable gene knock-out. On the other hand, morpholinos are widely used for gene knock-down experiments (Bill, Petzold, Clark, Schimmenti, & Ekker, 2009).

Decades of research and breading led to a large variability of zebrafish strains including about 30 different wildtype lines and numerous genetic engineered fishes (Sprague, Doerry, Douglas, & Westerfield, 2001). For the present study we used WT AB fish and the mitochondrial tagged

pSCAC69 line (Kim, Kang, Kim, & Choi, 2008) for all *in vivo* approaches. The transgenic pSCAC69 fish line, which bases on a genetic WT AB background, was obtained from the laboratory of Kim and colleagues. The group generated the pSCAC69 strain via genomic integration of a novel eGFP sequence fused to a mitochondrial localization signal and is regulated via the *elongation factor-1α* promoter. This approach allowed the ubiquitous expression of a green fluorescence protein targeted to mitochondria and thus improves several workflows addressed to mitochondrial *in situ* imaging (Kim et al., 2008). Moreover, the transgenic fish line was crossed into the *nacre* strain to generate albino animals which enhances imaging procedures.

1.6. Genomic engineering approaches

1.6.1 TALEN

The discovery of *Transcription activator-like effectors* (TALE's), as a part of a host-pathogen interaction in plants, gave rise to re-develop this system and to make it suitable for genomic engineering. In principle, TALE's are used by *Xanthomonas ssp.* to specifically modify the gene expression of the host (Bogdanove, Schornack, & Lahaye, 2010). A typical TALE sequence consists of several repeat-variable-di-residues (RVD) which are crucial for sequence recognition and interaction (Figure 2). Each RVD is defined by an array of two amino acids, specifying the binding affinity to a distinct nucleotide. Further, a transcriptional activator domain is fused at the C-terminal site to maintain the gene modulation in the infiltrated host. Via establishment of a RVD library, sequence specific TALE's can be constructed by ease *in vitro*. The natural occurring C-terminal transcription activator domain was replaced by a type IIS FokI endonuclease (TALE nuclease; TALEN) to make it suitable for precise genomic engineering. To establish a stable gene knock-out, mRNA's of two TALEN (TALEN pair) has to be injected into the host of choice. Hereby the space between the two binding sites (spacer region) is a crucial factor for the efficiency. Only if both effectors bind close enough, the heterodimeric FOK I domains can fuse, form a dimer and introduce a double strand break (DSB). Cell internal pathways are further activated to repair the broken DNA. In most of the cases the error prone non-homologous end joining (NHEJ) is carried out, which typically introduces insertions or deletions at the cleavage site.

For genotyping purposes, the TALEN construct should be designed in a way, so that the spacer region contains a unique restriction site. This method allows to easily screen for putative mutations due to an assumed change in the spacer sequence within the restriction site (Cermak et al., 2011; Miller et al., 2011; Zu et al., 2013).

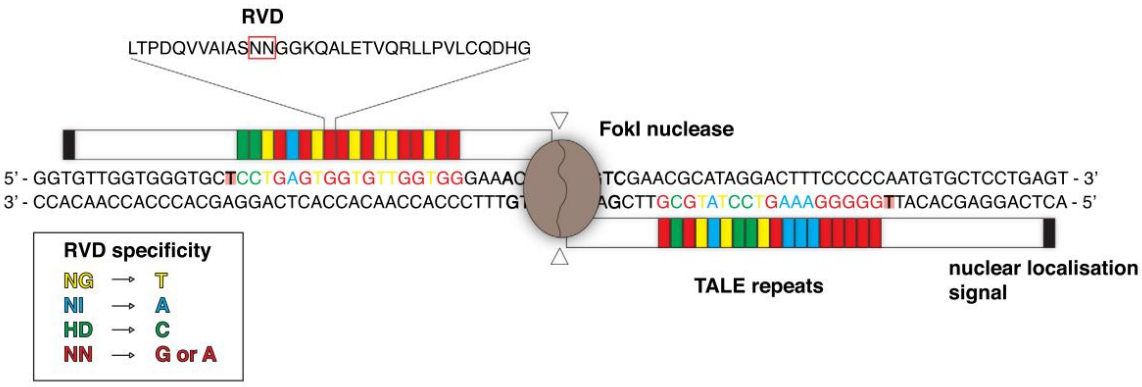

***Figure 2**: Schematic representation of a typical TALEN pair. Two arrays consisting of several RVD's and an attached heterodimeric FOKI domain are used to introduce a locus specific DSB. Each utilized RVD recognizes a particular nucleotide which allows highly accurate DNA interaction. Only if both TALEN effectors bind close enough, the FOKI domains can fuse and introduce the DSB. (Graphic adapted and modified from* Auer & Del Bene, 2014)

Besides the classical TALEN approach to disrupt the gene functionality, the inverted *TALEN (iTAL)* technique is a reliable method to establish a specific knock-in at any desired genomic locus. A typical iTAL sequence is characterized by a small nucleotide array consisting of both genomic TALEN binding sites including the spacer region in between. Furthermore, the TALEN recognition sites are inverted: The left TALEN effector binds at the 5' end of the lagging strand, while the right TALEN effector binds at the 5' region of the upper stand. However, the spacer region stays unaltered (Figure 3/A). This rearrangement is necessary to achieve the underlying iTAL principle: Micro-homologous recombination. Prior construction of a suitable expression vector, containing the respective iTAL sites, the construct is injected in the host of choice. Immediately post injection, the TALEN transcripts are translated into the final effector proteins which bind to their assigned genomic sequence and introduce a DSB. However, the proteins also recognize the provided iTAL sequences and cleave at these sites. Based on the inverted arrangement, the resulting termini show a micro homology to the prior cleaved genomic locus. In contrast to the common principle of homologous recombination (HMR) to repair a DNA cleavage, the hereby exerted process is a combination of (micro-) HMR and NHEJ (Auer & Del Bene, 2014).

In this present study, a fluorescent reporter gene, controlled by a ubiquitous promoter, was planned to be integrated in the middle of the letm1 sequence in zebrafish. This approach allows genotyping after few hours post fertilization and ensures disruption of the letm1 gene (Figure 3/B).

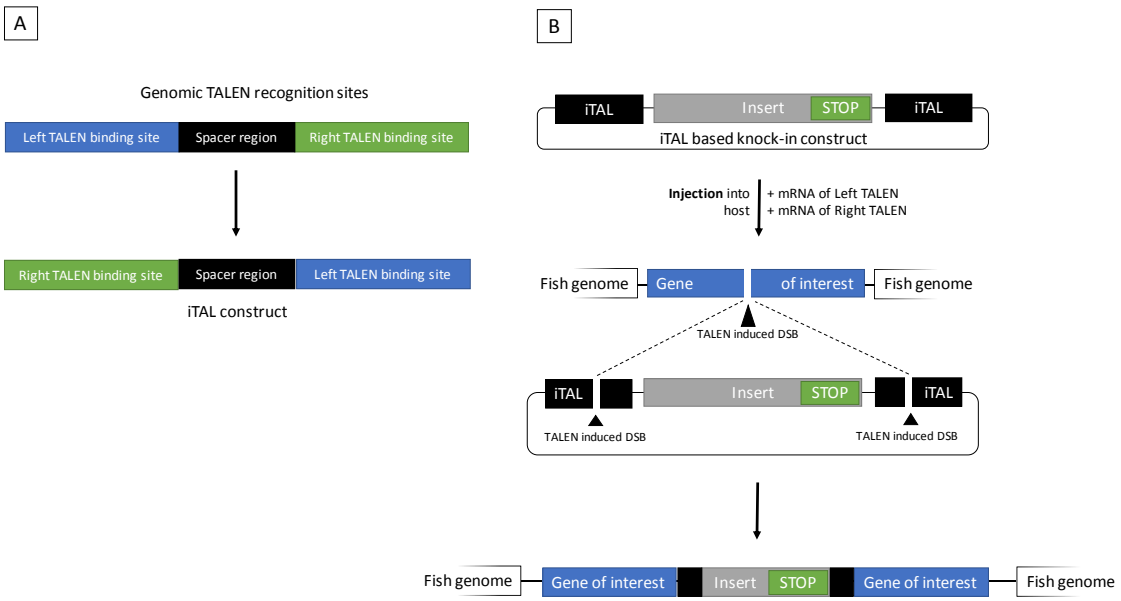

Figure 3: (A) *Illustration of the basic principle of an iTAL mediated gene insertion. The most essential features of the insertion sequence are the flanking iTAL sites. These arrays are the reversed TALEN target sequences. The respective left TALEN pair would interact with the right side of the target region and vice versa. Moreover, the spacer region between the targeting sites stays untouched.* ***(B)*** *A suitable iTAL vector, carrying the insertion sequence is further co-injected with the associated TALEN mRNA's into the host of choice. After translation of the provided TALEN transcripts in vivo, the resulting effector proteins recognize their genomic target locus and introduce a DSB. However, the TALEN proteins also recognize the iTAL sequences and perform a restriction at these sites. The introduced nuclear DSB initiates HMR or NHEJ depended pathways, which can also involve a template guided repair. Therefore, the cleaved iTAL sequences can be used to "correct" the DNA cleavage.*

1.6.2 The CRISPR/Cas9 system

In principle, clustered regularly interspaced palindromic repeats/CRISPR associated (CRISPR/Cas) is a bacterial defense system against foreign DNA (Barrangou et al., 2007). Similar to the TALEN approach, also this native mechanism was genetically modified to establish a tool for high precise genomic engineering. The adapted system consists of two major components (Figure 4). The single guiding RNA (sgRNA) which is a short RNA sequence complementary to the targeted locus (approximately 16 nucleotides) and fused to a so called tracerRNA which allows interaction with the second component, the enzyme Cas9.

By now, two different Cas9 approaches are available (Figure 4). The commonly used Cas9 nuclease requires just one sgRNA to introduce a DSB at any genomic locus. On the other hand, the novel Cas9 nickase is capable to cleave only one strand. Therefore, the latter requires a pair of sgRNAs to introduce two single strand breaks which results in a DSB, comparable to TALEN. Using the nickase drastically reduces the amount of offset targets due to higher specificities.

Therefore, designing an efficient pair of sgRNA's is very similar to TALEN. A unique restriction site in the spacer region should be considered to improve the genotyping workflow. In opposite to

the TALEN, sgRNA's require a genomic protospacer adjacent motif (PAM) immediately before the binding site for proper function. This motif depends on the bacterial origin of the utilized Cas9. For example, the commonly used Cas9, derived from *Streptococcus pyogenes*, requires a *5'-NGG-3'* PAM sequence.

Via injection of specific sgRNA's in combination with the related Cas9 mRNA, or the recombinant protein, a stable knock-out in zebrafish can be realized (Auer & Del Bene, 2014; Makarova et al., 2011; Mali, Aach, et al., 2013). Besides, the CRISPR/Cas9 system is also capable to establish a specific knock-in, following a very similar protocol as already described in the former section (Section 1.6.1; *inverted TALEN*). Moreover, while TALEN cut unpredictable somewhere in the spacer region, the Cas9 cleavage always occurs 3 basepairs downstream of the PAM sequence, which makes them perfectly suitable for high precisely gene insertions (Auer & Del Bene, 2014).

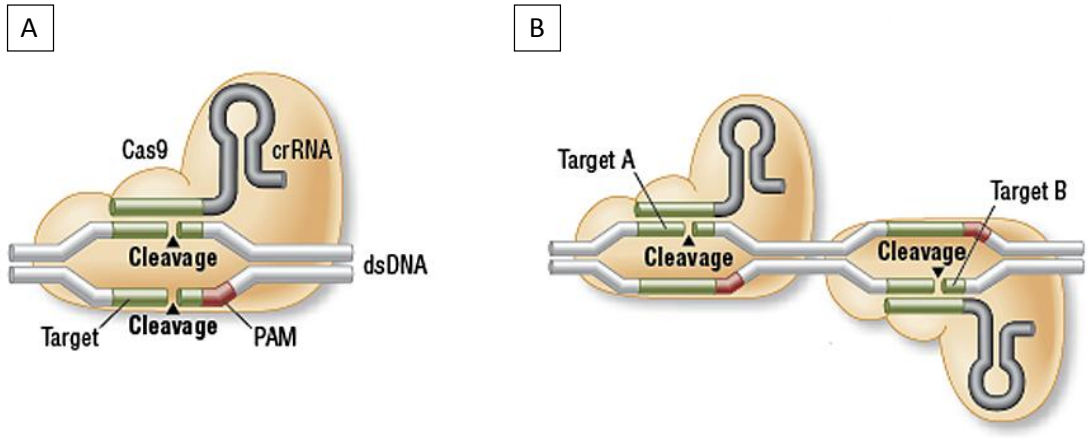

***Figure 4**: Schematic representation of the two commonly used CRSIPR/Cas9 systems. Both methods rely on the presence of a Cas9 specific PAM sequence immediately upstream of each targeted locus. Section **(A)** illustrates one sgRNA bound to the Cas9 nuclease which introduces a single DSB. **(B)** The illustrated CRISPR/Cas9 nickase introduces two single strand breaks, which results in a DSB if the restriction occurs within a proper distance. This approach drastically increases specificity due to minimizing the amount of offset targets. (Graphic adapted and modified from* Reis, Hornblower, Robb, & Tzertzinis, 2014)

1.6.3 Multisite Gateway Cloning

The fundamental principle of the Gateway Cloning technique is based on a recombination method derived from bacteriophages. The bacteriophage λ usually makes use of this system to integrate and excise its own genome via specific recombination in a host (Karimi, Depicker, & Hilson, 2007). Transferring the mechanism into the field of molecular biology led to the establishment of a sophisticated, fast and less labor-intensive cloning method. The procedure relies on two recombination reactions.

First, so called *entry clones* (pEntry or pME (Middle entry)), flanked by attB1 (5 prime end) and attB2 (3 prime end) sites have to be available. These clones usually act as libraries, each carrying a specific element. To synthesize such plasmids, the sequence of interest is amplified by means of PCR with specific primers encoding the necessary attB sites. Furthermore, another plasmid characterized by an attP1 and an attP2 recombination site is required to serve as a donor (pDONOR). To construct an entry clone, the linear DNA fragment (flanked by attB1/attB2 sites) and a donor plasmid (harboring the attP1/attP2 sites) are mixed in presence of a BP-clonase-enzyme reagent to transfer the sequence of interest into the provided vector. Via recombination of attB1/attB2 with attP1/attP2 sites, a novel attL1/attL2 recombination site is created (Figure 5).

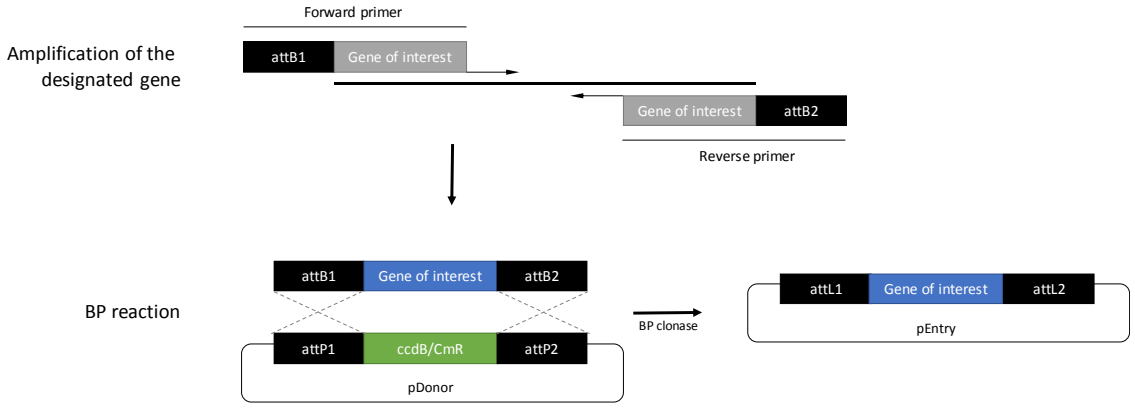

Figure 5: *Representation of the basal BP reaction used to create suitable entry vectors for more complex Gateway Cloning approaches. Within the first step, the coding sequence of a certain gene, or any nucleotide sequence of interest is amplified via PCR. A special primer pair is therefore necessary to detect the related sequence and to add the flanking recombination sites (attB1/attb2) within one reaction. The generated construct will be further used to create the final pEntry vector via recombination. This so called BP reaction bases on the availability of appropriate recombination sites at the donor plasmid (pDonor; attP1/attP2) and the PCR fragment (attB1/attB2). Moreover, recombination between attB and attP sites form the attL site, indispensable for the upcoming LR reaction. To allow selection of successfully recombined clones, a ccdB sequence in pDonor induces lethality if not excised during the BP reaction.*

The construction of the final expression vector also relies on specific recombination sites. Similar to the BP-recombination reaction, this process requires a specific donor vector, termed destination vector (pDest), bearing attR1/attR2 recombination sites.

Currently there are two widely used approaches. The first one, designed as a single clone Gateway system, is based on a destination vector which already contains a promoter sequence, followed by attR1 and attR2 sites, and optionally a fluorescence tag, stop sequence or other features. Hereby the sequence of the entry vector is cloned immediately after the promoter of pDest (Karimi et al., 2007).

The other approach, the Multisite gateway cloning technique gives more freedom to develop complex constructs (Figure 6). This system recombines three specific entry clones and a destination vector, which only carries an attL1 and attL2 site. The used entry plasmids are characterized by different attL or attR sites, which define their final position in the expression vector. According to the principles of gene expression, the first element usually carries a promoter sequence (5 prime element; p5E), the middle clone the gene of interest (middle element; pMe) and the last element the sequence of a tag or a stop codon (3 prime element; p3E). To generate the final expression plasmid, three suitable entry clones are mixed with the destination vector and the LR-clonase-enzyme reagent.

In the present study, the TOL2Kit Multisite gateway cloning method was applied to create two different sets of expression plasmids (Kwan et al., 2007b; Urasaki, Morvan, & Kawakami, 2006).

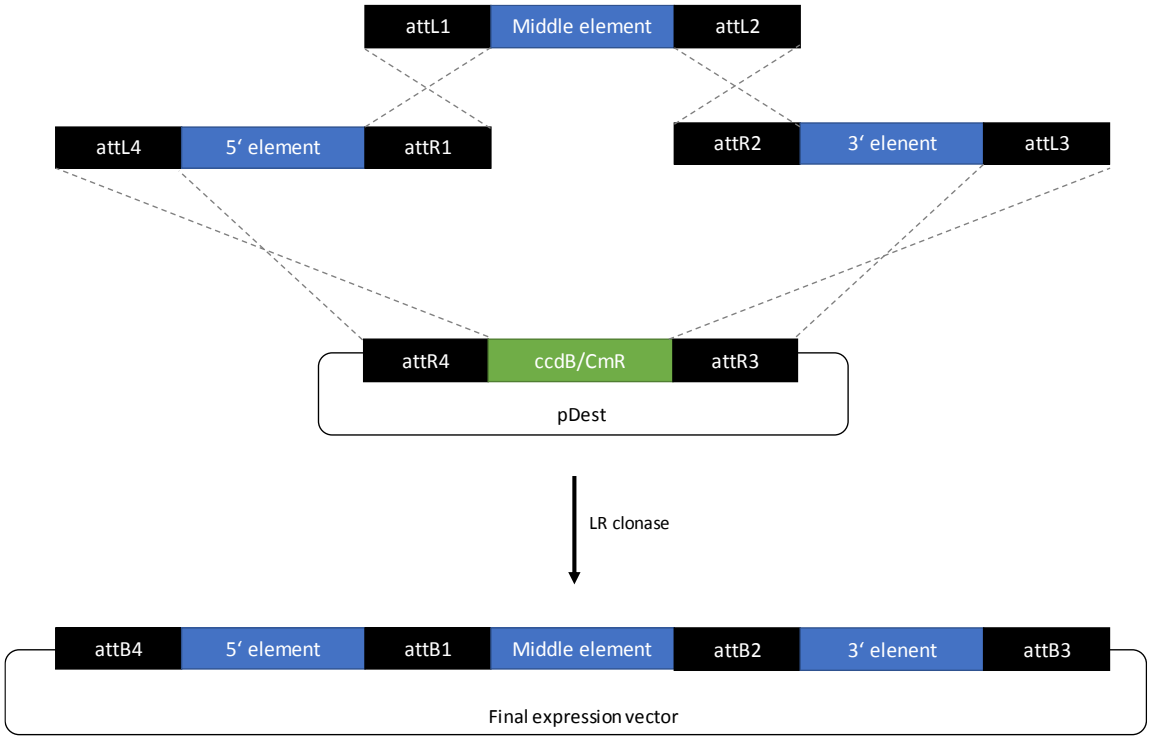

Figure 6: *Schematic overview of the LR reaction. Within the illustrated recombination reaction, functional expression vectors are generated. Prerequisite for the approach is the availability of several entry clones, defined by their specific recombination sites. These short sequences define their position in the definite vector and form the basis of the whole method. According to the principles of gene expression, the 5’ element usually carries a promoter sequence, the middle element contains the gene of interest and the 3’ element can be used to add an additional tag. Similar to the BP reaction, also the LR recombination reaction bases on a plasmid (pDest) which provides the final backbone and carries a ccdB sequence for further selection purposes. Besides, recombination between attL and attR sites creates attB recombination sequences. (Picture adapted from* Kwan et al., 2007b)

1.7. Studying different aspects of LETM1 and LETM2 *in vivo* and *in vitro*

The primary goal of the study was to investigate several aspects of Letm1 and Letm2 in a novel model system, the zebrafish. Moreover, additional experiments were conducted in human tissue samples to expand, or link the available data beyond species.

First steps were dedicated to analyze the evolutionary track of Letm1 and Letm2. Hence protein sequences of different species were aligned and a phylogenetic tree was calculated. These studies should further reveal conserved domains of Letm1 and Letm2 throughout the investigated kingdoms.

Based on the gathered insights, *in situ* hybridizations (ISH) in zebrafish larvae and adult brain samples were carried out to determine the *letm1* and *letm2* mRNA distribution within the chosen model system. Subsequent quantification of the gene expression in larvae and several adult organs was conducted to eventually spot tissues with a significantly different *letm1* and/or *letm2* expression pattern.

To investigate the role of both investigated proteins *in vivo,* respective haploinsufficient knock-out strains were established, using the TALEN or CRISPR/Cas9 technology.

Previous studies described an altered locomotor behavior in *letm1* deficient model systems. Hence, we assessed the activity levels of the generated *letm1*$^{+/-}$ fish line to investigate potential abnormalities in the mutant specimens. Additional treatment with PTZ and nigericin should reveal their harmful of beneficial effect on the animal's locomotor behavior.

To conduct localization studies, Multisite Gateway cloning was utilized to establish two sets of expression vectors, carrying the zebrafish *letm1* or *letm2* sequence. One subset was injected into zebrafish embryos and the other one was transfected into HeLa cells. The latter approach should reveal the conservation and approximate localization of the fish Letm1 and Letm2 in a human cell line.

2. Material and Methods

2.1. Animal handling

2.1.1 Husbandry

All animal procedures were conducted according to Austrian and European guidelines for animal research. Zebrafish (*Danio rerio*) strains AB and pSCA69 were kept in a constant circulating system at 28 °C on a 16 h light/8 h dark cycle.

2.1.2 Breeding and nutrition

Suitable breeding pairs (1:1 male/female ratio) were transferred to separate breeding tanks in the evening. The day after, fertilized eggs were collected, rinsed with fresh fish water and transferred to petri dishes containing E3 medium (Section 2.9). After hatching at around 2-3 days post fertilization (dpf), the medium was replaced by fresh one. At an age of around 8 dpf, the animals were transferred to bigger tanks, connected to a circulating water flow and routinely feeding with paramecia was carried out. When the larvae reached an appropriate size (approx. 2-3 weeks post fertilization) artemia and flakes were additionally offered. Adult fish (approx. 3 month post fertilization) were transferred to the main tank system and genotyping, as described in section 2.1.4, was conducted if necessary.

2.1.3 Microinjections

Before starting the main procedure several arrangements had to be met in advance:

- Injection molds: To increase the injection efficiency and to prevent damaging the fish embryos a stable scaffold is required. Therefore, 50 mL of a 1.5% agarose solution in E3 medium was prepared, poured into a 10 cm petri dish and cooled down to approximately 60 °C. Afterwards, a plastic scaffold for microinjection molds was put on top of the gel until complete polymerization. Finally, the scaffold was carefully removed and the plate was ready to use.
- Injection needle: By means of a micropipette puller (Flaming/Brown Micropipette Puller; Model P-97), 0.87x1.00x1000 mm glass capillaries (Science Products GmbH; GB100TF-10) were pulled into two needles (Heat: 490; Pull:120; Vel:100; Time: 150) and the tips were carefully opened with forceps.

- Zebrafish embryos: Similar to the breeding procedure, adult fish were transferred to breeding tanks the evening prior injection (1:1 male/female ratio). Via adding a shutter between the male and female fish premature fertilization was prevented.
- Injection solution: It is highly recommended to prepare the injection solution at least one day before the injection. For evaluation purposes, 0.3% TRITC-dextran (Sigma Aldrich; #D1819) can be added to the mixture to visualize the distribution of the injected material the day after.

The microinjection procedure started with removal of the fish divider in the morning. While giving the animals enough time for mating, the injection system[1] was assembled and an automatic calibration was performed. The constant pressure was set to 0-5 hpa and the injection pressure was set to 100-160 hpa. A former prepared needle was loaded with 3 µL of the injection solution and further mounted into the corresponding holder. Fertilized eggs were immediately collected, rinsed with fresh fish water and transferred to a petri dish containing E3 medium. Depending on the amount of gathered eggs, approximately 80% were further transferred into the injection molds and arranged as shown in Figure 7. The residual eggs served as a control to monitor the basal viability of the clutch. Immediately before starting the injections, it was crucial to ensure that the embryos were not developed past the 2nd cell stage. The injection material was further applied into the yolk sac and after completion of the whole plate the specimens were gently rinsed with E3 medium into a fresh petri dish. Injected fish embryos were raised until adulthood receiving the same environmental and nursing conditions as untreated samples.

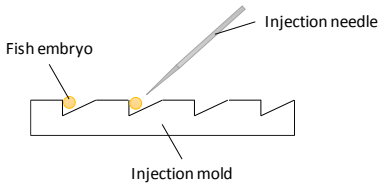

***Figure 7**: Arrangement of zebrafish embryos for micro injections. The animals were placed in pre-assembled injection molds to avoid damaging the embryos during the process and to improve the general work flow.*

2.1.4 Genotyping

To evaluate the efficiency of micro-injections or to determine the genotype of a recent offspring, specimens were screened at early larval stages (3-7 dpf). Approximately 24 larvae were therefore transferred into single tubes and euthanized in liquid nitrogen.

[1] Microinjection system: Stereo Microscope (Stemi 2000) with light source (CL 1500 ECO); Micro Maninpulator (Eppendorf; Femto Jet express and InjectMan NI 2)

Adult fish on the other side were anesthetized in 4% tricaine (Section 2.9) and a short segment of the tail fin was cut with a sterile scalpel. Afterwards, treated fish were moved to separate tanks to avoid confounding.

To isolate genomic DNA, two possible approaches were available:

- Proteinase K digest: The gathered samples (larvae or fins) were transferred to single tubes containing 1 µL Proteinase K (20 mg/mL; VWR, #1.245680100), 1 µL HotStar Taq Plus polymerase buffer (10x; Quiagen, #203605) and 7 µL H2O. After incubation at 55 °C for approximately 16 h the enzyme was inactivated at 99 °C for 15 min. The samples were further diluted in water (1:20) and 1.5 µL were used for amplification via PCR.
- HotShot digest: Obtained tissue samples were transferred to single tubes, 100 µL (fins) or 50 µL (larvae) of 50 mM NaOH were added and incubation at 95 °C on a shaker rotating at 1,200 rpm for 15 minutes was carried out. Afterwards, the lysis process was stopped via addition of 1/10th volume of Tris-HCl (pH 8). The gathered lysates were directly used for PCR amplification without dilution (1 µL per reaction).

The genomic locus of interest was further amplified by means of the HotStarTaq Plus DNA polymerase approach (Section 4.2.6), followed by a restriction assay with the corresponding enzyme (Section 2.2.1). Digested samples were further analyzed by agarose gel electrophoresis (Section 2.2.2) and convincing bands were isolated (Section 2.2.3). To obtain reliable sequencing results, the purified DNA fragments were further sub-cloned into a pJET1.2 vector (Section 2.9), following the manufacturer's protocol. Generated plasmids were further transformed into XL1-Blue E. Coli cells (Section 2.2.4), 3 single colonies were cultivated in LB medium (Section 2.9) with the corresponding antibiotics (Section 2.2.4) the day after, followed by DNA isolation (Section 2.2.5) and sequencing (Section 2.2.8.)

Zebrafish tagged with a fluorescent protein (e.g. expression studies or TALEN mediated knock-in) didn't undergo the typical genotyping procedure. Based on their genotype, phenotyping by means of fluorescence microscopy was conducted at around 2 dpf.

2.1.5 Euthanasia

Zebrafish not applicable for further experiments or breeding were euthanized in liquid nitrogen.

2.2. General procedures

2.2.1 Restriction digest

For genotyping, cloning and several other applications a DNA restriction assay was indispensable. A practical amount of DNA (1 µg - 5 µg; approach dependent) was mixed with the related restriction enzyme together with the corresponding buffer and water. The following incubation was done according to the manufacturers recommendations. Some of the performed cloning procedures implied the usage of multiple restrictions within one template. Such constructs were designed in a way to use enzymes with similar activity conditions to conduct the assay in one reaction.

2.2.2 Agarose gel electrophoresis

Depending on purpose and expected size of the samples a proper gel density was chosen (<500 kb: 3%, 500 bp-1 kb: 2%, 1 kb-1.5 kb: 1.5%, >1.5 kb: 1%). The correct amounts of agar and TAE buffer (Section 2.9) were mixed and boiled in a microwave until the solution appeared clear. A nucleotide gel staining solution (10,000x; Invitrogen SYBR Safe DNA Gel Stain, #S33102) was added and a gel tray with suitable combs was assembled. Furthermore, the liquid agarose gel solution was poured into the prepared container. After complete polymerization, the gel was transferred to a designated running chamber, the combs were removed, followed by loading of the samples and application of proper voltage for an approach dependent period.

DNA samples were mixed with a DNA loading dye (Section 2.9) and respective RNA samples with formaldehyde containing loading dye (Ambion; Formaldehyde Load Dye). Besides, a reference ladder (NEB, #N3200) was used within each experiment. After completion, the gel was imaged and bands were excised if desired.

2.2.3 Agarose gel extraction

Correct sized bands were excised from an agarose gel and transferred to 2 mL tubes. DNA isolation was carried out according to the manufacturer's protocol (Section 2.9).

2.2.4 Bacterial transformation and Inoculation

To amplify plasmids, transformation into XL1-Blue E. Coli cells (Agilent Technologies; #200268) or NEB 5-alpha Competent E. coli cells (NEB, #C2987) was carried out as described in Table 1.

***Table 1**: Instructions for bacterial transformation*

Protocol: Bacterial transformation
• Thaw aliquot with bacteria (50 µL) on ice for 5 min. • Apply 2 µL – 5 µL of your sample and gently flick the tube • Incubation (on ice; 30 min.) • Heat shock (42°C; exactly 30 sec.) • Add 250 µL SOC medium (2.9) • Incubation (shake with 300 rpm; 37 °C; 1 h) • [Optional] Mix 40 µL X-Gal (20 mg/mL) with 40 µL IPTG (0.1 M) and distribute over the agar plate • Depending on the expected transformation efficiency, distribute 100 µL - 300 µL of the transformation mix on agar plates, containing the plasmid-specific antibiotic • Incubation (37 °C;~16 h)

The day after, a number of colonies were picked and grown in 3 mL LB medium, containing the appropriate antibiotics (Ampicillin: 100 µg/ml, Kanamycin: 50 µg/mL) at 37°C overnight. For higher yield or endotoxin free DNA isolation, the cultures were increased to 250 mL LB medium. Besides, agar plates containing the respective antibiotics, LB and SOC media were kindly prepared and provided by the lab technicians.

2.2.5 DNA Isolation

Low scale DNA isolation (Table 2) was carried out for almost all conducted experiments if not otherwise stated. For that purpose 3 mL of a bacterial culture were sufficient.

***Table 2**: Instructions for low scale DNA isolation*

Protocol: Low Scale DNA isolation
• Transfer 2 mL culture to a 2 mL tube • Centrifuge (max speed; 1 min.) and carefully discard the supernatant • Add 200 µL of chilled P1 buffer (Section 2.9) and resuspend the pellet • Add 200 µL of buffer P2 (Section 2.9) and invert the tube(s) several times • Add 200 µL of chilled P3 buffer (Section 2.9) and invert the tube(s) several times • Centrifuge (max speed; 10 min) • Carefully transfer the supernatant to a fresh tube • Add 450 µL Isopropanol and mix well • Centrifuge (max speed; 10 min) and carefully discard the supernatant • Add 1 mL Ethanol (70%) • Centrifuge (max speed; 5 min) and carefully discard the supernatant • Air-dry the pellet for approximately 2 min. • Resuspend the pellet in 30 µL - 50 µL H_2O

To ensure embryonic viability an endotoxin free DNA preparation was indispensable. Hence, the *EndoFree Plasmid Maxi Kit* (Section 2.9) was utilized prior microinjection into zebrafish embryos.

2.2.6 RNA isolation and cDNA synthesis

Various conducted techniques (e.g. *In situ* hybridization or qPCR analysis) relied on the availability of a cDNA library, derived from larval or adult zebrafish tissues.

Larvae were euthanized in 15% ice cold tricaine, followed by decapitation as illustrated in Figure 8. Three heads and tails were independently pooled and immediately snap frozen in liquid nitrogen.

Similar to the larval sampling, adult zebrafish were anesthetized in 30% ice cold tricaine. The unconscious fish were further transferred to a former prepared 10 cm petri-dish, covered by a 1 cm thick agarose gel to fixate the specimen. Subsequently, the spinal cord was cut to ensure pain freedom and death, respectively. By means of fine hypodermic needles (Henry Schein U.K. Holdings Ltd.; 27G x ¾'') the fish was fixated and isolation of eyes, brain, liver, heart, swim-bladder and gonads as described by Gupta & Mullins (2010) was conducted. The gathered organs were immediately snap frozen in liquid nitrogen to preserve the RNA integrity. Afterwards, 3 organs were pooled to one biological replicate and stored at -80 °C.

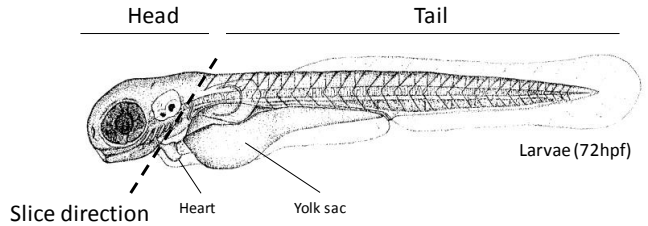

Figure 8: *Schematic overview of the larval sample definition for RNA isolation and further processes. Specimens at an age of 3 or 7 dpf were euthanized and decapitated with a sterile scalpel. It was crucial to separate the head cranial of the heart to get a clean sample distribution. (Picture adapted and modified from* Kimmel, Ballard, Kimmel, Ullmann, & Schilling, 1995)

The collected tissue samples were further prepared for cDNA synthesis. During the whole process it was crucial that the RNA samples were kept under ice cold conditions to prevent RNA degradation. First, the tissues were homogenized by means of the Qiagen TissueLyser II (Qiagen, #85300). Therefore, a sterile steel bead (Ø2.8 mm; Peqlab, #91-PCS-MK28), 350 µL of RLT buffer (Provided by the Quiagen RNeasy Mini Kit; Section 2.9) and 3.5 µL β-Mercapto-Ethanol were added to each sample, followed by homogenization (30x/sec; 30 sec.). The gathered homogenates were immediately transferred to -80 °C or further utilized for RNA isolation (Section 2.9). To increase the efficiency, only 6 samples were processed at the same time. Afterwards, the concentration of the isolates was determined and 2 µL were loaded on an Agraose gel to quick-evaluate the RNA integrity.

Finally, cDNA synthesis was carried out according to the manufacturer's protocol (Section 2.9) and stored at -20 °C for further applications.

RNA isolates of HEK-293 cells were kindly prepared by Shane Austin. The gather samples were further processed and cDNA synthesis was carried out by means of the High-Capacity cDNA Reverse Transcription Kit (Section 2.9).

2.2.7 PCR Protocols and primer

DNA amplification was indispensable for most of the conducted approaches. Depending on the desired accuracy and amplification speed, one of three available PCR protocols was applied (Table 3). Respective primer sequences are listed in the *Supplemental Materials* section (5.1).

Table 3: *Compilation of the utilized protocols for the conducted PCR approaches*

Protocol: DNA amplification protocols

FIREPol DNA Polymerase (Solis Biodyne; #01-01-00500)	
Reagents	Volume / Reaction
Reaction buffer (10x)	2.5 µL
$MgCl_2$ (25 mM)	3.0 µL
dNTP's (10 mM)	1.0 µL
Forward primer (5 µM)	1.0 µL
Reverse primer (5 µM)	1.0 µL
FIREPol polymerase (2.5 U/µL)	0.5 µL
H_2O	x µL
Template (5-100 ng/µL)	x µL
Total volume	25 µL

HotStarTaq Plus DNA Polymerase (Quiagen; #203203)	
Reagents	Volume / Reaction
Coral load (10x; 15 mM $MgCl_2$)	2.5 µL
$MgCl_2$ (25 mM)	1.5 µL
dNTP's (10 mM)	1.0 µL
Forward primer (5 µM)	1.5 µL
Reverse primer (5 µM)	1.5 µL
HotStarTaq Plus (0.7 U/µL)	0.14 µL
H_2O	x µL
Template (5-100 ng/µL)	x µL
Total volume	25 µL

Phusion HF DNA Polymerase (NEB; #M0530S)	
Reagents	Volume / Reaction
HF buffer (5x; 7,5 mM $MgCl_2$)	5.0 µL
$MgCl_2$ (25 mM)	1.5 µL
dNTP's (10 mM)	1.0 µL
Forward primer (5 µM)	1.5 µL
Reverse primer (5 µM)	1.5 µL
Phusion polymerase (0.5 U/µL)	0.25 µL
H_2O	x µL
Template (5-100 ng/µL)	x µL
Total volume	25 µL

Thermocycler setup

	Hotstart	Denaturation	Annealing	Elongation	Final elongation	Store
Temperature	95 °C	95 °C	Primer dependent[1]	72 °C	72 °C	4 °C
Time	5 min.	30 sec.	30 sec.	Size dependent[2]	10 min.	∞
		Cycles: 30x-40x				

[1]The annealing temperature depends on the selected primer pair. Section 5.1 illustrates a compilation of all primers used for the present study, including annealing temperature.

[2]The elongation time depends on the expected size of the final amplicon and elongation speed of the selected polymerase. FIREPol DNA Polymerase: 1 kb/min; HotStarTaq Plus DNA Polymerase: 2-4 kb/min; Phusion HF DNA Polymerase: 4 kb/min

2.2.8 Sequencing

An aliquot of the isolated DNA sample was diluted to a final concentration of 85±5 ng/µL in a total volume of 15 µL and sent to Microsynth for sequencing purposes. Most of the screening primers were available at the screening facility. Hence, 3 µL of specific sequencing primer (10 µM) were only supplied if necessary.

2.3. Genetic modifications

2.3.1 Gateway Cloning

To conduct localization and gene expression studies *in vivo* and *in vitro*, several expression vectors were constructed by means of a Multisite Gateway cloning approach (Table 4; Kwan et al., 2007a).

Table 4: *Overview of the constructed expression clones by Multisite Gateway Cloning. The figure illustrates the principal arrangement of the utilized entry clones and pDestTol2pA2 was used as a backbone for all plasmids.*

Overview: Constructed expression clones via Multisite Gateway Cloning

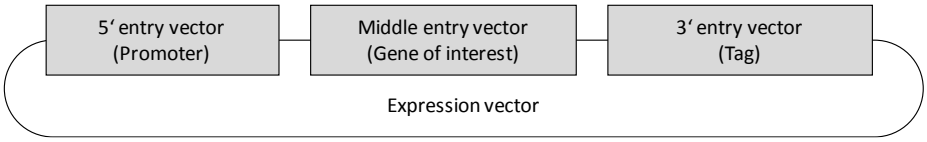

	Backbone: pDestTol2pA2		
	5’ entry vector	**Middle entry vector**	**3’ entry vector**
#1	p5E-CMV/SP6	pMe-Letm1_CDS	p3E-EGFPpA
#2	p5E-CMV/SP6	pMe-Letm1_CDS	p3E-mCherrypA
#3	p5E-CMV/SP6	pMe-Letm1_CDS	p3E-polyA
#4	p5E-CMV/SP6	pMe-Letm1_CDS_6xHis	p3E-polyA
#5	p5E-CMV/SP6	pMe-Letm2_CDS	p3E-EGFPpA
#6	p5E-CMV/SP6	pMe-Letm2_CDS	p3E-mCherrypA
#7	p5E-CMV/SP6	pMe-Letm2_CDS	p3E-MTpA
#8	p5E-CMV/SP6	pMe-Letm2_CDS	p3E-polyA
#9	p5E-h2afx	pMe-Letm1_CDS	p3E-EGFPpA
#10	p5E-h2afx	pMe-Letm1_CDS	p3E-mCherrypA
#11	p5E-h2afx	pMe-Letm1_CDS	p3E-polyA
#12	p5E-h2afx	pMe-Letm1_CDS_6xHis	p3E-polyA
#13	p5E-h2afx	pMe-Letm2_CDS	p3E-mCherrypA
#14	p5E-h2afx	pMe-Letm2_CDS	p3E-MTpA
#15	p5E-h2afx	pMe-Letm2_CDS	p3E-polyA

As already described in section 1.6.3, the utilized TOL2Kit cloning approach is a constitutive technique. Entry vectors with appropriate recombination sites must be available to synthesize an expression clone. The conventional entry clones were ordered from the TOL2Kit developer if they were not already available in the laboratory (Kwan et al., 2007b).

Entry clones with the CDS of letm1 (Accession number: NM_001045208), letm1 including a histidin tag and letm2 (Accession number: ENSDART00000131819), were ad hoc synthesized (Figure 9). The respective sequences were amplified using the former prepared cDNA library as a template (Section 2.2.6). The emerging amplicons were designed in a way to exclude the stop

codon and to extend the CDS with the specific recombination sites (Figure 9). Besides, the utilized primer pairs are listed in section 5.1.

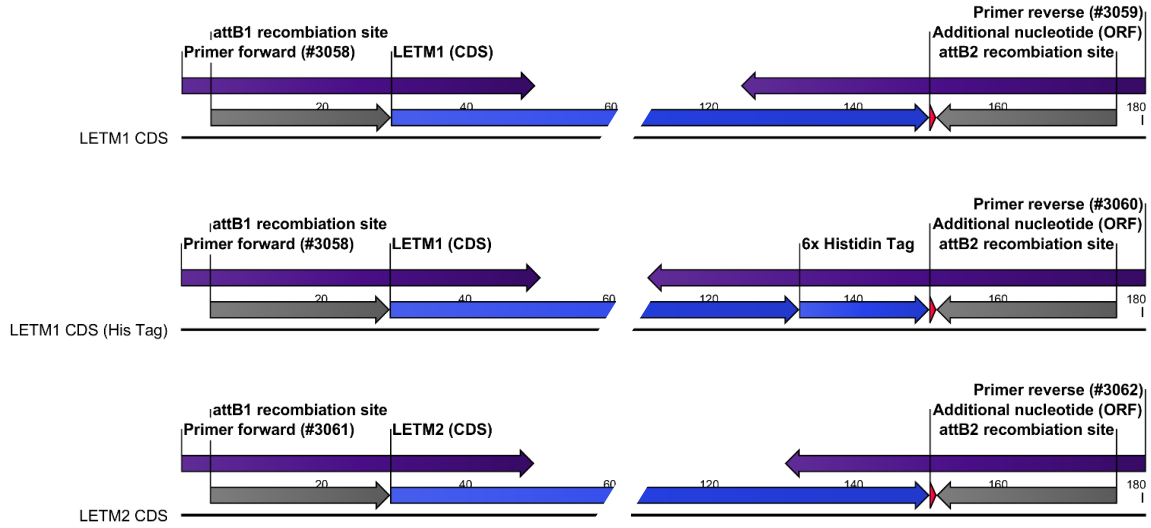

Figure 9: *Representation of the designed entry vectors, carrying the CDS of letm1 or letm2. Both genes were amplified using the stated primer which also flanked the sequences with respective attB recombination sites. All of the utilized reverse primer were designed in a way to replace the terminal 3 nucleotides of the respective CDS with a thymine. This crucial step removed the stop codon and ensured an unchanged reading frame to provide expression of a fused fluorescence protein. Moreover, to generate a certain tagged letm1 clone, an elongated reverse primer was utilized to insert a six times histidine sequence.*

The PCR amplified samples were loaded on a 1.5% Agarose gel, correct sized bands were excised followed by purification. The necessary amounts of these attB-PCR products were calculated and the BP reaction was carried out (Table 5). After incubation of approximately 16 h at room temperature, the reaction was stopped via addition of 4 µg Proteinase K and another incubation step at 37 °C for 10 minutes was conducted. The constructed entry clones were further transformed into XL1-Blue E. Coli cells, grown on Kanamycin-agar-plates, colonies were picked and inoculated, followed by DNA isolation and sequencing.

The upcoming procedure was designed to synthesize the final expression clones. Hence the LR recombination reactions were carried out (Table 5). Similar to the BP reaction, also this process was terminated by Proteinase K treatment after 16 h incubation at room temperature. Constructed clones were transformed into NEB 5α Competent E. coli cells, grown on ampicillin agar plates and further handled as already described.

Table 5: *Instructions for the BP and LR recombination reaction. To calculate the necessary amounts of plasmids or linear DNA products, the stated equation was applied before each reaction (Adapted from the Gateway Cloning Manual). Moreover, the compilation of utilized DNA's shows their required amount per reaction according to their sequence length.*

Protocol: Multisite Gateway Cloning, the BP and LR recombination reaction

BP Reaction	
attB-PCR clone (100 fmol)	x µL
pDONOR221 (100 fmol)	x µL
BP-Clonase Mix II (Section 2.9)	2 µL
H_2O	x µL
Total volume	10µL
Incubation at room temperature overnight	

LR Reaction	
Destination clone (33 fmol)	
5' entry clone (33 fmol)	x µL
Middle entry clone (33 fmol)	x µL
3' entry clone (33 fmol)	x µL
LR-Clonase Mix II (Section 2.9)	2 µL
H_2O	x µL
Total volume	10µL
Incubation at room temperature overnight	

Equation to calculate the amount of necessary plasmids

$$\frac{100\ fmol\ x\ plasmid\ or\ PCR\ product\ size\ [bp] x\ 660\ fg\ x\ ng}{10^6\ fg\ x\ fmol}$$

Necessary amount and length of attB-PCR products

	Length	Amount
attB1-LETM1-attB2	2,300 bp	152 ng
attB1-LETM1-His-attB2	2,318 bp	99 ng
attB1-LETM2-attb2	1,500 bp	153 ng

Necessary amount and length of entry clones

	Length	Amount
pDestTol2pA2	5,883 bp	128 ng
p5e-H2AFX	3,604 bp	78 ng
p5e-CMV/SP6	3,704 bp	80 ng
pMe-LETM1	4,816 bp	317 ng
pMe-LETM1_His	4,834 bp	317 ng
pMe-LETM2	3,987 bp	319 ng
pMe-mCherry	3,261 bp	71 ng
p3e-mCherrypA	3,586 bp	78 ng
p3e-eGFPpA	3,634 bp	79 ng
p3e-polyA	2,838 bp	61 ng
p3e-MTpA	3,151 bp	68 ng

Expression clones intended for micro injection into zebrafish embryos were additionally grown in 250 mL LB medium and purified by means of an endotoxin free, high scale DNA isolation procedure to remove life threatening bacterial endotoxins (Section 2.2.5). This treatment was not necessary if the clones were utilized for transfections *in vitro*.

To establish a stable integration into the zebrafish genome, *in vitro* transcription (IVT) of a transposase was necessary. For that purpose, the pCS2FA-transposase (Kwan et al., 2007b) clone was linearized by means of NotI (NEB; #R0189), purified via agarose gel extraction and further *in*

vitro transcribed by the *mMessage mMachine SP6 transcription kit* (Section 2.9). Agarose gel electrophoresis was further performed to validate the mRNA integrity.

2.3.2 Generation of zebrafish, overexpressing *letm1* or *letm2*

Expression vectors containing the h2afx promoter (Construction at section 2.3.1) were co-injected with the previously generated transposase mRNA into zebrafish eggs (Concentration of all injected components: 20 ng/µL each). Evaluation of the integration efficiency was further determined by common fluorescence microscopy. Positive specimens were further raised until 5 dpf, anesthetized in 1% tricaine, embedded in 3% Methylcellulose and investigated via confocal imaging (Zeiss LSM 700). Post imaging, the larvae were rinsed with fresh E3 medium, transferred to their aquarium and raised until adulthood.

2.3.3 TALEN induced knock-out

To predict suitable targeting sequences and to circumvent large numbers of offset targets, different exons of the *letm1* and *letm2* gene were screened by means of the TAL Effector Nucleotide Targeter 2.0 (Cermak et al., 2011; Doyle et al., 2012) using the parameters shown in Table 6.

Table 6: *Utilized parameters to predict suitable TALEN targeting sites for the letm1 and letm2 gene, using the TAL Effector Nucleotide Targeter 2.0*

Applied parameters to predict suitable TALEN target sites	
Mode	Provide custom Spacer/RVD Lenghts
Spacer width	Minimum: 15 bp; Maximum: 16 bp
RVD length	Minimum: 15 bp; Maximum: 20 bp
G-Substitute	NN
Filter Options	Hide redundant TALENs
Streubel et al. guidelines	Off
Pre-loaded Sequence	Danio rerio (genome)
Upstream base	(T)hymine

The optimal TALEN pair was selected upon fulfilling following criteria:

- Minimal offset targets
- Presence of a unique restriction site in the spacer region

- TALEN pairs with a high composition of the HD RVD and/or a low composition of NN RVD's show higher binding affinities, which makes them more preferable

For *letm1* as well as for *letm2*, two individual TALEN pairs were selected and constructed (Table 7). Besides sticking to the given criteria, the protein structure was also accounted. Hence, it was crucial that the TALEN pairs bind upstream of the transmembrane domain to prevent insertion into the inner mitochondrial membrane, in case of a successful mutation. Furthermore, TALEN pairs binding in the 5 prime untranslated region were also excluded.

***Table 7**: Compliation of the constructed TALEN pairs; Primer numbers refer to the respective table in section 5.1*

Overview of the constructed TALEN pairs	
Letm1-Exon1	
Nucleotide sequence of the left TALEN array	5'-GGCATCGATTTTGCTCACC-3'
Nucleotide sequence of the right TALEN array	5'-GACCTGGATGTTTTCAACAA-3'
Restriction enzyme for screening purposes	PleI (NEB; #R0515)
Screening primer (Forward/Reverse)	#2489 / #2864
Letm1-Exon3	
Nucleotide sequence of the left TALEN array	5'-GGATCGACACGACCATCGCT-3'
Nucleotide sequence of the right TALEN array	5'-GTGTCCATTCAACACCCT-3'
Restriction enzyme for screening purposes	FokI (NEB; #R0109)
Screening primer (Forward/Reverse)	#2796 / #2797
Letm2-Exon2	
Nucleotide sequence of the left TALEN array	5'-TTTCCATCACAAAATGGCA-3'
Nucleotide sequence of the right TALEN array	5'- CTTGTTACCGCAAGAAGCAC-3'
Restriction enzyme for screening purposes	AluI (NEB; #R0137)
Screening primer (Forward/Reverse)	#2413 / #2414
Letm2-Exon3	
Nucleotide sequence of the left TALEN array	5'-GCCACTCAACCACCGCCAGC-3'
Nucleotide sequence of the right TALEN array	5'-TCTGTCCCAGGGACTTCCTT-3'
Restriction enzyme for screening purposes	BpmI (NEB; #R0565)
Screening primer (Forward/Reverse)	#2798 / #2799

The construction of the TALEN pairs occurred in two consecutive steps as described by Cermak et al. (2011). Step one addressed the assembly of intermediary arrays consisting of 6-10 RVD's into pFUS backbone vectors. Hence, a single Digestion-Ligation-Reaction (Table 6) followed by subsequent transformation into XL1-Blue E-Coli cells was performed. To increase the screening efficiency for positive colonies, a mixture of 40 µL X-Gal (20 mg/mL) and 40 µL IPTG (0.1 M) was equally distributed over Spectinomycin-agar plates, 20 minutes before streaking the transformed bacteria. The day after, 6 colonies were picked and a colony PCR was conducted (Protocol at section 2.2.7; FirePol polymerase; Primer #1821/#1822). The synthesized PCR amplicons were evaluated by Agarose-gel-electrophoresis and convincing cultures were incubated in LB-spectinomycin medium overnight. DNA isolation followed by sequencing to ensure the correct arrangement of the RVD's was performed (Sequencing primer: #1821/#1822) the day after.

Table 8: *Protocol for the first TALEN Digestion-Ligation reaction*

Protocol: First TALEN ligation cycle

- Setup the Digestion-Ligation mix (Total volume/reaction: 20 µL)

Components	Volume / reaction
pFUS-A or pFUS-B[1] (150 ng/µL)	1 µL
Each RVD (150 ng/µL/RVD)	1 µL/RVD
BsaI (NEB; #R0535)	1 µL
BSA (2 mg/mL)	1 µL
Quick Ligase (NEB; #M0202)	1 µL
Ligase buffer (10x, NEB; B0202S)	2 µL
H_2O	x µL

[1]pFUS-A is used for the first array (RVD 1-10), pFUS-B for the second array (max. 9 further RVD's)

- Incubate the reaction in a PCR machine following the stated program

	Temperature	Time
10x	37°C	5 min.
	16°C	10 min.
	37°C	15 min.
	50°C	5 min.
	80°C	5 min.
	4°C	∞

- Degradation of reaction based DNA fragments via nuclease treatment

Components	Volume / reaction
Plasmid Safe Nuclease (Epicentre; #E3105K)	1 µL
ATP (25 mM; Epicentre; #E3105K)	1 µL

- Incubation (37 °C, 60 min.)
- Transformation of 5 µL in XL1-Blue E. coli cells (or store at 4 °C)

The second step was designated to join the respective arrays into the TALEN backbone vector (pCS2TAL3-DD or pCS2TAL3-RR) to form the final construct. Thus, another Digestion-Ligation-Reaction, followed by the same procedure as already described in step one was carried out (Table 9). Besides, primer pair #1823/#1824 was utilized for the associated colony PCR and sequencing purposes.

***Table 9**: Protocol for the second (final) TALEN Digestion-Ligation reaction*

Protocol: Second TALEN ligation cycle

- Setup the Digestion-Ligation mix (Total volume/reaction: 20 µL)

Component	Volume / reaction
pCS2TAL3-DD or pCS2TAL3-RR[1] (150 ng/µL)	1 µL
Last RVD (150 ng/µL)	1 µL
pFUS-A with related RVD array (150 ng/µL)	1 µL
pFUS-B with related RVD array (150 ng/µL)	1 µL
Quick Ligase (NEB; #M0202)	1 µL
Ligase buffer (10x, NEB; B0202S)	2 µL
Esp3I (Thermo Scientific; #ER0452)	1 µL
H_2O	x µL

[1] pCS2TAL3-DD is used for the final left TALEN array, pCS2TAL3-RR for the final right TALEN array

- Incubate the reaction in a PCR machine following the stated program

	Temperature	Time
10x	37°C	5 min.
	16°C	10 min.
	37°C	15 min.
	50°C	5 min.
	80°C	5 min.
	4°C	∞

- Transformation of 5 µL in XL1-Blue E. coli cells (or store at 4°C)

The definite TALEN constructs were further linearized with NotI, purified by using the QUIAGEN MinElute Reaction Cleanup Kit followed by SP6 mediated IVT (Section 2.9). Agarose gel electrophoresis was further utilized to evaluate the RNA integrity.

To determine the efficiency of the former prepared TALEN mRNA's *in vivo*, 300 ng/µL/pair were microinjected into zebrafish embryos. Treated specimens were raised until 7 dpf and genotyped as already described in section 2.1.4. Functional TALEN pairs were re-injected and the resulting larvae were raised until adulthood. Adult fish were genotyped and positive animals were used for further experimental and breeding purposes.

2.3.4 TALEN mediated knock-in

Lacking a readout to distinguish between WT and mutant larvae, genotyping was directly linked to euthanasia. To circumvent the issue an iTAL based approach was developed. A primary expression vector was therefore generated by means of the Multisite Gateway Cloning technology. Hence, an h2afx promoter was fused with a mCherry CDS, followed by several stop codons (polyA tail). Simultaneously, single stranded oligo nucleotides for the iTAL *letm1* recognition sites, including 5' extensions (necessary for cloning purposes), were ordered and annealed as described in Table 10 (Respective sequences can be found in section 5.1).

Table 10: *Protocol for the oligo annealing reaction*

Protocol: Oligo annealing reaction

- Preparation of the reaction (Total volume/reaction: 14 µL)

Component	Volume / reaction
Top oligo (5 µM)	2 µL
Bottom oligo (5 µM)	2 µL
Annealing buffer (1x)	46 µL

- Incubation (95 °C, 3 min.)
- Change the temperature of the heating block to 25 °C and keep the tubes inside until the temperature is reached
- Store at -20°C

The complete h2afx-mCherry construct was digested with HindIII (NEB; #R0104), XhoI (NEB; #R0146), BglII (NEB; #R0144) and ClaI (NEB; #R0197) and further evaluated on an agarose gel (Figure 10). The two emerged fragments were excised, purified and ligated with the recently synthesized iTAL sequences, using a T4 ligase (Section 2.9). Thus, the expression vector containing the expression cassette, flanked by iTAL sites, was finalized. Post transformation into NEB-5α cells, screening for viable colonies and the endotoxin free plasmid isolation, 25 ng/µL of the construct were co-injected with the corresponding *letm1* specific TALEN mRNAs (300 ng/µL each) into zebrafish embryos. Two days later, genotyping was conducted by means of fluorescence microscopy.

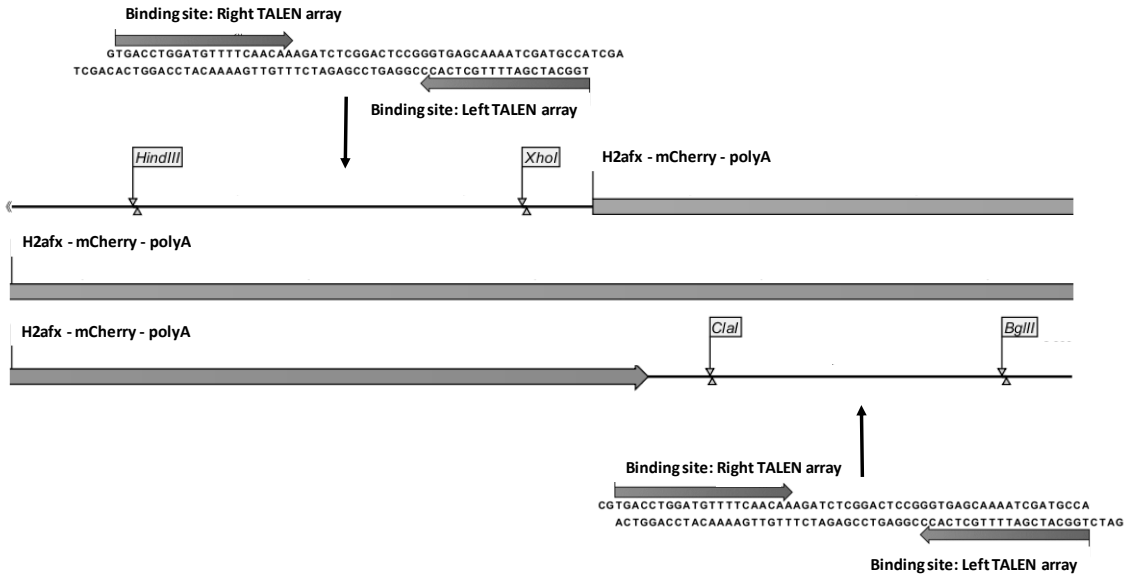

Figure 10: *Schematic illustration of the cloning procedure to generate an expression vector, suitable for an iTAL mediated gene insertion. After synthesis of the expression cassette (H2afx-mCherry-polyA), the annealed nucleotide arrays with the appropiate iTAL seqeunces and respective sticky ends were cloned into the backbone. Based on the elaborated cloning strategy, the postion and orientation of each array was predertermined due to individual chosen restriction enzymes.*

2.3.5 CRISPR/Cas9 induced knock-out

The inefficient character of the constructed TALEN pairs against *letm2* led to the development of a CRISPR/Cas9 mediated gene knock-out approach. For this purpose three different CRISPR pairs were constructed and validated (Table 11). First trials were performed using the Cas9 nickase. However, due to very high lethality rates (>98%), we switched to the Cas9 nuclease to improve viability. Hence, construction of sgRNA pairs for the nickase was conducted in the first place. The latter approach required at least one of synthesized sgRNA's. Nevertheless, a mixture of all effectors was injected to increase the efficiency.

Table 11: *Compliation of the constructed sgRNA pairs; Primer numbers refer to the respective table in section 5.1*

Overview of the generated sgRNA pairs	
LETM2-Exon3-Locus A	
Nucleotide sequence of the left sgRNA	5'-GCGGATATGCAACCAGGG-3'
Nucleotide sequence of the right sgRNA	5'-GCTCTTGTTCGTGGCTGC-3'
Restriction enzyme for screening purposes	BmgBI (NEB; #R0628)
Screening primer pair (Forward/Reverse)	#2798 / #2799
LETM2-Exon3-Locus B	
Nucleotide sequence of the left sgRNA	5'-GTGGTTGAGTGGCAGAGG-3'
Nucleotide sequence of the right sgRNA	5'-GCACCTCCAGCGTTGCCA-3'
Restriction enzyme for screening purposes	BpmI (NEB; #R0565)
Screening primer pair (Forward/Reverse)	#2798 / #2799
LETM2-Exon4	
Nucleotide sequence of the left sgRNA	5'-GCATGAAGGGCACAAGC-3'
Nucleotide sequence of the right sgRNA	5'-TGTTATTGTTCCCTTCA-3'
Restriction enzyme for screening purposes	BaeGI (NEB; #R0708)
Screening primer pair (Forward/Reverse)	#3048 / #3049

Using the ZiFiT Targeter Version 4.2 (Hwang et al., 2013; Mali, Yang, et al., 2013) suitable targeting loci on the *letm2* gene were identified. Similar to the TALEN design, the gathered results were carefully analyzed to spot sgRNA pairs meeting following criteria:

- Minimal amount of offset targets
- Unique restriction site(s) in the spacer region
- Cas9 specific PAM sequence immediately upstream of the target site
- Ideal length of 17-18 nucleotides per sgRNA
- Proper spacer size (< 30 nucleotides).

To synthesize specific sgRNA's each targeting sequence has to be cloned in a *T7-sgRNA* vector, which already carries the tracerRNA array (Table 12). Construction started via annealing of two complementary oligo nucleotides (Table 12). The "Top oligo" contains the genomic target region and is extended by a 5'-TAGG-[Top oligo]-3' sequence, indispensable for the subsequent ligation

procedure. The complementary "Bottom oligo" is necessary to form the double stranded DNA fragment. Besides, also this short sequence was expanded by 5'-AAAC-[Bottom oligo]-3'.

The generated recognition sequence was further ligated into a supplied *T7-sgRNA* vector[2], following the protocol in Table 12. Similar to previous approaches, also this method required transformation into XL1-Blue E. Coli cells, bacterial selection (Ampicillin) and sequencing to gather the final sgRNA templates.

Table 12: *Protocol for generation of a template vector, used for sgRNA IVT. The provided illustration shows the conducted cloning strategy to fuse the DNA recognition sequence to the tracrRNA array. The figure further shows the necessary BbsI sites for the cloning procedure and the DraI restriction site to linearize the plasmid.*

Protocol: sgRNA construction

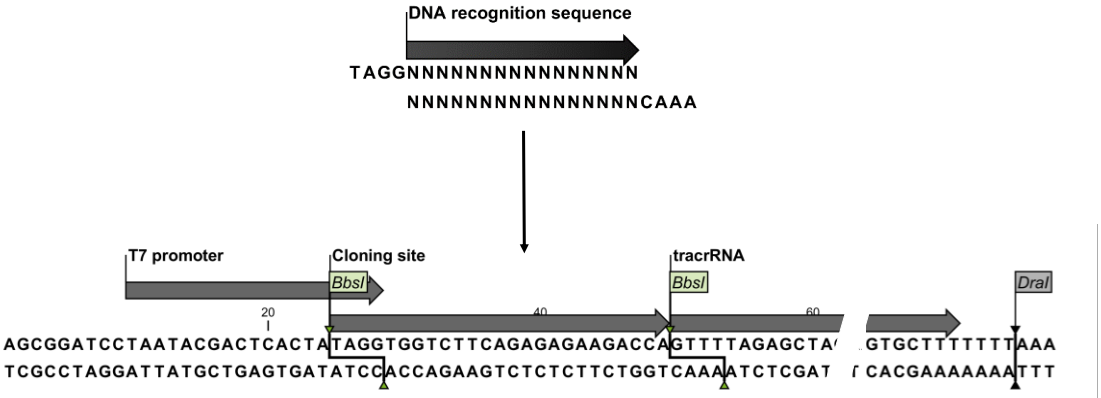

- Preparation of the oligo annealing reaction (Total volume/reaction: 50 µL)

Component	Volume / reaction
Top oligo (5 µM)	2 µL
Bottom oligo (5 µM)	2 µL
Annealing buffer (1x)	46 µL

- Incubation (95°C, 3 min.)
- Change the temperature of the heating block to 25°C and keep tubes inside until the temperature is reached
- Preparation of the Digestion-Ligation mix (Total volume/reaction: 20 µL)

[2] The Cas9 and sgRNA template vectors were kindly provided by Dr. Stephanie Bannister and Mirta Resetar, M.Sc.

Component	Volume / reaction
Annealed oligo nucleotides	2 µL
T7_sgRNA vector (75 ng/µL)	1 µL
T4 Ligase buffer (Section 2.9)	2 µL
T4 Ligase (Section 2.9)	1 µL
BSA (2 mg/mL)	2 µL
BbsI (NEB; #R0539)	1 µL
H_2O	x µL

- Incubate the reaction in a PCR machine following the stated program

	Temperature	Time
3x	37°C	10 min.
	16°C	10 min.
	37°C	10 min.
	65°C	20 min.
	4°C	∞

- Transformation of 5 µL in XL1-Blue E. coli cells (or store at 4°C)

To perform an IVT the provided Cas9 vector was linearized by NotI and the previously generated sgRNA template(s) were linearized by DraI (NEB; #R0129). Resulting DNA fragments were loaded on a 1.5% agarose gel and correct sized bands were isolated. Besides, products of the restriction assay were analyzed in comparison with respective uncut samples. While sgRNA's were further synthesized by means of the T7 Quick High Yield RNA Synthesis Kit (Section 2.9), Cas9 mRNA was amplified by the mMESSAGE mMACHINE T7 Ultra Kit including a subsequent capping and polyadenylation reaction (Section 2.9). The prepared RNA's were finally isolated and the integrity was quick-evaluated by agarose gel electrophoresis.

Similar to the TALEN, several microinjections of constructed CRISPR/Cas9 effectors were performed to evaluate functionality, efficiency and viability. Based on the obtained results, we decided to use 100 ng/µL of the Cas9 nuclease and 12 ng/µL of each sgRNA for further procedures.

2.4. In situ hybridization

2.4.1 Preparation of probes

To generate digoxigenin labeled probes for in situ hybridizations, the former established cDNA library of adult zebrafish brains was used as a template to amplify a distinct region of the *letm1* and *letm2* CDS.

The applied PCR was performed with the HotStarTaq Plus polymerase in combination with the appropriate primer pairs (Section 5.1; *letm1*: 2400/2401; *letm2*: 2402/2403). The synthesized amplicons were evaluated by agarose gel electrophoresis and convincing bands were isolated. The obtained DNA fragments were further ligated into a *pGEM-T easy* vector (Section 2.9) following the manufacturer's protocol. The synthesized plasmids were transformed into XL1-Blue E. Coli cells immediately after the ligation process. The next days, colonies were picked and cultivated in LB/Ampicillin medium, followed by DNA isolation and sequencing. The sequences were finally evaluated and one suitable construct per gene was chosen for IVT. A suitable construct was defined by none to minor PCR errors and a convincing chromatogram.

Sequencing revealed that both inserts were ligated in 5' to 3' direction into the backbone vector. To synthesize anti-sense digoxigenin labeled RNA probes, an aliquot of the isolated plasmids was linearized with SacII (NEB; #R0157). Moreover, a template for control probes (sense RNA) was digested with SacI (NEB; #R0156). Both reactions were catalyzed at 37°C for 2 h, followed by evaluation on a 1.5% agose gel and purification. Finally, the digoxigenin labeled anti-sense probes were *in vitro* transcribed by the SP6 RNA polymerase (NEB; #M0207) and sense probes by a T7 RNA polymerase (NEB; #M0251), as shown in Table 13.

Table 13: *Protocol to synthesize digoxigenin labeled probes, suitable for ISH*

Protocol: Synthesis of digoxigenin labelled ISH probes

- Preparation of the reaction (Total volume/reaction: 20 µL)

Component	Volume / reaction
10 µg linearized DNA	x µL
NTP-Dig labelling mixture (Roche; #11277073910)	2 µL
Reaction Buffer (10x: NEB; #B9012)	2 µL
RNA polymerase	1 µL
DTT (100 mM; Sigma Aldrich; #D0632)	4.5 µL
RNase Inhibitor (40 U/µL; Thermo Scientific; #EO0381)	0.5 µL
H_2O	x µL

- Incubation (37°C, ≥2 h)
- Add 1 µL of DNase
- Incubation (37°C, 15 min.)
- RNA purification

The integrity of synthesized RNA's was further evaluated on a 1.5% agarose gel, convincing samples were diluted to 500 ng/µL in Hyb+ buffer (Section 2.9) and stored at -20°C.

2.4.2 Whole mount in situ hybridization

WT AB larvae were raised until 3 or 7 dpf and thereafter euthanized in 15% ice cold tricaine. To inhibit pigmentation, 0.003% of 1-phenyl-2-thiourea was added at 1 dpf. The samples were further fixated in 4% PFA (Section 2.9) for at least 4 h at room temperature or overnight at 4°C. Afterwards, the samples were washed twice in PTW (Section 2.9) for 5 min. each, followed by incubation in 100% Methanol for 5 min. Finally, the methanol was replaced by a fresh aliquot and the samples were stored at -20°C for at least 24 h until ISH was conducted (Table 14).

Table 14: *Instruction for whole mount ISH*

Protocol: Whole mount in situ hybridization

- The used solutions and buffers are listed in section 2.9
- If not mentioned, the procedures were conducted on room temperature

Day 1

- Replace methanol by 75% methanol and incubate for 5 min.
- Replace methanol by 50% methanol and incubate for 5 min.
- Replace methanol by 25% methanol and incubate 5 min.
- Replace methanol by PTW and incubate for 5 min.
- Repeat the last step
- Digest embryos with proteinase K (10 µg/mL)
  - Larvae (3 dpf) for exactly 15 min.
  - Larvae (7 dpf) for exactly 25 min.
- Rinse twice with glycine (2 mg/mL) for 2 min. each
- Post fixate the samples in 4% PFA on a shaker for 30 min.
- Wash three times with PTW for 5 min. each

- Replace PTW with Hyb+ solution and incubate at 65°C for at least 2 h
- Replace Hyp+ with your probe (2 ng/µL in 200 µL), diluted in Hyp+ solution and incubate at 65°C overnight

Day 2

- Wash 2 times with 50% Formamide / 2x SSCT at 65°C for 30 min.
- Wash 3 times with 25% Formamide / 2x SSCT at 65°C for 10 min.
- Wash with 2x SSCT at 65°C for 5 min.
- Wash 2 times with 0.2x SSCT at 65°C for 30 min.
- Replace solution with 50% MABT / 50% SSCT (1x) and incubate for 5 min.
- Replace solution with MABT and incubate for 5 min.
- Block your samples in 2% DIG block for 2 h
- Incubate in *anti-DIG-AP* antibody solution (1:3,000 dilution in 2% DIG block) at 4°C overnight

Day 3

- Wash throughout the whole day with MABT at 4°C (at least 5x)
- Transfer your samples to a 6 well plate with MABT and further incubate at 4°C overnight

Day 4

- Replace MABT with BM-Purple to induce the staining reaction and keep your samples in a dark environment
- Constantly, evaluate the staining progress and stop the reaction if necessary

- Wash 2x with PTW for 5 min.
- Re-fixate in 4% PFA for 30 min.
- Wash 2x with PTW for 5 min.
- Incubate in 70% glycerol / H_2O
- Store at 4°C in a dark environment

The stained samples were finally mounted on object slides and imaged by microscopy (Zeiss Axioplan 2).

2.4.3 Brain sections

Brains of adult wild type zebrafish (AB strain) were carefully isolated and immediately transferred to vials containing 4% ice cold PFA (Section 2.9) followed by incubation at 4°C for 24 h. Afterwards, the specimens were washed 5 times in PTW (Section 2.9) for 5 min. each and were further dehydrated in 100% methanol. The brains were stored at -20°C for at least 24 h until ISH was conducted (Table 15).

Table 15: *Instructions for ISH's of adult zebrafish brain slices*

Protocol: In situ hybridization of adult zebrafish brains
• The used solutions and buffers are listed in section 2.9 • If not mentioned, the procedures were conducted on room temperature **Day 1** • Replace methanol by 75% methanol and incubate for 5 min. • Replace methanol by 50% methanol and incubate for 5 min. • Replace methanol by 25% methanol and incubate 5 min. • Replace methanol by PTW and incubate for 5 min. • Repeat the previous step • Digest embryos with proteinase K (10 µg/mL) for exactly 30 min. • Rinse twice with glycine (2 mg/mL) for 2 min. each • Post fixate the samples in 4% PFA on a shaker for 30 min. • Wash 5 times with PTW for 5 min. each • Separate each brain to a single 2 mL tube • Replace PTW with Hyb+ solution and incubate at 65°C for at least 2 h • Replace Hyp+ with your probe (2 ng/µL in 200 µL), diluted in Hyp+ solution and incubate at 65°C overnight **Day 2** • Wash 2 time with 50% Formamide / 2x SSCT at 65°C for 45 min. • Wash with 2x SSCT at 65°C for 45 min. • Wash 2 times with 0.2x SSCT at 65°C for 45 min. • Transfer the brains to a 10 cm petri dish • Melt 3% agarose in PBS (50 mL), wait for a few minutes to let the solution cool down (~70°C) and pour it over the brains • Position the samples in a way that they are parallel to the bottom • Wait until full polymerization of the gel • Carefully cut out each brain and temporarily store it in a 6 well plate (1 well per brain), containing PTW • By means of a vibratome, slice the blocks into 100 µm thick pieces and collect them • Block your samples in 10% sheep serum for 2 h • Incubate in *anti-DIG-AP* antibody solution (1:3,000 dilution in 10% sheep serum) at 4°C overnight **Day 3** • Wash throughout the whole day with PTW at 4°C (at least 5x) • In the evening, store the samples at 4°C

Day 4

- Equilibrate your slices 2 times in staining buffer for 5 min. each
- Replace the buffer with a NBT/BCIP mix (in SB-PVA) to induce the staining process
  Keep your samples in a dark environment and constantly evaluate the staining progress
- The developmental is stopped by washing several times in PTW (2x for 5 min.)
- Replace PTW with 4% PFA and incubate at 4°C without shaking

Day 5

- Wash 2x with PTW for 5 min.
- Mount and seal the samples on an objected slide
- Image the samples or store at 4°C in a dark environment

The stained slices were finally mounted on object slides and imaged by microscopy (Zeiss Axioplan 2).

2.5. Quantitative gene expression analysis

2.5.1 qPCR analysis

All prior established cDNA libraries (Section 2.2.6) of HEK-293 cells and juvenile and adult zebrafish were utilized for gene expression studies via qPCR.

Before starting the main experiment, a dilution series (1:1, 1:10, 1:100, 1:1000) of newly synthesized sets of cDNA templates (Section 5.1) was prepared and analyzed. These titrations were indispensable to optimize the working concentration for the investigated samples. Afterwards, aliquots of the libraries were diluted according to the obtained results, followed by qPCR analysis as technical duplicates (Table 16).

Table 16: *Protocol for gene expression analysis via qPCR*

Protocol: qPCR analysis

Component	Volume / reaction
Power Sybr Green Master Mix (10x; Invitrogen, #4367660)	10 µL
Forward primer (10 µM)	1 µL
Reverse primer (10 µM)	1 µL
Template	x µL
H_2O	x µL
	20 µL

Thermocycler setup			
	Holding stage	**Denaturation**	**Annealing and Elongation**
Temperature	95°C	95°C	60°C
Time	10 min.	15 sec.	1 min.
		40 cycles	

2.6. Localization studies in HeLa cells

To perform localization studies in HeLa cells, a subset of prior generated expression vectors (Section 2.3.1) was transfected. Plasmids driven by a CMV promoter and carrying the fish derived *letm1* or *letm2* CDS, fused to an eGFP tag were therefore utilized. HeLa cells were kindly seeded in *µ-Slide 8 Well* plates (Ibidi; #80821) by Shane Austin and further incubated at 37°C (5% CO_2) approximately two days before transfection. The culture medium (Dulbecco's Modified Eagle Medium; Gibco; #41966-029) was supplemented with 10% FCS (Gibco; #16000-036), 100 u/mL Penicillin and 0.1 mg/mL Streptomycin (Gibco; #15140-122). After reaching a cell confluency of approximately 80%, 250 ng of DNA were individually transfected following the manufacturer's instructions (Section 2.9). One day after, mitochondria and nuclei were stained with MitoTracker-Red FM (Thermo Scientific; #M22425) and Hoechst (Thermo Scientific; #62249), respectively. Immediately after the staining process, confocal live cell imaging was carried out (Zeiss LSM780). To provide a viable environment, the imaging chamber was heated to 37°C under constant CO_2 flow (5%).

2.7. Locomotor behavior

The locomotor performance of zebrafish larvae was investigated by means of a DanioVision Tracking system and further analyzed with the corresponding software suite (Noldus Information Technology). *Letm1*$^{+/-}$ zebrafish were outcrossed with wild type animals (AB strain) and raised until 7 dpf. Based on mendelian inheritance the obtained clutch consisted of *letm1*$^{+/+}$ and *letm1*$^{+/-}$ genotypes in an expected ratio of 50%:50%. Hence the measurements were conducted blindly (without knowing the genotype). The 7 dpf larvae were transferred to a 96 well plate (1 larvae/well) and an equal volume of 200 µL/well was established. Moreover, to provide a constant and natural environment the temperature of the observation chamber was set to 28.5°C. The tracking experiment started with assessment of a baseline, as illustrated in Table 17.

Thereafter, 15 mM PTZ (Sigma Aldrich; #P6500) were added to each well and the light cycle was applied again. To distinguish between *letm1*$^{+/+}$ (Control) and *letm1*$^{+/-}$ animals, genotyping was conducted after the tracking experiment.

Table 17: *Illustration of the applied conditions for conducted locomotor assessments in zebrafish larvae (7 dpf). Each experiment was separated into two different sections. During the first period (Baseline) the specimens were exposed to a short light/dark cycle (10 min. each) repeating three times. Subsequently after, 15 mM PTZ were added to each well and the light cycle was repeated (Treatment).*

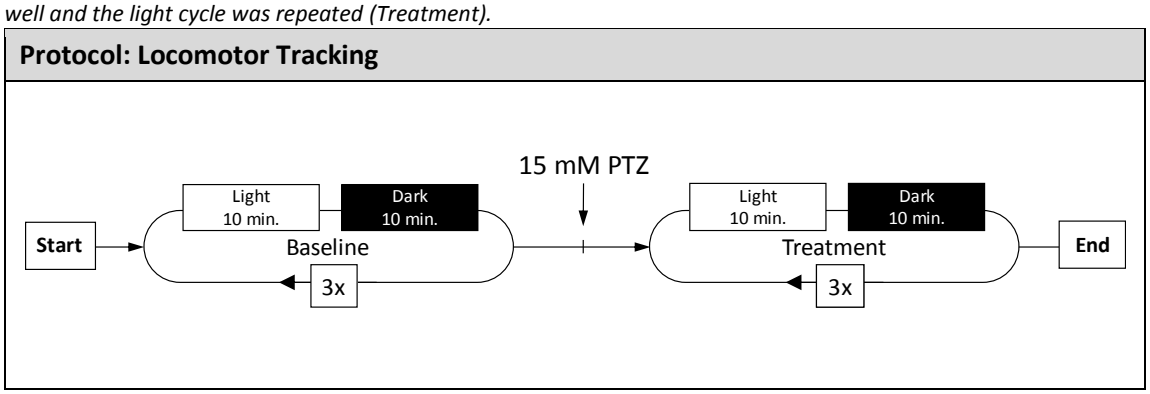

2.8. Bioinformatical approaches and data evaluation

2.8.1 Phylogenetic analysis

To visualize the evolution of LETM1 and LETM2, protein sequences of relevant organisms (Table 18) were collected using the ENSEMBL (Cunningham et al., 2014) and the NCBI BioSystems databases (Geer et al., 2010).

Table 18: *Compilation of protein accession numbers used for the phylogenetic analysis*

Accession numbers of proteins used for the phylogenetic analysis		
Protein	**Organism**	**Accession number**
Letm1	*Danio rerio*	XP_009305455.1
LETM1	*Homo sapiens*	AAD13138.1
LETM1	*Mus musculus*	AAD13139.1
LETM1	*Rattus norvegicus*	NP_001005884.1
Letm1	*Oryzias latipes*	XP_004082779.1
DmLETM1	*Drosophila melanogaster*	AAM68316.1
CeLETM1	*Caenorhabditis elegans*	NP_506382.1
Letm2	*Danio rerio*	XP_001339387.1
LETM2	*Homo sapiens*	NP_001186588.1
LETM2	*Mus musculus*	NP_766600.2
LETM2	*Rattus norvegicus*	AAH87079.1
Letm2	*Oryzias latipes*	XP_004072229.1
Mdm38p	*Saccharomyces cerevisiae*	NP_014615.1
Mrs7p	*Saccharomyces cerevisiae*	NP_015450.1
AtLETM1	*Arabidopsis thaliana*	At3g59820
AtLETM2	*Arabidopsis thaliana*	AT1G65540.1
HCCR1	*Mus musculus*	AAH21361.1
HCCR1	*Rattus norvegicus*	AAI59427.1
HCCR1	*Homo sapiens*	AAH19274.1
Hccr1	*Danio rerio*	NP_001124088.1

The phylogenetic analysis was further calculated by *phylogeny.fr* (Dereeper et al., 2008), a free accessible online tool. Therefore, protein sequences were imported and the settings shown in Table 19 applied.

Table 19: *Utilized parameters to calculate and render a phylogenetic tree by means of phylogeny.fr*

Parameters used for phylogenetic protein analysis

• Step 1: Workflow setup
  ○ Multiple Alignment: MUSCLE
  ○ Alignment curation: Gblocks
  ○ Construction of phylogenetic tree: PhyML
  ○ Visualisation of phylogenetic tree: TreeDyn
 	
• Input Data
  ○ Pasted protein sequences of interest (FASTA format)
 	
• Alignment (MUSCLE)
  ○ MUSCLE run mode: Full mode
  ○ Maximum numbers of iterations: 16
 	
• Curation (Gblocks)
  ○ No selections made
 	
• Phylogeny (PhyML)
  ○ Approximate Likelihood-Ratio Test (aLRT): SH-like
  ○ Substitution model: Default
  ○ Number of substitution rate categories: 4
  ○ Gamma distribution parameter: estimated
  ○ Proportion of invariable sites: estimated

2.8.2 Software

Most of the bioinformatic approaches such as sequence analysis or design and simulation of cloning procedures were performed in CLC Main Workbench 6.7.1 (http://www.clcbio.com).

Images were assembled, annotated and edited by means of Photoshop CS3, Version 10.0 (http:// http://www.adobe.com).

Conducted calculations, data analysis and generation of graphs was carried out in Microsoft Excel 2013 (http://products.office.com) or Prism 6.0 (http://www.graphpad.com).

Confocal and common light microscopy was supported by the manufactures supplied software suites (Confocal imaging: Carl Zeiss Microscopy GmbH, ZEN2012; Light microscopy: Carl Zeiss Microscopy GmbH, AxioVs40 4.8.1.0).

2.9. Utilized buffers and commercial kits

Reaction Kits		
Purpose	**Description**	**Catalog number**
cDNA synthesis (HEK-293 cells)	Invitrogen High-Capacity cDNA Reverse Transcription Kit	#4368813
cDNA synthesis (Zebrafish)	Quiagen QuantiTect Reverse Transcription Kit	#205311
Gateway Cloning – BP recombination reaction	Invitrogen Gateway BP Clonase II Enzyme mix	#11789-020
Gateway Cloning – LR recombination reaction	Invitrogen Gateway LR Clonase II Enzyme mix	#11791-019
High scale, endotoxin free DNA isolation	Quiagen EndoFree Plasmid Maxi Kit	#12362
In vitro transcription (SP6)	Ambion mMESSAGE mMACHINE SP6 Transcription Kit	#AM1340
In vitro transcription (T7)	mMESSAGE mMACHINE T7 ULTRA Transcription Kit	#AM1345
In vitro transcription of sgRNA's	NEB T7 Quick High Yield RNA Synthesis Kit	#E2050
pGEM-T easy cloning	Promega pGEM-T Easy Vector System	#A1360
pJET1.2 cloning	Thermo Scientific; CloneJET PCR Cloning Kit	#K1231
RNA isolation	Quiagen RNeasy Mini Kit	#74104
T4 mediated ligation	NEB T4 ligase NEB T4 ligase buffer (10x)	#M0202 #B0202
Cell transfection	Thermo Scientific TurboFect Transfection Reagent	#R0531

Fish related materials	
E3 medium	5 mM NaCl, 170 µM KCl, 330 µM $CaCl_2$, 330 µM $MgSO_4$, 10^{-4}% Methylene blue (Sigma Aldrich; #M9140), H_2O
Tricaine	400 mg Tricaine powder (ABCR GmbH; #AB142950),2.1 mL TRIS (1M; pH 9); pH ~7

Common materials	
TAE (1L)	242 g TRIS, 57.1 mL glacial acetic acid, 100 ml EDTA (0.5 M, pH8), H_2O
DNA loading dye	10 mM Tris-HCl (pH 7.6), 60 mM EDTA, 60% Glycerol, 0.15% Orange G (Fluka; #75380)

Bacterial handling	
Agar plates	15 g agarose, 1 L low salt-LB medium (5 g NaCl, 10 g Tryptone, 5 g yeast extract)
LB-medium (1 L)	10 g NaCl, 10 g Tryptone, 5 g yeast extract, filled up with autoclaved H_2O
SOC-medium (1 L)	20 g Tryptone, 5 g yeast extract, 0.5 g yeast extract, 10 mL KCl (0.25 M), 5 mL $MgCl_2$ (2 M), Glucose 20 mL (1 M), filled up with autoclaved H_2O
P1 buffer (Resuspension buffer)	10 mM Glucose, 25 mM Tris (pH 8), 10 mM EDTA (pH 8), 100 mg RNase A
P2 buffer (Lysis buffer)	0.2 M NaOH, 1% SDS
P3 buffer (Neutralization buffer)	3 M Potassium acetate, 11.5% glacial acetic acid

ISH – Common buffers	
4% Paraformaldehyde (PFA)	4% PFA in 1x PBS; pH 7.4
PTW	1xPBS, 0.1% Tween-20
Methanol	100% Methanol diluted in 1xPBS
Proteinase K	10 µg/mL Proteinase K in 1x PTW
Glycine	2 mg/mL glycine in 1x PTW
SSC (20x)	175.3 g NaCl, 88.2 g Na_3citrate-$2H_2O$ to 1 L with H_2O; pH 7.0
Hybridization buffer (Hyb+)	50% Formamide, 5xSSC (pH6.0), 0.1% Tween-20, 0.5 mg/mL Torula RNA, 50 µg/mL Heparin
Anti-DIG-AP antibody	Roche; #11214667001

ISH of brain slices of adult zebrafish	
Anti-Digoxigenin-antibody-AB (sheep)	Diluted in 10% sheep serum (Sigma Aldrich; #C3263)
Staining buffer (SB)	100 mM Tris (pH 9.5), 100 mM NaCl, 0.1% Tween-20, in H_2O
PVA	10% PVA powder (Merck; #821038) in H_2O
Staining buffer with PVA (SB-PVA)	100 mM Tris (pH 9.5), 100 mM NaCl, 0.1% Tween-20, in 10% PVA
NBT/BCIP	Roche; #11383213001/#11585002001

Whole mount ISH of zebrafish larvae	
MABT	100 mM Maleic acid, 150 mM NaCl, H_2O, pH7.5
DIG-blocking solution	2% blocking reagent(Roche; #11096176001) dissolved in MABT
Anti-Digoxigenin-antibody-AB (sheep)	Diluted in DIG-blocking solution
BM-Purple	Roche; #1142074001

3. Results

3.1. The gene duplication of LETM1 generated an evolutionary conserved protein family

A large diversity of studies addressed to investigate basal aspects of proteins led to our current understanding of homologies, conserved regions and how sequences changed during evolution. Based on that knowledge, sequences of *Leucine-Zipper-EF-hand-containing proteins* (LETM) were collected and analyzed. The LETM1-like protein family includes LETM1, LETM2 and LETM1 domain containing proteins. The ubiquitous LETM1 or respective orthologues are widely distributed found in all so far sequenced eukaryotic species (Dimmer et al., 2008; Karin Nowikovsky & Bernardi, 2014). In contrast to LETM1, studies on the protein function and localization of the related LETM2, its orthologues or on LETMD1 (Hccr1; Master Thesis of Roland Baumgartner, 2009) are rare.

To cluster and analyze the evolutionary track of these proteins, a phylogenetic tree was calculated taking into account the most representative and relevant organisms for the present study (Figure 11). Hccr1 was defined as an outside group which sets the root of the tree (red asterisk). Furthermore, the numbers on the branches represent the amount of genetic change, relative to the root.

The phylogenetic tree reveals that vertebrates, invertebrates, plants and yeast are independently clustered. Interestingly, as recently described and also illustrated in the present study, the vertebrate LETM2 originated by gene duplication of LETM1 (Karin Nowikovsky et al., 2012). However, protein sequences for LETM2 in invertebrate species are absent so far. Thus, it can be hypothesized that this taxon does not carry a letm2 gene, has lost it during evolution or that it was not yet discovered.

Comparisons between vertebrate and invertebrate species point to a more common ancestor as when correlated to plants or yeast. Both latter taxon's harbor two LETM1 like proteins named AtLETM1 and AtLETM2 in *Arabidopsis Thaliana* and Mdmd38p and Mrs7p in *Saccharomyces cerevisiae*. However the plant nomenclature is misleading and it is not clear which of these proteins is the LETM1 or the LETM2 orthologue. Hence, it can only be assumed that all LETM1 or orthologues proteins share conserved functions throughout the species.

Of note, while a homozygote LETM1 deficiency leads to embryonic lethality in animals, plants just exhibit a mild growth retarded phenotype. These observations can be linked to the fact that plants use chloroplasts additionally to mitochondria. Thus, some evolutionary changes of the LETM1, respectively LETM2 sequences may have been necessary to adapt the functionality to the organism.

Based on the phylogenetic analysis, it can be concluded that the vertebrate and invertebrate LETM1 may act in a similar manner due to a common ancestor and similar phenotypes in knock-out mutants. The conserved gene duplication in vertebrates may point to an important but still totally unknown homologous function of LETM2.

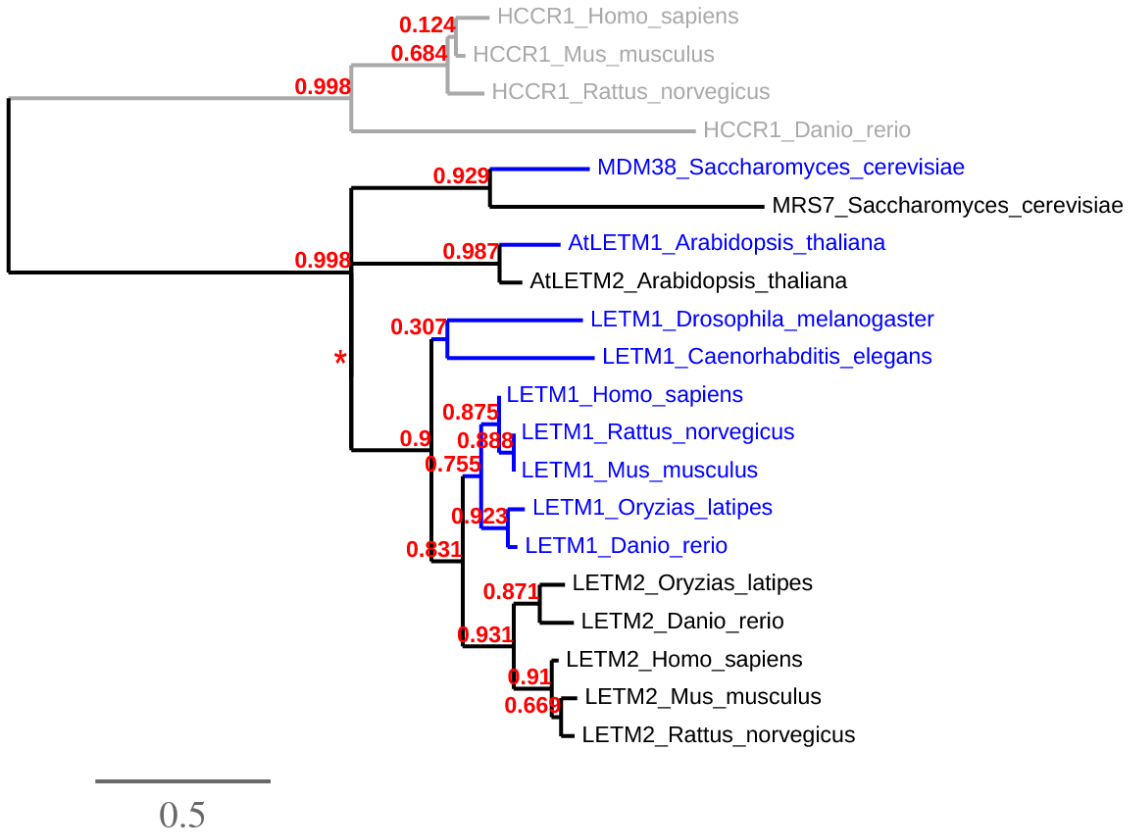

Figure 11: *Phylogenetic analysis of LETM1, LETM2 and LETMD1 (HCCR1) in several species across the eukaryotic kingdom. The highly related LETMD1 was selected to serve as outside group, which also defines the root of the tree (*). It is striking visible that LETM1 as well as LETM2 (if available) are significantly diverse across the investigated kingdoms, visualized by independent clusters. The tree further fortifies the common theory that LETM2 originated by gene duplication in vertebrates.*

Detailed sequence analysis revealed various very well conserved domains throughout the analyzed taxons. Besides Coil-coil and 14-3-3-like domains, the highly homologous TMR is the most prominent feature, as illustrated by the sequence alignment of the LETM1 and LETM2 TMR (Figure 12/A). Notably, many amino acids are identical and equally localized in both proteins, which strengthen the hypothesis of gene duplication during early evolution. Especially three proline residues, a crucial factor for protein structure, can be found without exception in all analyzed sequences (marked by an asterisk). Furthermore, also a negatively charged glutamic

acid and two lysine residues are ubiquitously present (Glutamic acid marked by a hash, Lysine marked by a paragraph sign).

Investigations of further regions revealed the occurrence of two CBD's in almost all aligned LETM1 sequences (Figure 12/B). Interestingly, comparison of the zebrafish Letm1 and Letm2 sequence revealed the unique existence of the CBD's in Letm1 (Figure 12/C) while not in Letm2. Furthermore, as shown in yeast, Mdm38p nor Mrs7p carry any CBD (Karin Nowikovsky et al., 2012).

While all analyzed vertebrate and plant species exhibit two CBD's, invertebrates show an inconsistency (Figure 12/B). For instance, *Drosophila melanogaster* carry two CBD's, but *C. elegans* harbors only one of them. Comparison between both CBD's of the fly shows a low level of variation in their amino acid sequence. Vertebrate and plant CBD's on the other side revealed a more heterogenic character. However, the second domain harbors three amino acids which are present in all analyzed vertebrate and invertebrate species (marked by an asterisk). Based on these observations it can be suggested that the second CBD may play an important role in various organisms, while the functionality of the first domain stays elusive. However, there are no available studies on the functionality of the CBD's. Hence it is difficult to judge the significance of these domains and it may be possible that the structures are just degenerated relicts of past times.

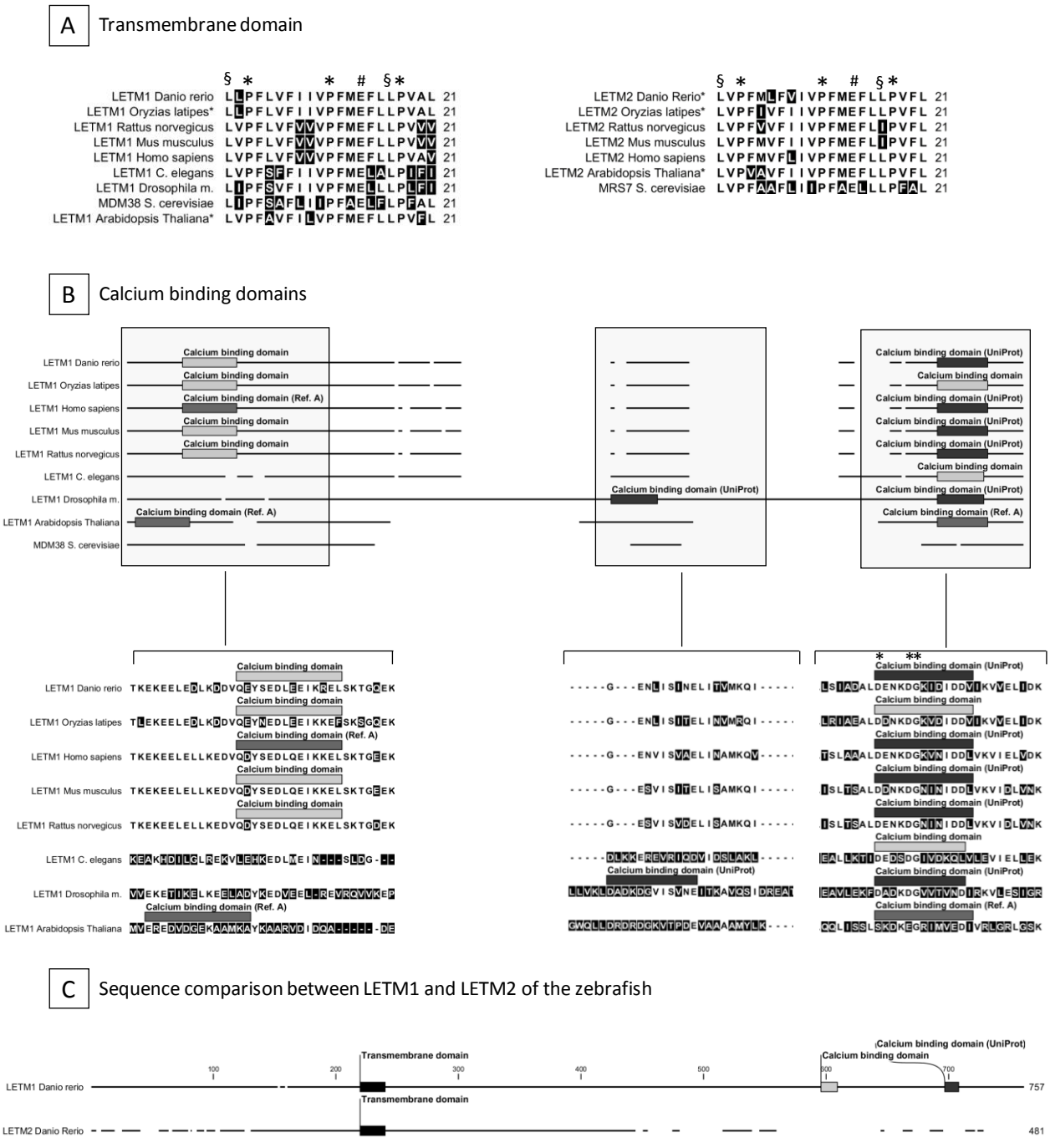

Figure 12: (A) *Sequence alignments of the LETM1 and LETM2 TMR revealed their siginficantly high conservation. It is striking visbile that several amino acids are equaly present in both proteins TMR's. Especially three proline (*), two lysine (§) and one glutamic acid (#) resides are ubiquitously present in all investigated species. These observations support the common theory that LETM2 arose by gene duplication. Annotations for species marked by an asterisk were not available in any database and were therefore predicted.* ***(B)*** *Most of the analyzed species carry two CBD's in their LETM1 protein. It was also found that invertebrates display a more heterogeneous occurrence of these domains. While the fly carry two CBD's, only one domain was predicted in C. elegans (so far). Interestingly, alignments of the second CBD revealed a very high level of conservation across all investigated vertebrates and invertebrates. It can be clearly seen that two aspartic acids and one glycine residue (*) are throughout present. Plants on the other side have a more variable CBD sequence.* ***(C)*** *Alignment of the investigated fish proteins revealed that the CBD's are explicitly present in LETM1 but not in LETM2.*
The annotations were obtained from the ENSEMBL database (Light grey), UniProt (Black) and the publication of B. Zhang et al., 2012 *(Ref. A).*

3.2. *Letm1* and *letm2* are ubiquitously expressed in larval and adult zebrafish tissues

ISH's are excellent approaches to visualize the expression of specific genes in several tissue types. For the present study, a digoxigenin labelled RNA probe, complementary to the zebrafish *letm1* or *letm2* was hybridized to their related mRNA transcripts in larval and adult tissue samples. The resulting staining intensities rely on several factors, such as probe quality, cells per area or developmental time of the digoxigenin labelled probe. Hence it has to be considered that the method is not suitable to determine the gene expression levels.

While the expression of LETM1 can be qualified as ubiquitous (Sabine Endele et al., 1999; Karin Nowikovsky et al., 2012; Tamai et al., 2008b; Wu, MacLeod, & Su, 2013), marginal knowledge about LETM2 is available. Indeed, there is only one study that demonstrated a tissue specific expression of LETM2 in adult rats so far (Tamai et al., 2008b).

3.2.1 Zebrafish larvae display a ubiquitous *letm*1 and *letm2* distribution

To investigate the expression of *letm1* and *letm2* in zebrafish larvae, *ISH's* in two developmental stages (3 and 7 dpf) were conducted (Figure 13). Strikingly, mRNA's of both observed genes are ubiquitously abundant at all observed time points.

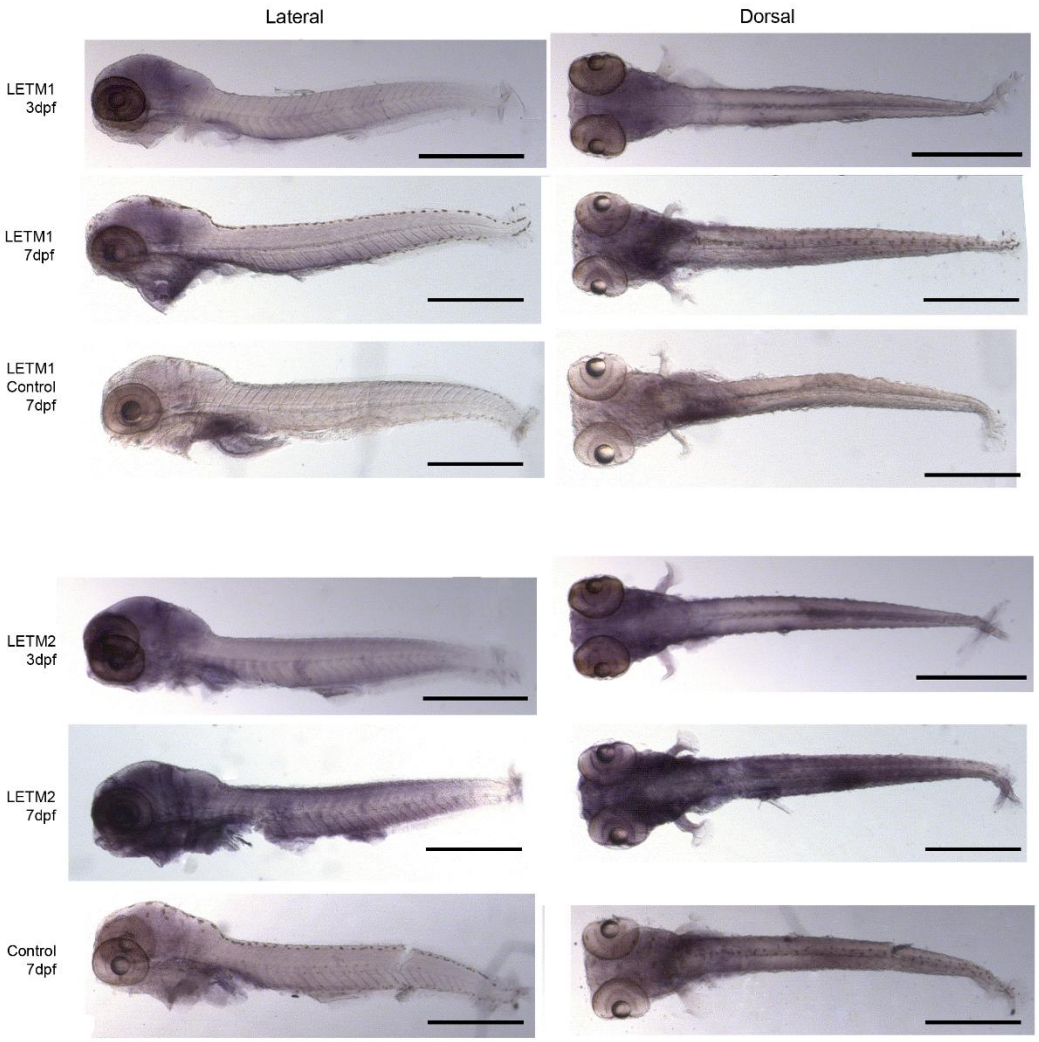

Figure 13: *Whole mount ISH of zebrafish larvae at an age of 3 and 7 dpf. It can be clearly seen that letm1 as well as letm2 are ubiquitously abundant. The scale bar represent 1 mm.*

3.2.2 *Letm1* and *letm2* are ubiquitously expressed in the adult zebrafish brain

Next, after visualizing the larval *letm1* and *letm2* mRNA distribution, ISH's of several adult zebrafish brains were conducted. Similar to the juvenile animals, the approximately 4 month old brain tissues also show a ubiquitous distribution of the investigated transcripts. Figure 14 illustrates the comparative expression of *letm1* and *letm2* in three different brain sections. The shown slices were chosen based to provide a through and informative overview of the most prominent structures.

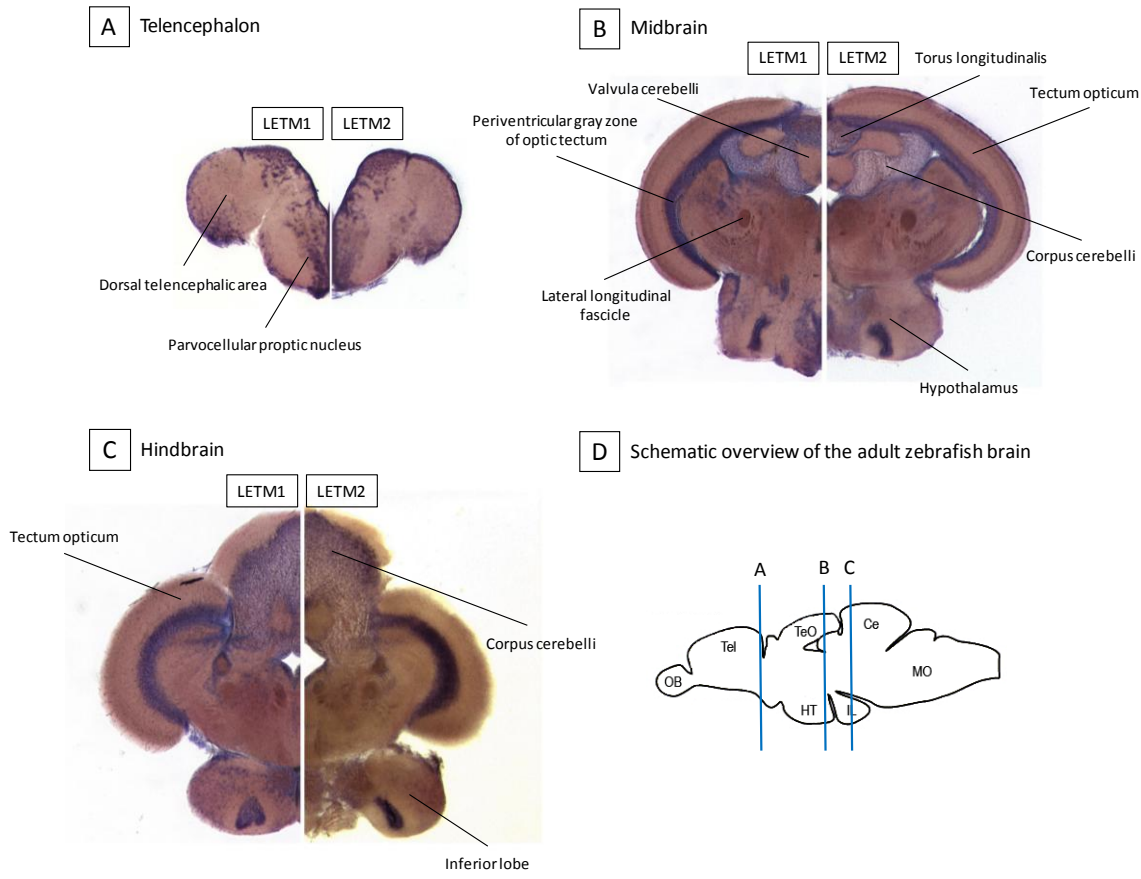

Figure 14: (A,B,C) *ISH in adult zebrafish brain slices revealed the ubiquitous expression of letm1 and letm2. Control samples with Sense-RNA probes were not conducted within the shown approach.* ***(D)*** *The schematic overview represents the localization of the illustrated slices (Picture adapted from Panula, Sundvik, & Karlstedt, 2014).*

3.2.3 *Letm1* and *letm2* are ubiquitously expressed in zebrafish and human cells

ISH's are excellent approaches to visualize and localize the gene expression in specific cells or areas. However, to study the exact amount of mRNA transcripts a more accurate method is indispensable. Hence qPCR analysis for *letm1* and *letm2* was carried out. Obtained values were normalized to the *eukaryotic elongation factor-1α* (eEF-1α) gene and are represented as relative gene expression (eEF-1α gene expression = 100%).

Messenger RNA of juvenile wild type zebrafish at an age of 1, 3 and 7 dpf was isolated, processed and further investigated. To improve the informational content, heads were carefully separated from the body (tail) and the gathered portions were independently utilized for the measurements (Figure 15/A). Based on the developmental stage of the embryos (1 dpf), these samples were not separated and therefore analyzed as a whole.

The low abundance of *letm1* and *letm2* transcripts are striking when compared to eEF-1α (<0.8%) at the assessed time points. However, the expression rates of both genes rose during

development. Interestingly, while the mRNA transcript distribution of *letm2* stayed almost equal in head and tail portions, *letm1* shows a more heterogeneous expression. The elevated abundance in tissue samples obtained from larval heads suggests an important role of letm1 during brain development and function. It is also noticeable that the observed *letm2* mRNA levels are modestly but not significantly higher than the *letm1* mRNA levels in the 1 and 7 dpf specimens.

To expand the knowledge of *letm1* and *letm2* gene expression, several organs of adult fish were isolated and analyzed independently (Figure 15/B). It is firstly evident that both genes are ubiquitously present in all analyzed tissue samples. Furthermore, while the *letm2* gene expression was slightly higher in the 1 and 7 dpf larvae (Figure 15/A), adult fish are clearly expressing *letm1* at higher rates than *letm2* (Figure 15/B). It can also be seen that accumulation of the *letm* transcripts is irregular throughout the adult organs. Similarly to the observed distribution of *letm1* transcripts in larval samples, also adult zebrafish showed a distinct higher expression in their head (brain and eyes). Furthermore, *letm1* mRNA transcripts were also elevated in the gonads, when compared to other body associated organs. Comparisons between male and female expression patterns did not show striking differences. This allowed to merge the data from both sexes.

Next, the *LETM1* and *LETM2* expression levels were analyzed in HEK-293 cells (Figure 15/C). Similarly to the adult zebrafish, we found that human cells express *LETM1* significantly higher ($p < 0.0001$) as *LETM2*. The expression values are visualized as relative gene expression normalized to the *human-TATA-box-binding-protein (TBP) gene.*

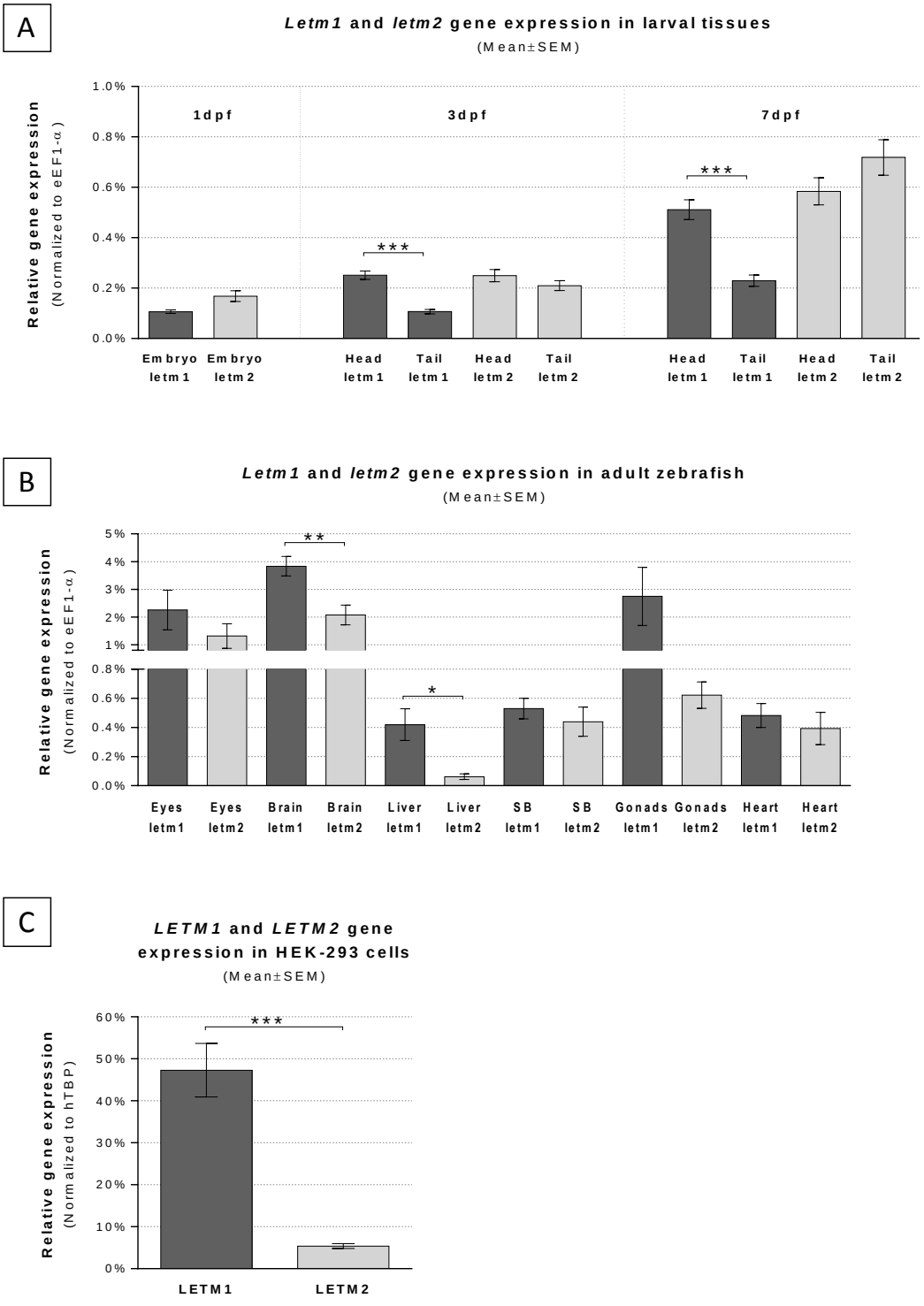

Figure 15: (A) *Quantitative gene expression analysis in juvenile zebrafish revealed a very low mRNA abundance of letm1 and letm2. It can be seen that the expression rates of both genes rose during the observed time points. While the distribution of letm2 mRNA transcripts stayed almost equal in head and tail portions, letm1 showed a more heterogeneous expression pattern. Interestingly, the observed letm2 mRNA levels are modestly but not significantly higher as for letm1 in the 1 and 7 dpf specimens. (1 dpf-letm1 (n:6); 1 dpf-letm2 (n:6); 3 dpf-head-letm1 (n:12); 3 dpf-tail-letm1 (n:9); 3 dpf-head-letm2 (n:12); 3 dpf-tail-letm2 (n:9); 7 dpf-head-letm1 (n:11); 7 dpf-tail-letm1 (n:9); 7 dpf-head-letm2 (n:13); 7 dpf-tail-letm2 (n:13))* ***(B)*** *Contrary to the observed expression rates in the fish larvae, adult specimens showed a throughout higher abundance of letm1 transcripts than for letm2 in all analyzed organs. It is*

furthermore striking that the head associated tissues (eyes and brain) display higher letm1 and letm2 expression rates as the other organs, except gonads. (Eyes-letm1 (n:6); Brain-letm1 (n:6); Liver-letm1 (n:5); Swimbladder-letm1 (n:7); Gonads-letm1 (n:5); Heart-letm1 (n:6); Eyes-letm2 (n:6); Brain-letm2 (n:7); Liver-letm2 (n:5); Swimbladder-letm2 (n:9); Gonads-letm2 (n:5); Heart-letm2 (n:9)) ***(C)*** *To investigate the LETM expression rates in human tissue samples, HEK293 were additionally analyzed and clearly show significantly higher LETM1 mRNA levels (n:5) than for LETM2 (n:7). Significances were calculated using the Student's t-test (P ≤ 0.05 = *; P ≤ 0.01 = **; P ≤ 0.001 = ***).*

3.3. Letm1 and Letm2 are highly conserved, mitochondrial associated proteins

While it is generally accepted that LETM1 plays an indispensable role in mitochondrial volume homeostasis, data for localization and function of LETM2 is still missing. Based on the conducted sequence alignments it can be suggested that also LETM2 may be a mitochondrial protein. To clarify this question, fish and mammalian expression vectors were generated and injected into mitochondrial, eGFP tagged pSCAC69 zebrafish embryos and transfected into HeLa cells, respectively. These vectors carried the CDS of the fish *letm1* or *letm2* in fusion with mCherry.

Live imaging of post injected zebrafish larvae at an age of 5 dpf revealed an explicit mitochondrial localization of Letm1 as well as for Letm2 (Figure 16). It has to be considered that living specimens (anesthetized) were utilized for the assessments. Hence a distal tail region was chosen for image acquisition. Volume, respectively thickness of more cranial areas (e.g. brain) prevented penetration of the imaging laser and were also out of the objectives range .

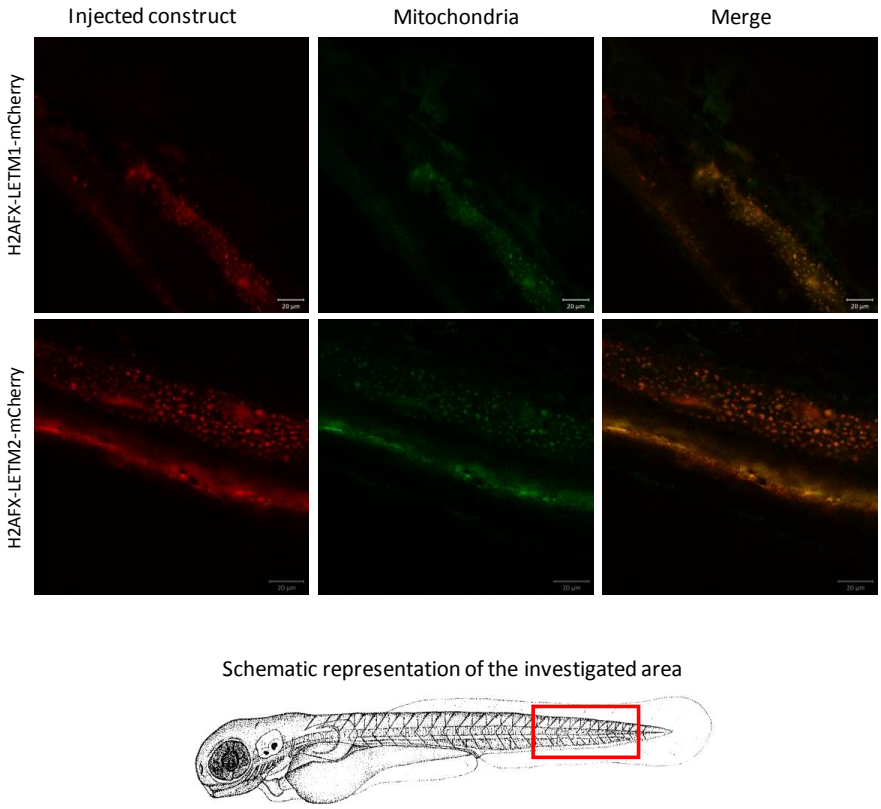

***Figure 16**: Expression vectors carrying the letm1 or letm2 CDS in fusion with mCherry and driven by the ubiquitous h2afx promoter were injected and further integrated into the pSCAC69 fish genome. Five days later, the animals where anesthetized and imaged by means of confocal microscopy. The ubiquitous eGFP expression in mitochondria of the utilized fish line (green) supported the localization of the introduced proteins (red). It can be seen that the fluorescent tagged Letm1 and Letm2 show the same localization pattern as the mitochondrial eGFP. Hence this data clearly shows that both proteins are explicitly localized in mitochondria. (Schematic representation adapted and modified from Kimmel, Ballard, Kimmel, Ullmann, & Schilling, 1995; The scale bar represents 20 µm)*

To investigate the effect of a Letm1 or Letm2 overexpression, imaged larvae were immediately rinsed with fresh E3 medium and raised. However, none of the transgenic fish survived longer than 2-3 weeks, suggesting a high toxicity due to an uncontrolled gene expression. To validate if the imaging process impacts fish development, microinjections were carried out again and the fish were quickly phenotyped under a common fluorescence microscope. However, also these specimens died within few weeks post fertilization. In contrast, untreated control fish from the same clutches developed as usual and reached adulthood.

Sequence alignments of LETM1 and LETM2 showed highly conserved domains throughout the animal kingdom. Especially the TMR was significantly well preserved. To investigate if the zebrafish *letm* genes can also be expressed in mammalian mitochondria, a localization study in Hela cells was conducted. The respective expression vectors were transfected and additional staining of mitochondria (red) and nuclei (blue) was carried out. Confocal imaging supported the

strong conservation of the zebrafish *letm* genes as demonstrated by their explicit mitochondrial localization in HeLa cells (Figure 17). The study was designed to investigate the localization pattern of the zebrafish Letm1 and Letm2 in a different species. Once this confirmed, additional experiments will be designed to draw further conclusions on the functional protein conservation.

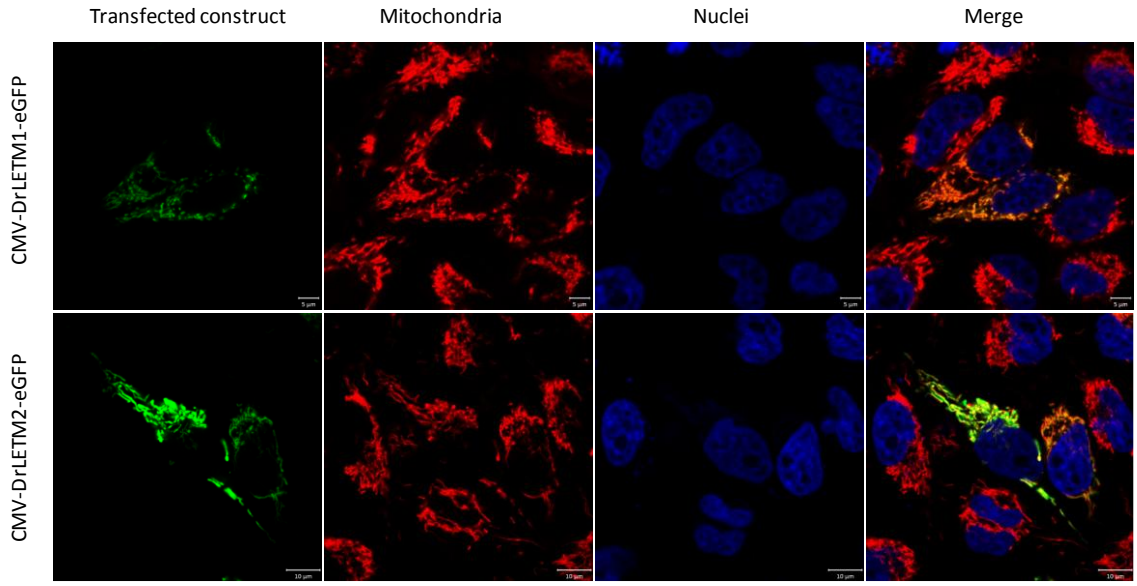

Figure 17: *Expression vectors carrying the zebrafish letm1 or letm2 CDS in fusion with eGFP and driven by the ubiquitous CMV promoter were transfected into HeLa cells. One day later, mitochondria were stained with MitoTracker-Red and nuclei with Hoechst. Subsequent confocal imaging revealed highly analogue localization patterns of the novel fish proteins when compared to mitochondria. Based on these findings it can be concluded that the TMR of the fish Letm1 and Letm2 is highly conserved, which allows integration of the proteins in human mitochondria. The scale bar represents 5 µm.*

3.4. Establishment of a vital, haploinsufficient letm1 zebrafish line

To generate a *letm1* haploinsufficient zebrafish strain, mRNA of a respective TALEN pair against exon 1 was micro-injected. The animals were raised until adulthood and further genotyped to characterize the type of introduced mutation. Figure 18/A illustrates the altered *letm1* sequences, characterized by a frameshift mutation leading to a premature stop codon of two obtained knock-out zebrafish. Hence, these mutants served for further breeding and experimental procedures. By outcrossing with the pSCAC69 line two stable *letm1*$^{+/-}$ strains were established.

Two different sets of TALEN pairs against letm1 were initially synthesized. While the first pair (specific for exon1) exhibited efficiency rates of >90%, the second pair (specific for exon 3) just showed mutation rates around 15%. Thus the first pair was used for further procedures.

After various genotyping approaches using proteinase K to isolate genomic DNA, the protocol was changed to a more efficient method. Hereby, the genetic material was isolated using the HotShot technique (Meeker, Hutchinson, Ho, & Trede, 2007), followed by PCR amplification and analysis on a 3.5% agarose gel. The higher percent gel concentration allowed to easily distinguish between all possible genotypes (Figure 18/B; Wildtype=349 bp, Heterozygote=333 bp, 349 bp and an unspecific hybrid band (>350 bp), Homozygote=333 bp) and yield quicker sequencing results. However, it has to be noted that this method is not suitable to detect size differences of less than 8 nucleotides and PCR amplicons bigger than 500 nucleotides.

Figure 18/B also shows a homozygote band of 333 bp. Based on available publications, no vertebrate organism is known to life with such a deletion so far. However, the shown specimens were screened at an age of 2 dpf. Hence no conclusion can be drawn yet. However, *letm1*$^{+/-}$ incrosses are in progress and will be evaluated soon.

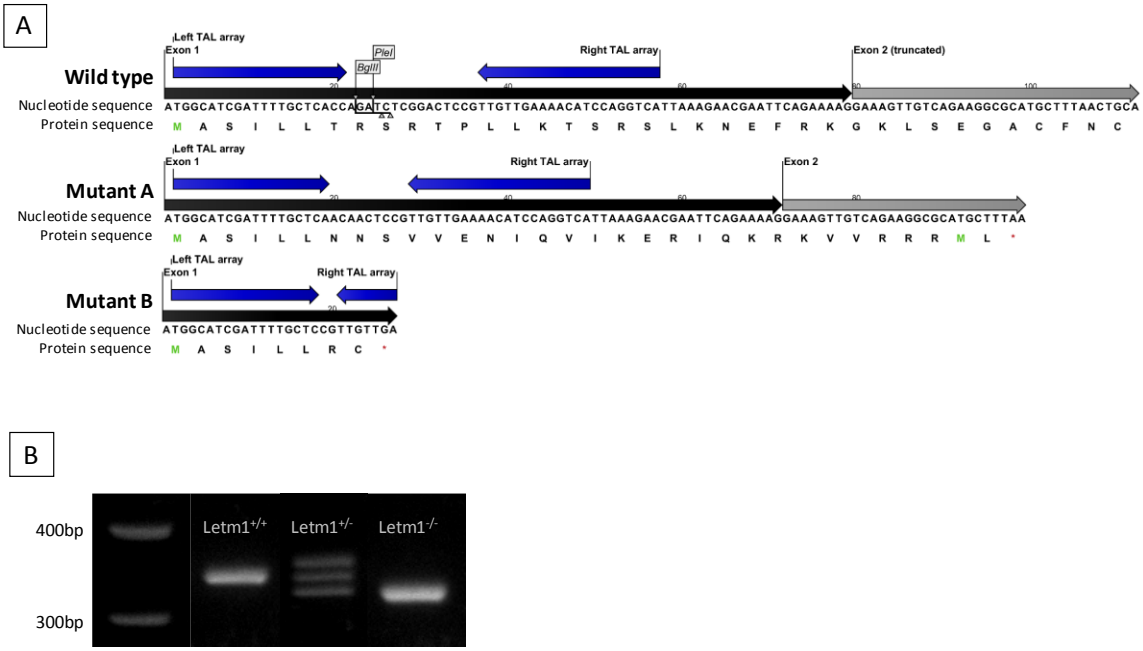

Figure 18: (A) *Illustration of the two obtained letm1*$^{+/-}$ *zebrafish mutants which were used for furhter breeding and experimental procedures. The shown specimens are characterized by a hemizygote frameshift mutation in exon1 of letm1 and are capable to heritage their gene alteration to further generations.* ***(B)*** *Genotyping of letm1*$^{+/-}$ *incrosses via agarose gel electrophoresis revealed viable letm1*$^{-/-}$ *mutants at an age of 2 dpf. The upper band of the illustrated letm1*$^{+/-}$ *sample is a common occuring artefact due to PCR ampflication of two highly similar (but nor equal) DNA templates.*

3.5. Generation of a CRISPR/Cas9 mediated letm2 knock-out strain yield first viable larvae

Besides the previously described disruption of the *letm1* gene, also *letm2* was chosen for a knock-out approach. The hereby generated hetero- and homozygous *letm2* knock-out zebrafish strains

will serve to investigate the *letm2* deletion phenotypes and thereby determine the protein function. However, evaluation of three different TALEN pairs targeted against exon 2 and exon 3 of *letm2* were disappointing. Hence we switched to the CRISPR/Cas9 nickase system. After experiencing very high lethality rates while using this approach, we replaced the nickase with the Cas9 nuclease. Microinjections of a mixture of four different sgRNA's against exon 3 in combination with the respective Cas9 mRNA, followed by genotyping at early larval stages (approx. 5 dpf) showed first positive results (Figure 19). Based on this outcome, further clutches were injected and are currently growing up.

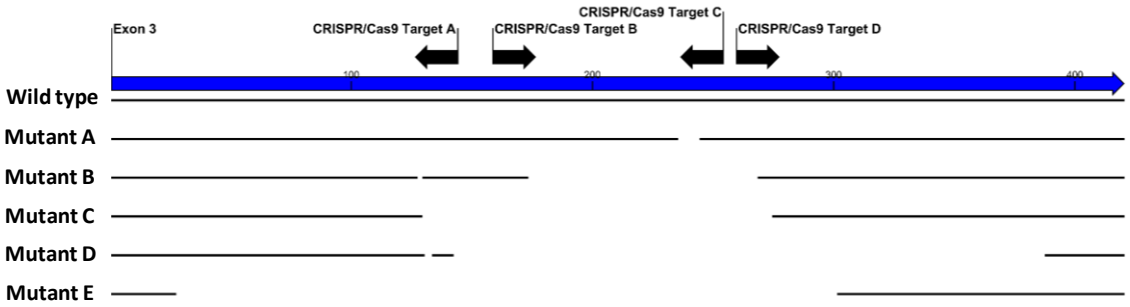

Figure 19: *Sequence alignment of exon3 of several genotyped letm2 deficient zebrafish larvae (5 dpf) in comparison to the WT sequence. Injection of a mixture of four different sgRNA's (Target A – Target D) resulted in a heterogeneous efficiency. For instance, it can be seen that just one sgRNA (Target C) disrupted the letm2 gene in mutant A and that three sgRNA's altered exon3 of letm2 in mutant B. The exact amount of deleted nucleotides (nt) are as following: Mutant A: 9nt, Mutant B: 97nt, Mutant C: 145nt, Mutant D: 248nt, Mutant E: 274nt.*

3.6. Letm1 haploinsufficient mutants reveal an unchanged locomotor behavior

Two studies demonstrated an increased susceptibility to artificially induced seizures in *Letm1* haploinsufficient rats (X. Zhang et al., 2013) and mice (Jiang et al., 2013). Furthermore, McQuibban and colleagues demonstrated that (untreated) flies with silenced, neuronal DmLetm1 expression are less mobile. To extend the knowledge to vertebrate species, several experiments to assess the locomotor activity of *letm1*$^{+/-}$ zebrafish larvae (7 dpf) were conducted.

First trials were performed to validate the experimental setup and to monitor the typical swimming behaviour in WT and *letm1*$^{+/-}$ specimens in bright and dark environments (Figure 20/B). It is widely known that zebrafish tend to be more active during light periods as in the dark. However, immediately after the *light-to-dark* transmission an increased locomotor activity can be observed, termed photokinesis *(*Figure 20/A*).* However, after a short period of approximately 15 minutes, this effect disappears and the movement drops below the activity levels as observed under bright light.

Comparison of the native swimming behaviour between WT and *letm1* haploinsufficient zebrafish larvae did not show significant differences (Figure 20/B). Also a subsequent treatment with 15 mM PTZ to induce seizures did not lead to a different locomotor pattern (Figure 20/C*)*. However, to validate the significance of the results, the swimming behaviour of untreated *letm1* control and mutant fish was set as baseline and the PTZ treated animals were normalized to these values, respectively (Figure 20/D). Unfortunately, also this method did not show any differences between WT and *letm1*$^{+/-}$ zebrafish.

Although the conducted experiments were not able to show any altered locomotor behaviour in our mutant fish, planned setups may lead to a more significant outcome. These will involve prolonged observation periods (e.g. 12 h bright light followed by 12 h darkness), usage of different stimuli (e.g. taping mechanism) or treatment with various compounds such as Valinomycin or Nigericin.

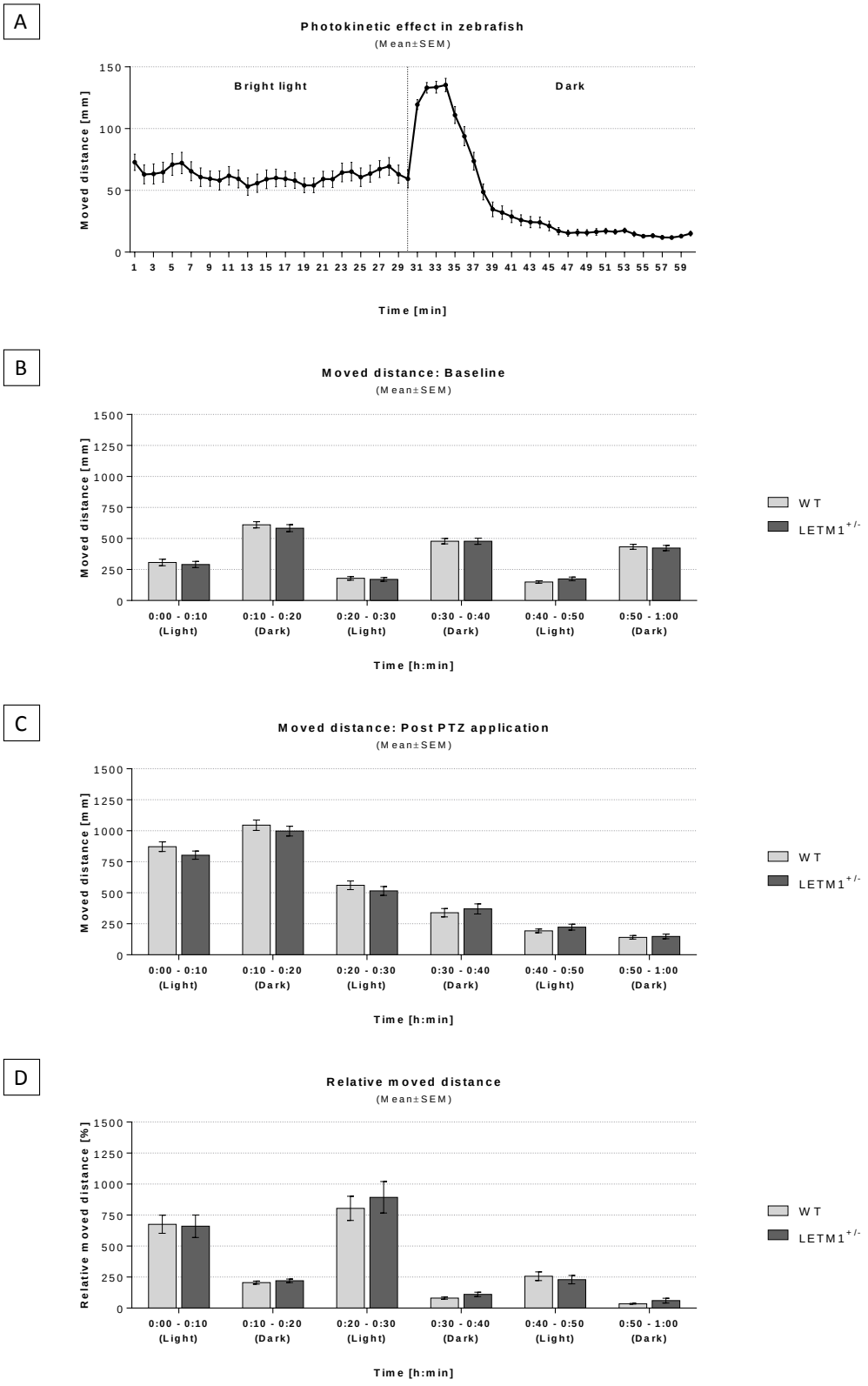

Figure 20: (A) *Assessment of the locomotor behavior in letm1 haploinsufficient zebrafish larvae at an age of 7 dpf. Figure A illustrates a typical behavioral phenomenon in zebrafish, termed photokinesis. Animals (n:64) exposed to bright light show elevated activity levels immediately after removal of the light stimulus. However, after a short period of approximately 15 minutes the effect subsided and the activity significantly decreased. Section* ***B*** *represents the average moved distance of each observation period (1 period = 10 min) under the given illuminations. The gathered results*

confirm that zebrafish are more active during light periods as in the dark, but did not show significant differences between WT (n:135) and letm1$^{+/-}$ (n: 117) specimens. Figure ***C*** *illustrates the average moved distance for each observation period after the subsequent addition of 15µM PTZ. The tracked behavior shows decreasing activity levels post PTZ treatment as already described by the group of Ellis* (Ellis et al., 2012). *However, also this approach did not display convincing differences between the analyzed genotypes.* ***(D)*** *To increase the expressiveness, the track of each PTZ treated specimen (C) was normalized the respective previously recorded baseline (B), but did not reveal different activity patterns.*

4. Discussion

4.1. LETM1 and LETM2 are highly conserved proteins throughout the eukaryotic kingdom

It has been shown that LETM1 and LETM2 are highly conserved proteins, sharing a series of homologous domains with other species. Especially the TMR of LETM1 and its orthologues is remarkably well preserved throughout all eukaryotic species including plants, vertebrates, invertebrates and yeast. Less preserved are the CBD's. While the second CBD is present in almost all investigated organisms, analysis of the first CBD revealed that the domain is less conserved in its sequence and does not occur in all species (e.g. *C. elegans*). It hast to be mentioned that the CBD's are just predicted domains. Hence it is very difficult to predict if these sequences have a functional role in the related species. However, studies dedicated to reveal the function of LETM1 progress and the number of interaction partners increases fast. These possible interactions may result from the existence of coiled-coils and the 14-3-3 like domain as found in (almost) all analyzed species (Lupo et al., 2011; Karin Nowikovsky et al., 2012). As well known, these domains enable a wide variety of interactions, thus broadening the functional range of the associated protein. Indeed, besides LETM1 mediated mitochondrial potassium efflux, single studies reported other linked functions and pathologies, besides WHS. While Wang et al. observed increased expression levels of *LETM1* in several human malignancies, Park and colleagues link LETM1 activity with obesity in mice (Park et al., 2014; Wang et al., 2015).

Sequence alignments and a phylogenetic analysis revealed a significant reciprocity between LETM1 and LETM2 throughout the eukaryotic kingdom. So far it can only be speculated if LETM2 is expressed or not and if so whether it shares similar function and localization as LETM1.

In yeast, two LETM1 family members are present and expressed. They are encoded by the ORF *YOL027c* and *YPL125w*, and respectively termed *MDM38* and *MRS7* (Karin Nowikovsky et al., 2012). While deletion of *MRS7* displays no phenotype, disruption of *MDM38* shows severe mitochondrial phenotypes. However, overexpression of *MRS7* can rescue the latter. Interestingly, the yeast LETM1 family proteins do not carry a CBD. In contrast, vertebrate, invertebrate and plant species harbor at least one CBD sequence in their letm1 gene, but not in letm2. It will be interesting to learn if this diversity may antagonize rescue approaches in letm1 deficient model systems via overexpression of letm2. It can be speculated that the CBD's may interact with other pathways important for various regulatory processes, which cannot be compensated by LETM2.

The present master thesis further demonstrates the high conservation of the fish Letm1 and Letm2. The localization studies illustrated that both zebrafish proteins are ectopically expressed in human cells and are exclusively localized within mitochondria. To investigate further functional aspects, respective approaches are already scheduled. Furthermore, complete substitution of the human LETM1 or LETM2 with the fish Letm1 or Letm2 will be additionally conducted. However, it will be crucial to initially determine and exclude the influence of the large fused fluorescence tag. Therefore, expression vectors with smaller labels (Myc- and His-Tag) were synthesized.

Knowledge about LETM2 is scarce and studies addressed to investigate the proteins function did not show any specific phenotypes. Hence, it will be very difficult to predict any effect of an altered LETM2 expression ectopically. Therefore, initial experiments have to be carried out in a native environment to find at least one pathway or phenotype which involves LETM2.

4.2. The ubiquitously abundant LETM proteins may play a crucial role during development

Studies in 1, 3 and 7 day old zebrafish larvae revealed an increasing gene expression of *letm1* as well as for *letm2* during development. While the abundance of *letm2* stays even distributed in head and tail portions, *letm1* is clearly higher expressed in the head when compared to the residual body. Furthermore, also the adult fish brain and the gonads harbor elevated levels of *letm1* mRNA transcripts in contrast to other organs such as liver or heart. Hence it can be speculated that *letm1* may play an important role in brain functions and mating.

As known, the developing brain heavily relies on mitochondrial functionality due to substantially higher demands of energy. The mitochondrial abundance increases during this developmental period and impairment of this process compromises neuronal maturation (Hagberg, Mallard, Rousset, & Thornton, 2014). Several studies demonstrated an altered mitochondrial physiology in letm1 deficient organisms. Hence, it can be reasoned that compromised mitochondria cannot sufficiently supply the energy demanding of neurons, which results in a pathogenic brain development. However, mitochondria in neurons lacking of letm1 and/or letm2 have not been fully investigated yet.

In accordance with the role of LETM1 in controlling the mitochondrial K^+ homeostasis, deficiencies result in severe mitochondrial swelling and depolarization. Whether this depolarization has any effect on the resting membrane potential which may elevate the probability for seizures is totally unknown. Besides the neuronal disturbance, letm1

haploinsufficient invertebrates, vertebrates and plants have shown to cause characteristic growth retardations within the first period of development.

Moreover, our data also illustrated a notable *letm1* expression in the gonads of male and female zebrafish. Sperm functional mitochondria have been linked to efficient fertilization (Amaral, Lourenco, Marques, & Ramalho-Santos, 2013). It could be therefore reasoned that *letm1*$^{+/-}$ sperm cells with reduced energy are less efficient in reaching oocytes. However, based on our preliminary data, male zebrafish tend to be more fertile than the females. A further explanation in favour to a female infertility could consist in an excess of impaired mitochondria not passing the bottleneck selection (Chappel, 2013). For instance, both *letm1*$^{+/-}$ founder fish were male and further breeding approaches of the originated F1 generation showed higher fertilization rates when *letm1* haploinsufficient males were crossed with female wild types than vice versa. Approaches dedicated to incross *letm1*$^{+/-}$ animals gave a very low number of vital, fertilized eggs (approx. 80% less than a typical WT breeding pair). Hence it can be concluded that the Letm1 deficiency affects the oocyte maturation more than the spermatogenesis.

Comparisons of the different splicing variations of the *letm1* gene throughout several vertebrate species (Human, mouse, rat and zebrafish) reveals a singular protein coding sequence which simplifies gene expression studies due to a full coverage of putative “isoforms”. *Letm2* on the other hand bears more difficulties. While the zebrafish processes 2 very similar splicing variants, 9 different transcript variations can be found in humans. Approximately half of these predicted human splicing types are just very short coding sequences. Hence it is difficult to predict if these fragments play any role in the related taxon.

For the present study, both *letm2* transcripts of the zebrafish were analyzed via qPCR. Additionally, 5 convincing human transcripts were included. It was demonstrated that the fish expresses *letm2* in a ubiquitous manner and likewise HEK-293 cells bear *LETM2* specific mRNAs. This data are in accordance to previous high throughput mRNA screens illustrating the ubiquitous expression of LETM2 in humans, mice and rats in all observed tissue types (Wu et al., 2009, 2013). Interestingly, the data also shows increased *LETM2* expression levels, in testes and the pineal gland in human tissue samples. However, while *letm2* gene expression in the fish gonads did not show striking differences in the present study, Tamai and colleagues observed elevated mRNA levels in rat testes (Tamai et al., 2008a). Based on these controversial findings, it can speculated that letm2 may have various roles, respectively functions in different species. It can be furthermore hypothesized that letm1 may overtake the function of letm2 in the rat testes due to its high transcript abundance.

The human pineal gland is another organ with an interesting letm2 expression pattern (Wu et al., 2009, 2013). It is well known that the *glandula pinealis* plays an important role in terms of circadian rhythms. Via synthesis and secretion of melatonin, a stable day/night cycle is maintained in almost all vertebrates (Macchi & Bruce, 2004). Non-mammalians such as the zebrafish have several photoreceptors in their pineal gland, which is also the reason for the term "third eye" (Lima-Cabello et al., 2014). Based on the high-throughput screening data, pineal *LETM2* expression is elevated during night periods in humans. While these differences were only observed for *LETM2* but nor for *LETM1*, a unique role of *LETM2* in the field of (human) circadian rhythms may be discovered.

4.3. Establishment of novel *letm1* and *letm2* zebrafish lines

4.3.1 The generated *letm1* haploinsufficient zebrafish strain will serve as an indispensable model to investigate several aspects of the mitochondrial protein

To study *letm1* deficiencies in the zebrafish, a TALEN based approach was designed and carried out. After injection of the respective TALEN mRNA's against exon1, two suitable adult founder fish with different mutations (deletion of 8 bp and 16 bp) were selected for further breeding and experimental procedures.

Several groups described a characteristic growth retardation in letm1 deficient model systems during the first period of development (Bergemann et al., 2005; Jiang et al., 2013; B. Zhang et al., 2012). For instance, the group of Jiang et al. observed a growth retardation in *Letm1*$^{+/-}$ mice at day 9.5 post fertilization. However, this delay completely subsided post 13.5 dpf.

To investigate this phenomenon in our *letm1*$^{+/-}$ zebrafish, similar experiments were conducted, but didn't lead to convincing results. The observed specimens were hereby imaged in regularly periods 3 times per day until 6 dpf. It has to be further considered that zebrafish develop much faster and *ex utero* when compared with mice. Hence, it may be possible that also *letm1*$^{+/-}$ zebrafish display the described growth delay, but for shorter terms and at earlier time points in their development. Therefore, our experimental design has to be refined and another technique to evaluate fish development has to be elaborated.

4.3.2 The challenging disruption of the *letm2* gene yielded first viable zebrafish larvae

Simultaneously to the TALEN approach dedicated to disrupt the *letm1* gene, the same principle was exerted for *letm2*. Unfortunately, none of the two constructed TALEN pairs introduced a mutation. Neither varying the concentration of injected TALEN mRNA's nor genotyping at earlier

time points led to a convincing outcome. A recent report from Valton et al. illustrated that 5-methylated cytosine (5mC) heavily impacts the TALEN efficiency. It has further been described that 5mC is present to approximately 70% in CpG islands and that it's abundance can be higher in proximal exons (Valton et al., 2012). Based on scarce information about the zebrafish methylome it was not possible to design a TALEN pair which considered the *letm2* methylation state. It has to be further noted, to establish a definite *letm2* knock-out a frameshift mutation has to be introduced in an early exon upstream of the TMR (Exon 4). Hence, proximal exons were emphasized. Moreover, chromatine accessibility of the target region is also a crucial factor which determines the TALEN efficiency.

To overcome the emerged difficulties we switched to the CRSIPR/Cas9 nickase method. This technique provides a faster workflow, more precise genomic interaction and is insensitive to methylation (Kuscu, Arslan, Singh, Thorpe, & Adli, 2014; Ran et al., 2013). In our lab the approach was successfully tested in *Oryzias latipes* (Medaka fish) and *Platynereis dumerilii* (Marine annelid). However, we observed very high lethality rates in zebrafish. To solve the advent issues, several sgRNA pairs against different genes were evaluated but did not lead to convincing results. Moreover, also various protocols for Cas9 *in* vitro transcription were tested. Unfortunately, also this process did not lead to higher viability rates.

Recently, we started to work with the Cas9 nuclease instead of the Cas9 nickase. In comparison to the latter, the nuclease introduces a DSB which requires at least one sgRNA against the targeted locus. First experiments with the novel Cas9 nuclease in combination with a mixture of four sgRNA's against exon 3 of letm2 yielded convincing surviving rates (>60%) and also successfully altered *letm2* sequences. Further experiments, will be conducted using one sgRNA to reduce the amount of putative off-set targets. Moreover, an approach to insert the CDS of a fluorescence protein, driven by a ubiquitous promoter, into exon 3 of *letm2* is already in progress.

4.3.3 An iTAL based approach will allow early larval genotyping while preserving animal welfare in the near future

Many of the planned experiments require high amounts of sample material. Based on our findings, *letm1*$^{+/-}$ larvae does not show any obvious phenotype. Hence, genotyping accompanied with sacrificing the specimen is necessary. To circumvent this issue, we recently started an iTAL based technique to genotype zebrafish larvae via phenotyping. The novel generated *letm1*$^{+/-}$ strain will additionally express the red fluorophore, mCherry in a ubiquitous manner. Such larvae

can be separated few days post fertilization according to their fluorescent phenotype. First trials showed an efficiency rate of approximately 8%, when observed by fluorescence microscopy. However, deeper screening approaches by means of PCR associated genotyping did not show any integration. Hence the observed results were rated false-positive due to the autofluorescent appearance of fish larvae (Figure 21). Upcoming experiments are addressed to vary the injected material and to re-develop the screening approach. However, if the method will not succeed, other approaches will be elaborated.

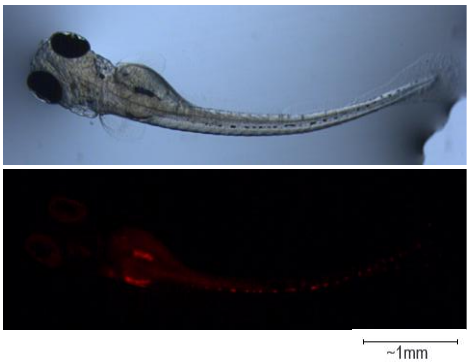

***Figure 21**: Illustration of the autofluorescent appearance of zebrafish larvae (7 dpf) which may lead to false-positive results. However, it can be hypothesized that positive specimens exhibit a much brighter fluorescence. Therefore, a positive mutant needs to be detected in the first place, to serve as a reference for further phenotyping approaches.*

4.3.4 Overexpression of *letm1* and *letm2* is not viable

By means of the Multisite Gateway Cloning technique, a set of expression vectors harbouring the CDS of the fish *letm1* and *letm2* was generated and injected into zebrafish embryos. While the ubiquitous h2afx promoter ensured a constitutive gene expression, the fluorescence tag allowed the localization of the final gene product. We further observed a very high lethality rate in the generated mutants, which demonstrates the negative dosage effect of Letm1 and Letm2 or a functional disturbance caused by the fused tag. In accordance with a negative dosage effect, Hasegawa et al. demonstrated that letm1 overexpression in mammalian cells and in *c. elegans* led to mitochondrial condensation and loss of the membrane potential (Hasegawa & van der Bliek, 2007). Thus, it can be hypothesized that zebrafish are not able to compensate for such an overexpression over longer time periods. However, the exact role of the investigated Letm proteins in the developmental process is still elusive. It may also be possible that Letm1 and/or Letm2 play an essential role during early development.

4.4. *Letm1* haploinsufficiency does not alter the locomotor behavior of zebrafish larvae

Mitochondrial volume homeostasis relies on well-balanced potassium fluxes. The KHE complex is therefore a most important system, responsible for K^+ extrusion to prevent mitochondrial swelling, a phenomenon linked to autophagy and various other malfunctions leading to cell death. Based on solid evidence, it is assumed that LETM1 is the regulatory subunit of the

complex. Several knock-down approaches of the letm1 gene revealed an altered locomotor behaviour in the investigated organisms. While invertebrates showed abnormalities without prior sensitizing chemical manipulation, vertebrates had to be exposed to convulsant substances to spot a specific phenotype.

In the present study juvenile *letm1*$^{+/-}$ zebrafish were treated with PTZ while experiencing a bright and dark surrounding. It can be summarized that the observed specimens did not show any differences in their locomotor activity, not prior or post PTZ application. Although our data shows no significant differences, we are still intrigued to spot a specific behavioural phenotype. For instance, two preliminary long-term experiments (24 h) revealed a decreased locomotor behaviour in *letm1*$^{+/-}$ zebrafish. Furthermore, treatment with nigericin partially restored the observed phenotype. However, these experiments has to be repeated and validated in the future.

Conducting experiments with nigericin is a complex task. The basal principle of the ionophore is to transport monovalent ions across biological membranes. However, the substance always exchanges the most abundant ions against H^+ (Crofts, 1996). Mitochondrial potassium homeostasis relies on LETM1 functionality. Hence, depletion of the protein results in mitochondrial potassium accumulation. Experiments of Nowikovsky and colleagues demonstrated that nigericin is capable to reverse mitochondrial swelling, caused by Mdm38p depletion (K Nowikovsky et al., 2007). Nevertheless, it has to be considered that nigericin gets also inserted in several other sub-cellular membranes, where it extrudes the most abundant monovalent ions against H^+. The following effects are difficult to rate due to a high range of linked consequences.

4.5. Summary and Outlook

The present thesis revealed several features of two novel mitochondrial proteins in the zebrafish. Here, it was shown that LETM1 as well as LETM2 are very well conserved throughout the eukaryotic kingdom and that human cells are capable to express the fish derived proteins. Moreover, *in situ* hybridization and qPCR analysis revealed their ubiquitous distribution in the fish. A noticeable higher *letm1* mRNA abundance in the brain and the reproductive organs points to an essential role in especially these tissue types. Furthermore, we shed new light on the scarce knowledge of *letm2* via showing its exclusive mitochondrial localization and the ubiquitous expression throughout the fish.

A haploinsufficient *letm1* zebrafish strain was generated and further investigated. Moreover, establishment of a haploinsufficient *letm2* fish line was more challenging than initially expected. However, via using the CRISPR/Cas9 nuclease instead of the TALEN yielded first positive results. Finally, a haploinsufficient *letm2* strain was generated, the fish are currently growing up and will be used for further procedures soon.

The herein established novel *letm1* and *letm2* deficient fish strains will serve as important models to investigate more features of the Letm proteins. Furthermore, generation of homozygote strains (*letm1*$^{-/-}$ and *letm2*$^{-/-}$) and possible double knock-out's (e.g. *letm1*$^{+/-}$ / *letm2*$^{+/-}$, *letm1*$^{-/-}$ / *letm2*$^{+/-}$, etc.) will be carried out in the future, if viable. Based on these fish lines, it can be determined whether Letm2 is capable to replace Letm1 functions, as well as how the gene expressions of *letm1* and *letm2* rely on each other. These strains will also allow deepening functional studies to assess the mitochondrial pathophysiologies caused by *letm1* or *letm2* mutations and ablations in the zebrafish.

Moreover, approaches to insert a reporter gene into the genomic *letm1* and *letm2* sequence are currently in progress. This method will allow quicker genotyping and selection of mutant fish at early larval stages. Most importantly, the mitochondrial KHE activity will be determined in these knock-out lines.

Furthermore, the synthesized set of minimal tagged *letm1* and *letm2* expression vectors (His- or Myc-Tag) will be injected into fish embryos. The tagged proteins can be further used for various proteomic approaches such as immunohistochemical investigations. It will be also interesting to investigate putative protein interactions between Letm1 and Letm2.

Data presented in this study on the locomotor behavior revealed an unaltered swimming behavior in the *letm1* deficient fish line. Despite these results, other strategies to evaluate the movement pattern of *letm1*$^{+/-}$ fish will be elaborated and conducted. For instance, one possibility is to test if valinomycin, a K^+ ionophore, would sensitize the *letm1* mutants to locomotor dysfunctions. Moreover, the activity pattern of the recently generated letm2$^{+/-}$ fish strain will be determined in the future.

To observe *letm1* and *letm2* deficiencies at the cellular level, the establishment of primary tissue cultures is currently in progress. Hereby, all possible genotypes will be included to investigate the cellular roles of both proteins. Moreover, treatment with nigericin will be conducted to rescue notable phenotypes (if any).

5. Supplemental Materials

5.1. Primer and oligo nucleotide sequences

Number	Purpose	Sequence [5' → 3']
89	pGem sequencing primer forward	CCATGGCGGCCGCGGGAATTC
90	pGem sequencing primer reverse	CAGGCGGCCGCGAATTCACTAGTG
140	pJet sequencing primer forward	CGACTCACTATAGGGAGAGCGGC
141	pJet sequencing primer reverse	AAGAACATCGATTTTCCATGGCAG
1821	pCR8 forward (TALEN)	TTGATGCCTGGCAGTTCCCT
1822	pCR8 reverse (TALEN)	CGAACCGAACAGGCTTATGT
1823	TALEN sequencing primer forward	TTGGCGTCGGCAAACAGTGG
1824	TALEN sequencing primer reverse	CATCGCGCAATGCACTGAC
3284	Top oligo for anterior iTAL site (letm1)	AGCTTGACCTGGATGTTTTCAACAAAGATC TCGGACTCCGGGTGAGCAAAATCGATGCCA
3285	Bottom oligo for anterior iTAL (letm1) site	TCGATGGCATCGATTTTGCTCACCCGGAGT CCGAGATCTTTGTTGAAAACATCCAGGTCA
3286	Top oligo for posterior iTAL (letm1) site	CGTGACCTGGATGTTTTCAACAAAGATCTC GGACTCCGGGTGAGCAAAATCGATGCCA
3287	Bottom oligo for posterior iTAL (letm1) site	GATCTGGCATCGATTTTGCTCACCCGGAGT CCGAGATCTTTGTTGAAAACATCCAGGTCA
3068	Top oligo for left sgRNA construction (Letm2-Exon3-Pair A)	TAGGGCGGATATGCAACCAGGG
3069	Bottom oligo for left sgRNA construction (Letm2-Exon3-Pair A)	AAACCCCTGGTTGCATATCCGC
3070	Top oligo for right sgRNA construction (Letm2-Exon3-Pair A)	TAGGGCTCTTGTTCGTGGCTGC
3071	Bottom oligo for right sgRNA construction (Letm2-Exon3-Pair A)	AAACGCAGCCACGAACAAGAGC
3072	Top oligo for left sgRNA construction (Letm2-Exon3-Pair B)	TAGGGTGGTTGAGTGGCAGAGG
3073	Bottom oligo for left sgRNA construction (Letm2-Exon3-Pair B)	AAACCCTCTGCCACTCAACCAC
3074	Top oligo for right sgRNA construction (Letm2-Exon3-Pair B)	TAGGGCACCTCCAGCGTTGCCA
3075	Bottom oligo for right sgRNA construction (Letm2-Exon3-Pair B)	AAACTGGCAACGCTGGAGGTGC
3076	Top oligo for left sgRNA construction (Letm2-Exon4)	TAGGGCATGAAGGGCACAAGC

3077	Bottom oligo for left sgRNA construction (Letm2-Exon4)	AAACGCTTGTGCCCTTCATGC
3078	Top oligo for right sgRNA construction (Letm2-Exon4)	TAGGTGTTATTGTTCCCTTCA
3079	Bottom oligo for right sgRNA construction (Letm2-Exon4)	AAACTGAAGGGAACAATAACA
2489	Letm1-Exon1 genotyping forward (TALEN)	GCTCTATCTACAGGAAGACGGAAGCA
2864	Letm1-Exon1 genotyping reverse (TALEN)	TAACCCACACACTTATCTACCC
2796	Letm1-Exon3 genotyping forward (TALEN)	CCTGGTGTTCTTGGAGGAATCGTC
2818	Letm1-Exon3 genotyping reverse (TALEN)	TCTCTCTCGGCGCGACAGAATGT
2413	Letm2-Exon2 genotyping forward (TALEN)	CGAGCGTAGTTTCCTGCAGT
2414	Letm1-Exon2 genotyping reverse (TALEN)	GTGACAGCAATACGTCCAAGC
2798	Letm2-Exon3 genotyping forward (TALEN and CRISPR/Cas9)	AAGACATGGCTGTGCTACACTCC
2799	Letm2-Exon3 genotyping reverse (TALEN and CRISPR/Cas9)	CTTCTCTCCCTCCTGGTAAGCTG
3048	Letm2-Exon4 genotyping forward (CRISPR/Cas9)	GGTAAGCGGTTTGACATTTGAAG
3049	Letm2-Exon4 genotyping reverse (CRISPR/Cas9)	AAGGCAACATTTCTGGGAAGAG
3238	Letm2-Exon4 genotyping forward (TALEN)	GCGGTTTGACATTTGAAGTT
3239	Letm2-Exon4 genotyping reverse (TALEN)	GCATACCTTTTTAGTCTCTGTCTCA
2800	qPCR primer (forward) for eEF1α	GTGGCTGGAGACAGCAAGA
2801	qPCR primer (reverse) for eEF1α	AGAGATCTGACCAGGGTGGTT
3052	qPCR primer (forward) for DrLETM1	CCACCTTCGAGACACAGTCC
3053	qPCR primer (reverse) for DrLETM1	GGCCATCTCCAACTTCACTC
2804	qPCR primer (forward) for DrLETM2	CCAGTGCCCAAACTGGAG
2805	qPCR primer (reverse) for DrLETM2	ACTGAGGAGGACAGGGGATT
ASCTR[3]	qPCR primer (forward) for hTBP	TCTTTGCAGTGACCCAGCATC
ASCTR	qPCR primer (reverse) for hTBP	GCAAACCAGAAACCCTTGCG
ASCTR	qPCR primer (forward) for hLETM1	GAGATTGTGGCAAAGGAAGC
ASCTR	qPCR primer (reverse) for hLETM1	CAAAATCCTTCGCCACCTC
ASCTR	qPCR primer (forward) for hLETM2	CAACTGCGACAACAGCTCAC
ASCTR	qPCR primer (reverse) for hLETM2	GTAGAAGGTGCGGGACAGG

[3] Stored at the *Anna Spiegel Center for Translational Research; Nowikovsky Group*

2400	ISH probe (forward) LETM1	ATGGCATCGATTTTGCTCAC
2401	ISH probe (reverse) LETM1	ACAGAGCCACCAGCTGCGGC
2402	ISH probe (forward) LETM2	ATGGCAGTTTTCAGCTCACAG
2403	ISH probe (reverse) LETM2	ACTCATCTTGGACTTCTGTGAC
3058	Gateway cloning: LETM1 CDS + attB1 site	GGGGACAAGTTTGTACAAAAAAGCAGGCTATGGCATCGATTTTGCTCACC
3059	Gateway cloning: LETM1 CDS without stop codon + attB2 site	GGGGACCACTTTGTACAAGAAAGCTGGGTAGTTTTGGATTTTAGCTGCCTGTTCCT
3060	Gateway cloning: LETM1 CDS w/o stop codon + 6xHistidin tag + attB2 site (reverse)	GGGGACCACTTTGTACAAGAAAGCTGGGTAGTGGTGGTGGTGGTGGTTTTGGATTTTAGCTGCCTG
3061	Gateway cloning: LETM2 CDS + attB1 site (forward)	GGGGACAAGTTTGTACAAAAAAGCAGGCTATGGCAGTTTTCAGCTCACA
3062	Gateway cloning: LETM2 CDS w/o stop codon + attB2 site (reverse)	GGGGACCACTTTGTACAAGAAAGCTGGGTTATGCCATTGGCACTCATCT
3063	Gateway cloning: Sequencing primer, upstream p5E	GAGCAGGAAACAGCTATGACCAT
3064	Gateway cloning: Sequencing primer, upstream pMe (CMV)	AAATGGGCGGTAGGCGTGCCTAA
3065	Gateway cloning: Sequencing primer, upstream pMe (H2AFX)	CAAATGTGTGGGCGGGACTATGC
3066	Gateway cloning: Sequencing primer, upstream p3E (LETM1)	AGTTGCAGAGATCATGGTGATGC
3067	Gateway cloning: Sequencing primer, upstream p3E (LETM2)	GCCGACACATCAGCCAAAGGGAA

5.2. Plasmids

If not otherwise stated, the shown plasmids carry an Ampicillin resistance gene for selection purposes.

5.2.1 TALEN: iTAL construct for a TALEN mediated knock-in

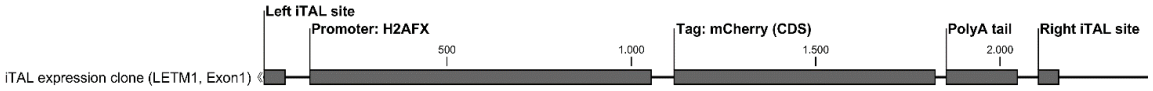

5.2.2 sgRNA constructs

5.2.3 TALEN: Final constructs for IVT, respectively injection

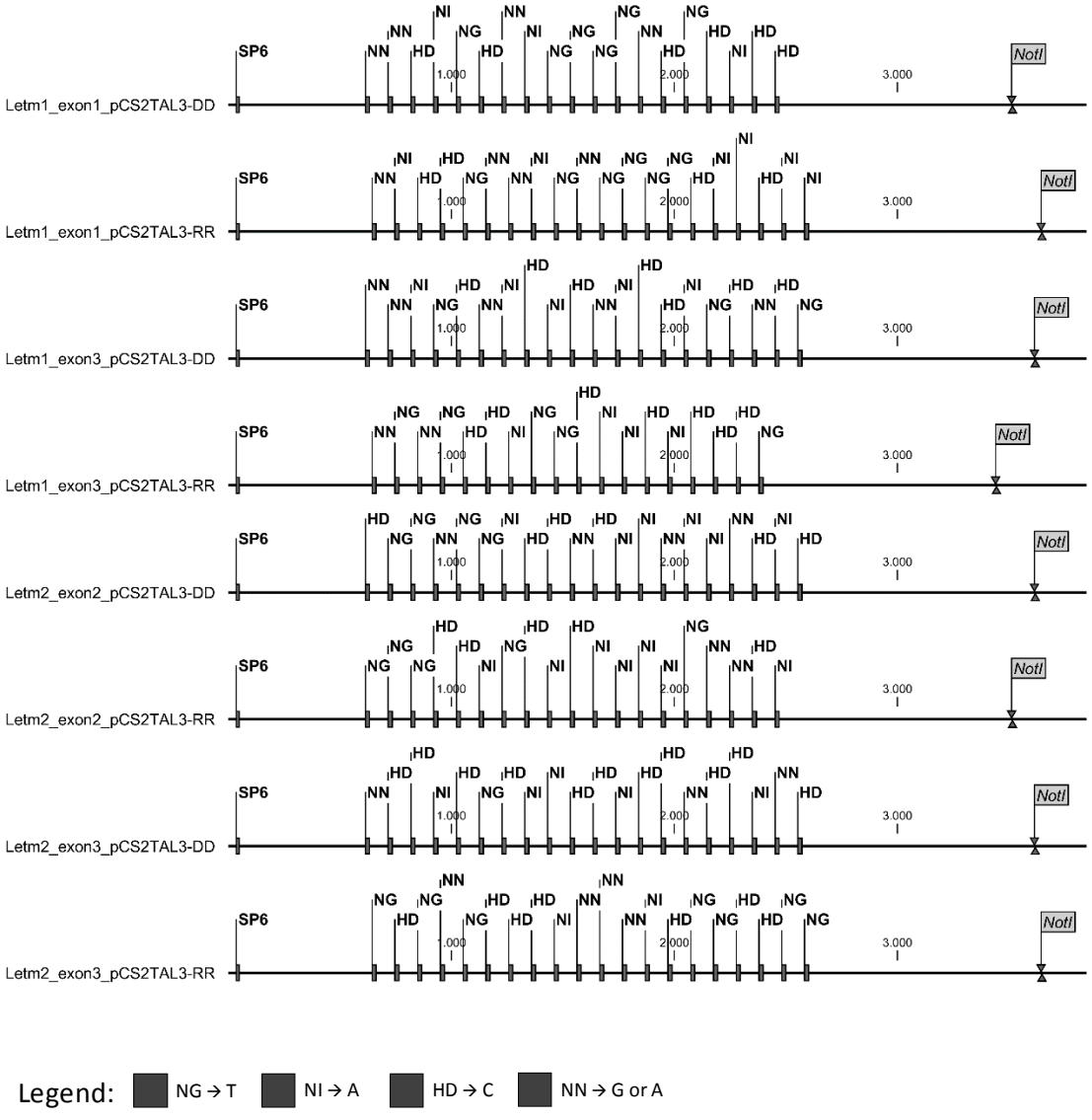

5.2.4 CRISPR/Cas9 related plamids

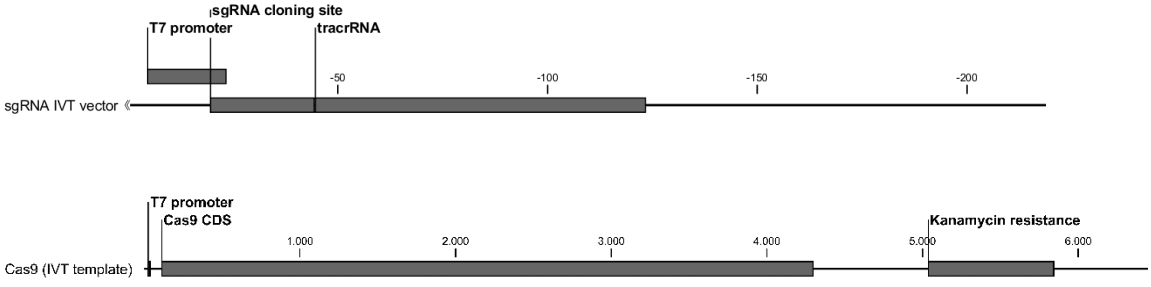

5.2.5 Digoxigenin labeled probes for ISH

5.2.6 Expression vectors: Zebrafish

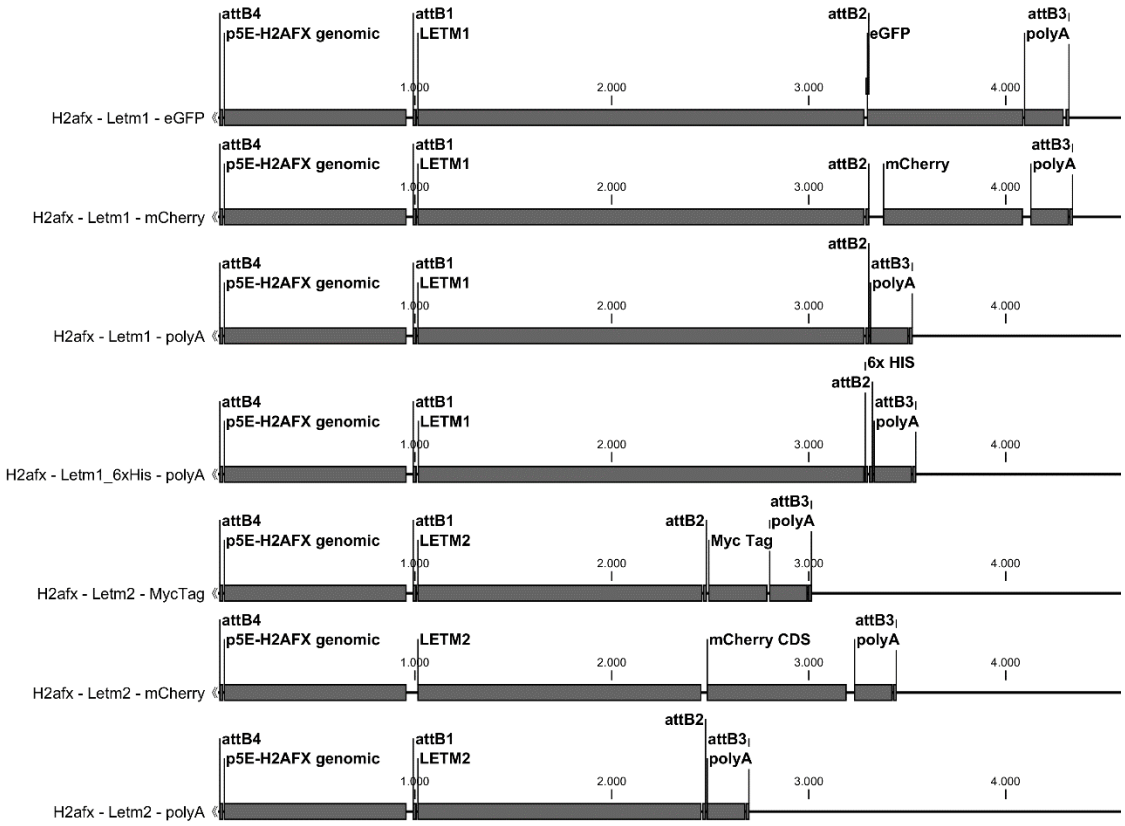

5.2.7 Expression vectors: Mammalian cell line

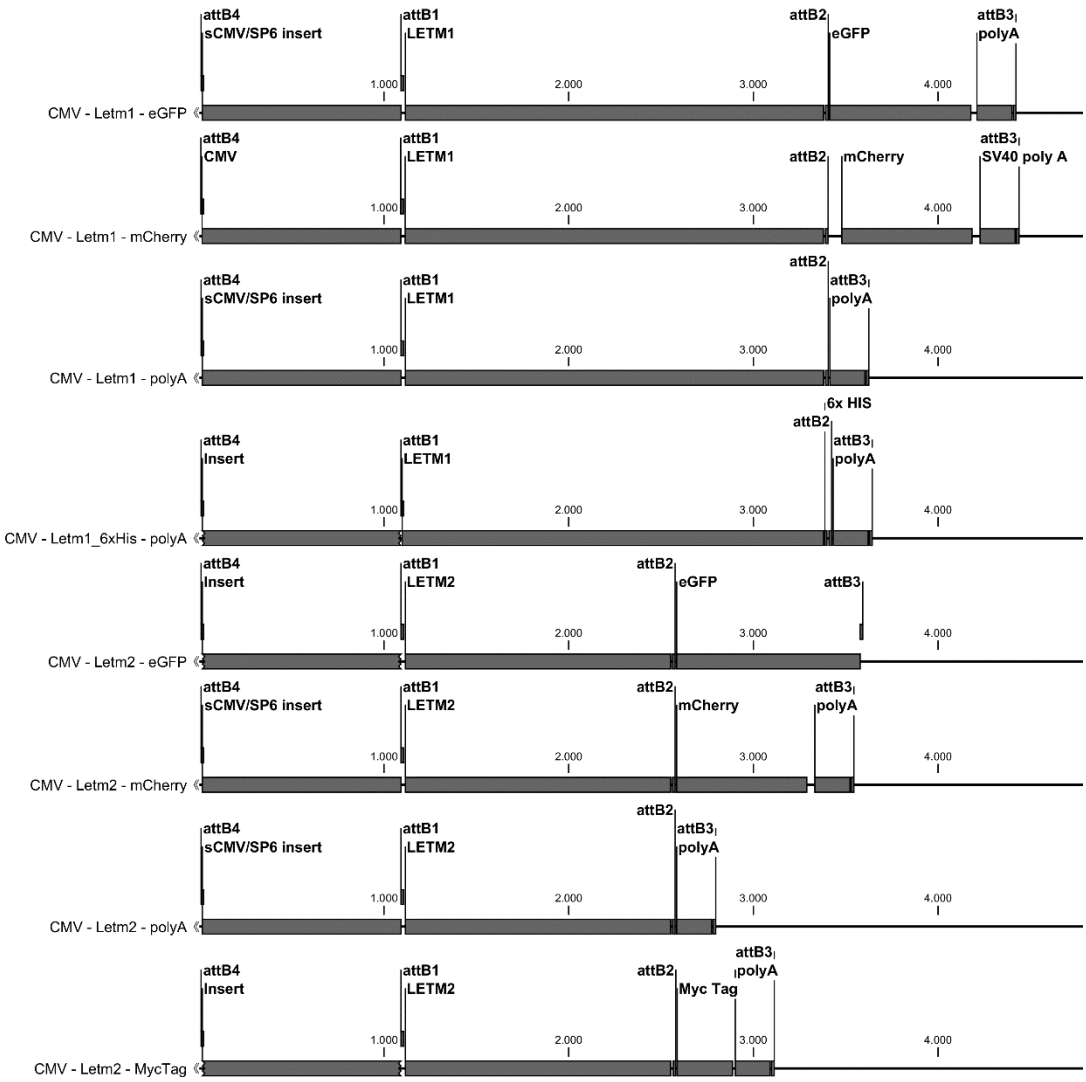

6. Abstract

Wolf Hirschhorn Syndrome (WHS) is severe gene deletion syndrome associated with a wide range of related symptoms. Different studies showed that WHS patients with seizures are LETM1 haploinsufficient. The *leucine zipper-EF-hand containing transmembrane protein 1* (LETM1) is an evolutionary conserved and nucleus encoded mitochondrial protein located in the inner membrane. Recent studies showed that LETM1 regulates the mitochondrial potassium homeostasis and is therefore a factor of the Potassium/Proton-Exchanger (KHE) complex. Disruption of LETM1 in various model systems revealed a temporary growth retardation and mitochondrial swelling, associated with mitophagy and cell death. Furthermore, while DmLetm1 deficient flies are less mobile than the controls, mice do not show any characteristic phenotype. However, injection of a convulsant substance induced prolonged and higher frequent seizures in the mutant rodents, compared to healthy specimens.

Besides LETM1, most eukaryotes also encode a LETM1-like protein, termed LETM2. Sequence alignments showed that LETM2 shares various domains with LETM1. However, the role and function of the novel protein is still elusive.

The current study was addressed to investigate several aspects of LETM1 and LETM2 in the zebrafish and human cells. Sequence alignments and a phylogenetic analysis of the studied proteins revealed their highly conservation throughout the animal kingdom. Furthermore, it was also found that especially the transmembrane and calcium binding domains are very well preserved. Visualization (*In situ* hybridization) and quantification (qPCR) of the *letm1* and *letm2* gene expression in larval and adult tissue samples was further conducted to determine their expression pattern in the zebrafish. The first method revealed a ubiquitous expression of both investigated proteins in larvae and adult fish brains. Quantification of the *letm1* expression levels showed a higher abundance in the head than in the residual body during development. However, the levels of *letm2* stayed almost even. Interestingly, while the *letm2* expression is modestly higher during some developmental stages, adult fish clearly display higher levels of *letm1* in all observed organs.

A novel *letm1* and *letm2* haploinsufficient zebrafish strain was generated by means of the TALEN and CRISPR/Cas9 technology.

The locomotor behavior of the generated *letm1*$^{+/-}$ mutants was further assessed, but did not show an abnormal movement behavior. Furthermore, the established fish lines will serve as important models to investigate additional aspects of Letm1 and Letm2. Moreover, to conduct localization studies two different sets of expression vectors, carrying the fluorescent tagged fish

letm1 or *letm2* were introduced in zebrafish embryos and HeLa cells. Confocal imaging revealed that both proteins were explicitly localized in the fish and human mitochondria.

7. Zusammenfassung (German abstract)

Das Wolf Hirschhorn Syndrom (WHS) ist eine schwerwiegende Gendeletionskrankheit, assoziiert mit einer Vielzahl an Symptomen. Verschiedene Studien haben demonstriert, dass WHS Patienten mit epileptischen Anfällen eine LETM1 haploinsuffizienz aufweisen. Das *leucine zipper-EF-hand containing transmembrane 1* (LETM1) Protein ist in der inneren mitochondrialen Membran lokalisiert und zeichnet sich besonders durch hohe evolutionäre Konservierung aus. Vorhergehende Studien haben gezeigt, dass LETM1 einen wichtigen Bestandteil der mitochondrialen Kalium Homöostase ausmacht, woraus sich die Assoziation mit *Potassium/Proton-Exchanger* Komplex ergibt. *Knock-down* oder *Knock-out* des letm1 Gens in verschiedenen Modellsystemen zeigte eine temporäre Wachstumsretadierung und einen geschwollenen mitochondrialen Phänotyp, zusammen mit Mitophagie und Zelltod. Während weitere Versuche in der Fruchtfliege eine erhöhte Trägheit in Letm1 defizienten Tieren offenbarten, zeigten ähnliche Experimente in Mäusen kein auffallendes Verhaltensmuster. Allerdings konnten längere und häufiger auftretende Krampfanfälle duch Injektion von konvulsiven Substanzen in Letm1 defizienten Mäusen beobachtet werden.

Nahezu alle sequenzierten eukaryontischen Genome kodieren des weiteren ein LETM1 ähnliche Protein: LETM2. Sequenzvergleiche zeigten, dass diverse LETM1 Proteindomänen auch in LETM2 auftreten. Allerdings ist die Funktionen des LETM2 Proteins unbekannt.

Die hier beschriebene Studie befasste sich mit der Analyse von *letm1* und *letm2* in Zebrafischen und humanen Zellen. Sequenzvergleiche und eine phylogenetische Analyse enthüllten ein hohes Maß an evolutionärer Konservierung in den untersuchten Spezies. Besonders auffallend waren hierbei die hoch konservierten Transmembran- und Calciumbindenden Proteindomänen. Visualisierung (*In situ* Hybridisierung) und Quantifizierung (qPCR) der *letm1* und *letm2* Genexpression in Zebrafischen wurden des weiteren durchgeführt um ein spezifisches Expressionsmuster zu erhalten. Basierend auf der visuellen Methode kann schlussgefolgert werden, dass sowohl *letm1* als auch *letm2* ubiquitär in Zebrafischlarven und adulten Gehirnen exprimiert wird. Die Quantifizierung der *letm1* Transkripte in Fischlarven zeigte im Kopf ein höheres Vorkommen als im restlichen Körper. Im Gegensatz dazu zeigten die Resultate von *letm2* keine signifikanten Unterschiede. Es wurde außerdem festgestellt, dass obwohl die *letm2* Expression in den Larven marginal höher als die von *letm1* war, die adulte Tiere eine deutlich ausgeprägtere *letm1* Expressionsrate aufwiesen.

Im Rahmen der Studie wurde mittels der TALEN und CRISPR/Cas9 Methode sowohl eine *letm1* als auch *letm2* haploinsuffiziente Zebrafischlinie etabliert. Diese Modellsysteme dienen als wichtige Grundlage zur Untersuchung verschiedener Aspekte von Letm1 und Letm2.

Anschließende Lokomotor Analysen in den generierten *letm1*$^{+/-}$ Fischen zeigten allerdings kein ungewöhnliches Schwimmverhalten. Des weiteren wurden Lokalisationsstudien durchgeführt. Hierfür wurden zwei Sets an Expressionsvektoren mit einer fluoreszenz markierten Fisch-*letm1* oder Fisch-*letm2* Sequenz hergestellt und in Zebrafischembryonen beziehungsweise HeLa Zellen transferiert. Mittels Konfokalmikroskopie konnte anschließend die explizite, mitochondriale Lokalisation von Letm1 und Letm2 im Zebrafisch und in den humanen Zellen festgestellt werden.

8. References

Amaral, A., Lourenco, B., Marques, M., & Ramalho-Santos, J. (2013). Mitochondria functionality and sperm quality. *Reproduction*. doi:10.1530/REP-13-0178

Auer, T. O., & Del Bene, F. (2014). CRISPR/Cas9 and TALEN-mediated knock-in approaches in zebrafish. *Methods*, pp. 142–150. Elsevier Inc. doi:10.1016/j.ymeth.2014.03.027

Azzone, G. F., & Azzi, A. (1965). Volume changes in liver mitochondria. *Proceedings of the National Academy of Sciences of the United States of America*, *53*(5), 1084–1089.

Barrangou, R., Fremaux, C., Deveau, H., Richards, M., Boyaval, P., Moineau, S., … Horvath, P. (2007). CRISPR provides acquired resistance against viruses in prokaryotes. *Science (New York, N.Y.)*, *315*, 1709–1712. doi:10.1126/science.1138140

Battaglia, A., Filippi, T., & Carey, J. C. (2008). Update on the clinical features and natural history of Wolf-Hirschhorn (4p-) syndrome: Experience with 87 patients and recommendations for routine health supervision. *American Journal of Medical Genetics, Part C: Seminars in Medical Genetics*, *148*(October), 246–251. doi:10.1002/ajmg.c.30187

Baumgartner, R. (2009). *Studies on mitochondria with special focus on human Letm1 and it's role in Wolf-Hirschhorn-Syndrom*. University of Vienna.

Bergemann, A. D., Cole, F., & Hirschhorn, K. (2005). The etiology of Wolf-Hirschhorn syndrome. *Trends in Genetics*, *21*(3), 188–195. doi:10.1016/j.tig.2005.01.008

Berghmans, S., Hunt, J., Roach, A., & Goldsmith, P. (2007). Zebrafish offer the potential for a primary screen to identify a wide variety of potential anticonvulsants. *Epilepsy Research*, *75*, 18–28. doi:10.1016/j.eplepsyres.2007.03.015

Bill, B. R., Petzold, A. M., Clark, K. J., Schimmenti, L. a, & Ekker, S. C. (2009). A primer for morpholino use in zebrafish. *Zebrafish*, *6*(1), 69–77. doi:10.1089/zeb.2008.0555

Bogdanove, A. J., Schornack, S., & Lahaye, T. (2010). TAL effectors: Finding plant genes for disease and defense. *Current Opinion in Plant Biology*, *13*(4), 394–401. doi:10.1016/j.pbi.2010.04.010

Cermak, T., Doyle, E. L., Christian, M., Wang, L., Zhang, Y., Schmidt, C., … Voytas, D. F. (2011). Efficient design and assembly of custom TALEN and other TAL effector-based constructs for DNA targeting. *Nucleic Acids Research*, *39*(12), e82. doi:10.1093/nar/gkr218

Chappel, S. (2013). The role of mitochondria from mature oocyte to viable blastocyst. *Obstetrics and Gynecology International*, *2013*, 183024. doi:10.1155/2013/183024

Crofts, A. (1996). Biological Energy Conservation, Course for Biophysics. Retrieved May 20, 2015, from http://www.life.illinois.edu/crofts/bioph354/lect22.html

Cunningham, F., Amode, M. R., Barrell, D., Beal, K., Billis, K., Brent, S., … Flicek, P. (2014). Ensembl 2015. *Nucleic Acids Research*, *43*(October 2014), 662–669. doi:10.1093/nar/gku1010

Dereeper, a, Guignon, V., Blanc, G., Audic, S., Buffet, S., Chevenet, F., … Gascuel, O. (2008). Phylogeny.fr: robust phylogenetic analysis for the non-specialist. *Nucleic Acids Research*, *36*(Web Server issue), W465–9. doi:10.1093/nar/gkn180

Dimmer, K. S., Navoni, F., Casarin, A., Trevisson, E., Endele, S., Winterpacht, A., … Scorrano, L. (2008). LETM1, deleted in Wolf-Hirschhorn syndrome is required for normal mitochondrial morphology and cellular viability. *Human Molecular Genetics*, *17*(2), 201–214. doi:10.1093/hmg/ddm297

Doyle, E. L., Booher, N. J., Standage, D. S., Voytas, D. F., Brendel, V. P., Vandyk, J. K., & Bogdanove, A. J. (2012). TAL Effector-Nucleotide Targeter (TALE-NT) 2.0: tools for TAL effector design and target prediction. *Nucleic Acids Research*, *40*(Web Server issue), W117–22. doi:10.1093/nar/gks608

Ellis, L. D., Seibert, J., & Soanes, K. H. (2012). Distinct models of induced hyperactivity in zebrafish larvae. *Brain Research*, *1449*, 46–59. doi:10.1016/j.brainres.2012.02.022

Endele, S., Fuhry, M., Pak, S. J., Zabel, B. U., & Winterpacht, a. (1999). LETM1, a novel gene encoding a putative EF-hand Ca(2+)-binding protein, flanks the Wolf-Hirschhorn syndrome (WHS) critical region and is deleted in most WHS patients. *Genomics*, *60*(2), 218–25. doi:10.1006/geno.1999.5881

Endele, S., Fuhry, M., Pak, S., Zabel, B. U., & Winterpacht, A. (1999). LETM1 , A Novel Gene Encoding a Putative EF-Hand Ca2+ Binding Protein , Flanks the Wolf – Hirschhorn Syndrome (WHS) Critical Region and Is Deleted in Most WHS Patients, *225*, 218–225.

Froschauer, E., Nowikovsky, K., & Schweyen, R. J. (2005). Electroneutral K+/H+ exchange in mitochondrial membrane vesicles involves Yol027/Letm1 proteins. *Biochimica et Biophysica Acta - Biomembranes*, *1711*, 41–48. doi:10.1016/j.bbamem.2005.02.018

Geer, L. Y., Marchler-Bauer, A., Geer, R. C., Han, L., He, J., He, S., … Bryant, S. H. (2010). The NCBI BioSystems database. *Nucleic Acids Research*, *38*(Database issue), D492–6. doi:10.1093/nar/gkp858

Goldsmith, J. R., & Jobin, C. (2012). Think small: Zebrafish as a model system of human pathology. *Journal of Biomedicine and Biotechnology*. doi:10.1155/2012/817341

Grunwald, D. J., & Eisen, J. S. (2002). Headwaters of the zebrafish -- emergence of a new model vertebrate. *Nature Reviews. Genetics*, *3*(September), 717–724. doi:10.1038/nrg892

Gupta, T., & Mullins, M. C. (2010). Dissection of organs from the adult zebrafish. *Journal of Visualized Experiments : JoVE*, (37), 4–8. doi:10.3791/1717

Hagberg, H., Mallard, C., Rousset, C. I., & Thornton, C. (2014). Mitochondria: Hub of injury responses in the developing brain. *The Lancet Neurology*, *13*(2), 217–232. doi:10.1016/S1474-4422(13)70261-8

Hammond, P., Hannes, F., Suttie, M., Devriendt, K., Vermeesch, Faravelli, F., … McMullan, D. (2011). Fine-grained facial phenotype-genotype analysis in Wolf-Hirschhorn syndrome. *European Journal of Human Genetics*, *20*(1), 33–40. doi:10.1038/ejhg.2011.135

Hasegawa, A., & van der Bliek, A. M. (2007). Inverse correlation between expression of the Wolfs Hirschhorn candidate gene Letm1 and mitochondrial volume in C. elegans and in mammalian cells. *Human Molecular Genetics*, *16*(17), 2061–2071. doi:10.1093/hmg/ddm154

Hwang, W. Y., Fu, Y., Reyon, D., Maeder, M. L., Tsai, S. Q., Sander, J. D., … Joung, J. K. (2013). Efficient genome editing in zebrafish using a CRISPR-Cas system. *Nature Biotechnology*, *31*(3), 227–9. doi:10.1038/nbt.2501

Jiang, D., Zhao, L., Clish, C. B., & Clapham, D. E. (2013). Letm1, the mitochondrial Ca2+/H+ antiporter, is essential for normal glucose metabolism and alters brain function in Wolf-Hirschhorn syndrome. *Proceedings of the National Academy of Sciences of the United States of America*, *110*(24), E2249–54. doi:10.1073/pnas.1308558110

Karimi, M., Depicker, A., & Hilson, P. (2007). Recombinational cloning with plant gateway vectors. *Plant Physiology*, *145*(December), 1144–1154. doi:10.1104/pp.107.106989

Kim, M. J., Kang, K. H., Kim, C.-H., & Choi, S.-Y. (2008). Real-time imaging of mitochondria in transgenic zebrafish expressing mitochondrially targeted GFP. *BioTechniques*, *45*(3), 331–4. doi:10.2144/000112909

Kimmel, C. B., Ballard, W. W., Kimmel, S. R., Ullmann, B., & Schilling, T. F. (1995). Stages of embryonic development of the zebrafish. *Developmental Dynamics : An Official Publication of the American Association of Anatomists*, *203*(3), 253–310. doi:10.1002/aja.1002030302

Kuscu, C., Arslan, S., Singh, R., Thorpe, J., & Adli, M. (2014). Genome-wide analysis reveals characteristics of off-target sites bound by the Cas9 endonuclease. *Nature Biotechnology*, *32*(7), 677–683. doi:10.1038/nbt.2916

Kwan, K. M., Fujimoto, E., Grabher, C., Mangum, B. D., Hardy, M. E., Campbell, D. S., … Chien, C. Bin. (2007a). The Tol2kit: A multisite gateway-based construction Kit for Tol2 transposon transgenesis constructs. *Developmental Dynamics*, *236*(October), 3088–3099. doi:10.1002/dvdy.21343

Kwan, K. M., Fujimoto, E., Grabher, C., Mangum, B. D., Hardy, M. E., Campbell, D. S., … Chien, C.-B. (2007b). The Tol2kit: a multisite gateway-based construction kit for Tol2 transposon transgenesis constructs. *Developmental Dynamics : An Official Publication of the American Association of Anatomists*, *236*(11), 3088–99. doi:10.1002/dvdy.21343

Lima-Cabello, E., Díaz-Casado, M. E., Guerrero, J. a, Otalora, B. B., Escames, G., López, L. C., … Acuña-Castroviejo, D. (2014). A review of the melatonin functions in zebrafish physiology. *Journal of Pineal Research*, 1–9. doi:10.1111/jpi.12149

Lupo, D., Vollmer, C., Deckers, M., Mick, D. U., Tews, I., Sinning, I., & Rehling, P. (2011). Mdm38 is a 14-3-3-like receptor and associates with the protein synthesis machinery at the inner mitochondrial membrane. *Traffic*, *12*(18), 1457–1466. doi:10.1111/j.1600-0854.2011.01239.x

Maas, N. M. C., Van Buggenhout, G., Hannes, F., Thienpont, B., Sanlaville, D., Kok, K., … Vermeesch, J. R. (2008). Genotype-phenotype correlation in 21 patients with Wolf-

Hirschhorn syndrome using high resolution array comparative genome hybridisation (CGH). *Journal of Medical Genetics*, *45*, 71–80. doi:10.1136/jmg.2007.052910

Macchi, M. M., & Bruce, J. N. (2004). Human pineal physiology and functional significance of melatonin. *Frontiers in Neuroendocrinology*, *25*, 177–195. doi:10.1016/j.yfrne.2004.08.001

Makarova, K. S., Haft, D. H., Barrangou, R., Brouns, S. J. J., Charpentier, E., Horvath, P., … Koonin, E. V. (2011). Evolution and classification of the CRISPR-Cas systems. *Nature Reviews. Microbiology*, *9*(June), 467–477. doi:10.1038/nrmicro2577

Mali, P., Aach, J., Stranges, P. B., Esvelt, K. M., Moosburner, M., Kosuri, S., … Church, G. M. (2013). CAS9 transcriptional activators for target specificity screening and paired nickases for cooperative genome engineering. *Nature Biotechnology*, *31*(9), 833–8. doi:10.1038/nbt.2675

Mali, P., Yang, L., Esvelt, K. M., Aach, J., Guell, M., DiCarlo, J. E., … Church, G. M. (2013). RNA-guided human genome engineering via Cas9. *Science (New York, N.Y.)*, *339*(6121), 823–6. doi:10.1126/science.1232033

Martin, W. H., Beavis, A. D., & Garlid, K. D. (1984). Identification of an 82,000-dalton protein responsible for K+/H+ antiport in rat liver mitochondria. *Journal of Biological Chemistry*, *259*(15), 2062–2065.

McQuibban, A. G., Joza, N., Megighian, A., Scorzeto, M., Zanini, D., Reipert, S., … Nowikovsky, K. (2010). A Drosophila mutant of LETM1, a candidate gene for seizures in Wolf-Hirschhorn syndrome. *Human Molecular Genetics*, *19*(6), 987–1000. doi:10.1093/hmg/ddp563

Meeker, N. D., Hutchinson, S. a., Ho, L., & Trede, N. S. (2007). Method for isolation of PCR-ready genomic DNA from zebrafish tissues. *BioTechniques*, *43*(5), 610–614. doi:10.2144/000112619

Miller, J. C., Tan, S., Qiao, G., Barlow, K. a, Wang, J., Xia, D. F., … Rebar, E. J. (2011). A TALE nuclease architecture for efficient genome editing. *Nature Biotechnology*, *29*(2), 143–148. doi:10.1038/nbt.1755

Mitchell, P. (2011). Chemiosmotic coupling in oxidative and photosynthetic phosphorylation. *Biochimica et Biophysica Acta - Bioenergetics*, *1807*(12), 1507–1538. doi:10.1016/j.bbabio.2011.09.018

Nowikovsky, K., & Bernardi, P. (2014). LETM1 in mitochondrial cation transport. *Frontiers in Physiology*. doi:10.3389/fphys.2014.00083

Nowikovsky, K., Froschauer, E. M., Zsurka, G., Samaj, J., Reipert, S., Kolisek, M., … Schweyen, R. J. (2004). The LETM1/YOL027 gene family encodes a factor of the mitochondrial K+ homeostasis with a potential role in the Wolf-Hirschhorn syndrome. *The Journal of Biological Chemistry*, *279*(29), 30307–15. doi:10.1074/jbc.M403607200

Nowikovsky, K., Pozzan, T., Rizzuto, R., Scorrano, L., & Bernardi, P. (2012). Perspectives on: SGP symposium on mitochondrial physiology and medicine: the pathophysiology of LETM1. *The Journal of General Physiology*, *139*(6), 445–54. doi:10.1085/jgp.201110757

Nowikovsky, K., Reipert, S., Devenish, R. J., & Schweyen, R. J. (2007). Mdm38 protein depletion causes loss of mitochondrial K+/H+ exchange activity, osmotic swelling and mitophagy. *Cell Death and Differentiation*, *14*, 1647–1656. doi:10.1038/sj.cdd.4402167

Nowikovsky, K., Schweyen, R. J., & Bernardi, P. (2009). Pathophysiology of mitochondrial volume homeostasis: Potassium transport and permeability transition. *Biochimica et Biophysica Acta - Bioenergetics*, *1787*(5), 345–350. doi:10.1016/j.bbabio.2008.10.006

Panula, P., Sundvik, M., & Karlstedt, K. (2014). Developmental roles of brain histamine. *Trends in Neurosciences*. Elsevier Ltd. doi:10.1016/j.tins.2014.01.001

Paradowska-Stolarz, A. M. (2014). Wolf-Hirschhorn syndrome (WHS) - literature review on the features of the syndrome. *Advances in Clinical and Experimental Medicine : Official Organ Wroclaw Medical University*, *23*(3), 485–9. Retrieved from http://www.ncbi.nlm.nih.gov/pubmed/24979523

Park, J., Li, Y., Kim, S. H., Yang, K. J., Kong, G., Shrestha, R., … Park, J. (2014). New players in high fat diet-induced obesity: Letm1 and Ctmp. *Metabolism: Clinical and Experimental*, *63*(3), 318–327. doi:10.1016/j.metabol.2013.10.012

Parng, C., Seng, W. L., Semino, C., & McGrath, P. (2002). Zebrafish: a preclinical model for drug screening. *Assay and Drug Development Technologies*, *1*(1), 41–48. doi:10.1089/154065802761001293

Ran, F. A., Hsu, P. D., Lin, C. Y., Gootenberg, J. S., Konermann, S., Trevino, A. E., … Zhang, F. (2013). Double nicking by RNA-guided CRISPR cas9 for enhanced genome editing specificity. *Cell*, *154*(6), 1380–1389. doi:10.1016/j.cell.2013.08.021

Reis, A., Hornblower, B., Robb, B., & Tzertzinis, G. (2014). CRISPR / Cas9 and Targeted Genome Editing : A New Era in Molecular Biology. *NEB Expressions*, (1). Retrieved from https://www.neb.com/tools-and-resources/feature-articles/crispr-cas9-and-targeted-genome-editing-a-new-era-in-molecular-biology

Schlickum, S., Moghekar, A., Simpson, J. C., Steglich, C., O'Brien, R. J., Winterpacht, A., & Endele, S. U. (2004). LETM1, a gene deleted in Wolf–Hirschhorn syndrome, encodes an evolutionarily conserved mitochondrial protein. *Genomics*, *83*(2), 254–261. doi:10.1016/j.ygeno.2003.08.013

Shannon, N. L., Maltby, E. L., Rigby, A. S., & Quarrell, O. W. (2001). An epidemiological study of Wolf-Hirschhorn syndrome: life expectancy and cause of mortality. *Journal of Medical Genetics*, *38*(10), 674–9. Retrieved from http://www.pubmedcentral.nih.gov/articlerender.fcgi?artid=1734744&tool=pmcentrez&rendertype=abstract

Sprague, J., Doerry, E., Douglas, S., & Westerfield, M. (2001). The Zebrafish Information Network (ZFIN): a resource for genetic, genomic and developmental research. *Nucleic Acids Research*, *29*(1), 87–90. doi:10.1093/nar/29.1.87

Steele, S. L., Prykhozhij, S. V., & Berman, J. N. (2014). Zebrafish as a model system for mitochondrial biology and diseases. *Translational Research*, *163*(2), 79–98. doi:10.1016/j.trsl.2013.08.008

Streck, E. L., Gonçalves, C. L., Furlanetto, C. B., Scaini, G., Dal-Pizzol, F., & Quevedo, J. (2014). Mitochondria and the central nervous system: Searching for a pathophysiological basis of psychiatric disorders. *Revista Brasileira de Psiquiatria*, *36*, 156–167. doi:10.1590/1516-4446-2013-1224

Tamai, S., Iida, H., Yokota, S., Sayano, T., Kiguchiya, S., Ishihara, N., … Oka, T. (2008a). Characterization of the mitochondrial protein LETM1, which maintains the mitochondrial tubular shapes and interacts with the AAA-ATPase BCS1L. *Journal of Cell Science*, *121*(Pt 15), 2588–600. doi:10.1242/jcs.026625

Tamai, S., Iida, H., Yokota, S., Sayano, T., Kiguchiya, S., Ishihara, N., … Oka, T. (2008b). Characterization of the mitochondrial protein LETM1, which maintains the mitochondrial tubular shapes and interacts with the AAA-ATPase BCS1L. *Journal of Cell Science*, *121*, 2588–2600. doi:10.1242/jcs.026625

Urasaki, A., Morvan, G., & Kawakami, K. (2006). Functional dissection of the Tol2 transposable element identified the minimal cis-sequence and a highly repetitive sequence in the subterminal region essential for transposition. *Genetics*, *174*(October), 639–649. doi:10.1534/genetics.106.060244

Valton, J., Dupuy, A., Daboussi, F., Thomas, S., Maréchal, A., Macmaster, R., … Duchateau, P. (2012). Overcoming transcription activator-like effector (TALE) DNA binding domain sensitivity to cytosine methylation. *Journal of Biological Chemistry*, *287*(46), 38427–38432. doi:10.1074/jbc.C112.408864

Wang, C., Liu, Q., Chen, Y., Liu, S., Xu, J., Cui, X., … Piao, L. (2015). Clinical implication of leucine zipper/EF hand-containing transmembrane-1 overexpression in the prognosis of triple-negative breast cancer. *Experimental and Molecular Pathology*, 1–6. doi:10.1016/j.yexmp.2014.12.012

Wright, T. J., Ricke, D. O., Denison, K., Abmayr, S., Cotter, P. D., Hirschhorn, K., … Altherr, M. R. (1997). A transcript map of the newly defined 165 kb Wolf-Hirschhorn syndrome critical region. *Human Molecular Genetics*, *6*(2), 317–24. Retrieved from http://www.ncbi.nlm.nih.gov/pubmed/9063753

Wu, C., MacLeod, I., & Su, A. I. (2013). BioGPS and MyGene.info: Organizing online, gene-centric information. *Nucleic Acids Research*, *41*(November 2012), 561–565. doi:10.1093/nar/gks1114

Wu, C., Orozco, C., Boyer, J., Leglise, M., Goodale, J., Batalov, S., … Su, A. I. (2009). BioGPS: an extensible and customizable portal for querying and organizing gene annotation resources. *Genome Biology*, *10*(11), R130. doi:10.1186/gb-2009-10-11-r130

Zhang, B., Carrie, C., Ivanova, A., Narsai, R., Murcha, M. W., Duncan, O., … Whelan, J. (2012). LETM proteins play a role in the accumulation of mitochondrially encoded proteins in Arabidopsis thaliana and AtLETM2 displays parent of origin effects. *Journal of Biological Chemistry*, *287*(50), 41757–41773. doi:10.1074/jbc.M112.383836

Zhang, X., Chen, G., Lu, Y., Liu, J., Fang, M., Luo, J., … Wang, X. (2013). Association of Mitochondrial Letm1 with Epileptic Seizures. *Cerebral Cortex (New York, N.Y. : 1991)*, (October), 1–8. doi:10.1093/cercor/bht118

Zollino, M., Di Stefano, C., Zampino, G., Mastroiacovo, P., Wright, T. J., Sorge, G., … Neri, G. (2000). Genotype-phenotype correlations and clinical diagnostic criteria in Wolf-Hirschhorn syndrome. *American Journal of Medical Genetics*, *94*, 254–261. doi:10.1002/1096-8628(20000918)94:3<254::AID-AJMG13>3.0.CO;2-7 [pii]

Zollino, M., Lecce, R., Fischetto, R., Murdolo, M., Faravelli, F., Selicorni, A., … Neri, G. (2003). Mapping the Wolf-Hirschhorn Syndrome Phenotype Outside the Currently Accepted WHS Critical Region and Defining a New Critical Region , WHSCR-2, *1*, 590–597.

Zollino, M., Murdolo, M., Marangi, G., Pecile, V., Galasso, C., Mazzanti, L., & Neri, G. (2008). On the nosology and pathogenesis of Wolf-Hirschhorn syndrome: Genotype-phenotype correlation analysis of 80 patients and literature review. *American Journal of Medical Genetics, Part C: Seminars in Medical Genetics*, *148*(October), 257–269. doi:10.1002/ajmg.c.30190

Zotova, L., Aleschko, M., Sponder, G., Baumgartner, R., Reipert, S., Prinz, M., … Nowikovsky, K. (2010). Novel components of an active mitochondrial K(+)/H(+) exchange. *The Journal of Biological Chemistry*, *285*(19), 14399–414. doi:10.1074/jbc.M109.059956

Zu, Y., Tong, X., Wang, Z., Liu, D., Pan, R., Li, Z., … Lin, S. (2013). TALEN-mediated precise genome modification by homologous recombination in zebrafish. *Nature Methods*, *10*(4), 329–31. doi:10.1038/nmeth.2374

9. Curriculum vitae

Personal Details

Name:	HAJNY Stefan
Nationality:	Austria
E-Mail:	hajnys3@univie.ac.at

Education

10/2009 - 09/2012	**Bachelor Study** of Biomedicine and Biotechnology at the University of Veterinary Medicine
10/2012 - 06/2015	**Master Study** of Molecular Biology at the University of Vienna (Specialization on Molecular Medicine)

Research Experience

02/2012 - 7/2012	**Bachelor Student**, Ludwig Boltzmann Institute for experimental and clinical Traumatology; Bachelor thesis: *Effect of ischemia/reperfusion on nitric oxide generation and mitochondrial function in rat limb.* Principal investigator: *Priv. Doz. Dr. Andrey Kozlov*
10/2012 - 12/2013	**Scientific employee**, Ludwig Boltzmann Institute for experimental and clinical Traumatology; *Continuation of the former bachelor project.* Principal investigator: *Priv. Doz. Dr. Andrey Kozlov*
03/2014 - 05/2015	**Master Student**, Anna Spiegel Center of Translational Research in collaboration with the Max F. Perutz Laboratories (Group of Dr. Kristin Tessmar-Raible); *Master thesis: A zebrafish model of Letm1 and Letm2 deficiency* Principal investigator: *Priv. Doz. Dr. Karin Nowikovsky*

Internships

02/2010 (2 weeks)	**VetOMICS**, University of Veterinary Medicine Vienna Principal investigator: *Ao.Univ.-Prof. Dr.med.vet.Dieter Klein*
07/2010 - 08/2010	**Institute of Pharmacology**, Medical University Vienna Principal investigator: *Ao.Univ.-Prof. Dr.med.univ. Christian Nanoff*
08/2010 (2 weeks)	**Institute of laboratory animal research**, University of Veterinary Medicine Vienna Principal investigator: *Dipl.-Ing. Dr.nat.techn. Dieter Fink*
02/2011 (2 weeks)	**Institute of laboratory animal research**, University of Veterinary Medicine Vienna Principal investigator: *Dipl.-Ing. Dr.nat.techn. Dieter Fink*
07/2011 - 09/2011	**Ludwig Boltzmann Institute for experimental and clinical Traumatology** Principal Investigator: *Priv. Doz. Dr. Andrey Kozlov*
08/2013 - 09/2013	**Institute for Pathophysiology**, University of Veterinary Medicine Vienna Principal investigator: *Ass.-Prof. Dr.rer.nat. Olena Andrukhova*